INVESTIGATIONS INTO THE CHEMISTRY OF PROTEIN TYROSINE PHOSPHATASE REDOX REGULATION

A Dissertation presented to the Faculty of the Graduate School

at the University of Missouri-Columbia

In Partial Fulfillment

of the Requirements for the Degree

Doctor of Philosophy

---

by

JASON N. LABUTTI

Dr. Kent S. Gates, Dissertation Supervisor

MAY 2009

The undersigned, appointed by the Dean of The Graduate School, have examined the dissertation entitled:

INVESTIGATIONS INTO THE CHEMISTRY OF PROTEIN TYROSINE PHOSPHATASE REDOX REGULATION

Presented by Jason N. LaButti

A candidate for the degree of Doctor of Philosophy

And hereby certify that in their opinion it is worthy of acceptance.

_____

Professor Kent S. Gates

_____

Professor Thomas Reilly

_____

Professor Michael Harmata

_____

Professor John Tanner

This dissertation is dedicated to Ralph and Yolanda Lotito.

ACKNOWLEDGEMENTS

I would like to acknowledge those who have made this dissertation possible:

My advisor, Professor Kent S. Gates for his guidance and advice throughout my graduate career.

My doctoral committee for their insight and ideas.

Past and present Gates Group members including my amazing friends Dr. Venkatraman Junnotula, Derrick Seiner, Ujjal Sarkar and Mostafa Fekry for making our lab a fun place to be.

Dr. John Scott Daniels for helping me find my way to the Gates Lab.

My brothers Erik and Kurt for helping me see the lighter side of life.

My Uncle Ralph, whose generosity, care and love helped us immeasurably.

My Nana who I wish could be here with us.

My Papa who showed me very early in my life that the world is full of wonder.

My mother and father for *always* being there for me.

My daughter Anna Regina who makes me smile (unless she is not using her listening ears…and even then I usually smile).

Last and most importantly my wife Gretchen, who has helped me become a better person.

TABLE OF CONTENTS

LIST OF FIGURES

LIST OF SCHEMES

Scheme Page

LIST OF TABLES

Table Page

Chapter 1

Introduction

1.1 Cell Signal Transduction and Protein Tyrosine Phosphatases

The binding of extracellular hormones such as insulin or epidermal growth factor to receptors on the surface of cells triggers complex intracellular signal transduction cascades.[1, 2] These signal cascades, in turn, can induce cells to perform a myriad of biochemical tasks ranging from cell division to taking up glucose from the blood. Transmission of these signals within cells is often accomplished through the reversible phosphorylation of specific protein tyrosine residues.[3] This reversible phosphorylation serves as a biochemical "rheostat" that alters a protein's functional properties and leads to propagation of the signal. The phosphorylation status of these tyrosine residues, thus transmission of the cellular signal itself, is tightly controlled by the opposing actions of protein tyrosine kinases that catalyze the addition of phosphoryl groups and protein tyrosine phosphatases (PTPs) that catalyze their removal (Scheme 1.1).[4, 5] The removal of these phosphoryl groups, in many cases, serves as an "off switch" to terminate the cellular responses to the extracellular stimulus. PTPs, therefore, play a central role in the

regulation of diverse cellular processes including glucose metabolism, cell cycle control and immune responses.[6]

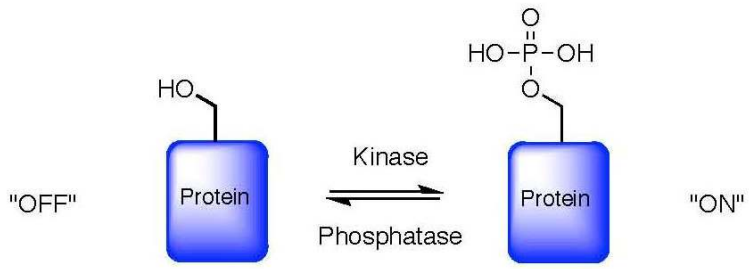

Scheme 1.1 The phosphorylation state of tyrosine residues can alter a protein's enzymatic function.

When considering the state of the art in PTP research, it is interesting to note that the field of PTP investigation lags that of kinases by approximately ten years. This is, in part, due to the fact that it was once thought that phosphatases, in contrast to kinases, were relatively unimportant "housekeeping" enzymes with little or no substrate specificity and/or regulation mechanism.[4] In the past 10 to 15 years, however, research has shown that these enzymes have exquisite substrate specificities and are actually tightly regulated by a number of mechanisms.[7, 8] Furthermore, the complex mechanisms by which PTPs exert their control over cell communications have yet to be fully elucidated. Regardless of the body of knowledge related to PTPs, due to their important roles in cell signal transduction and links to disease states such as cancer and diabetes, many PTPs have been identified as potential drug targets and in general the field of PTP research is subject of intense scientific study.[9]

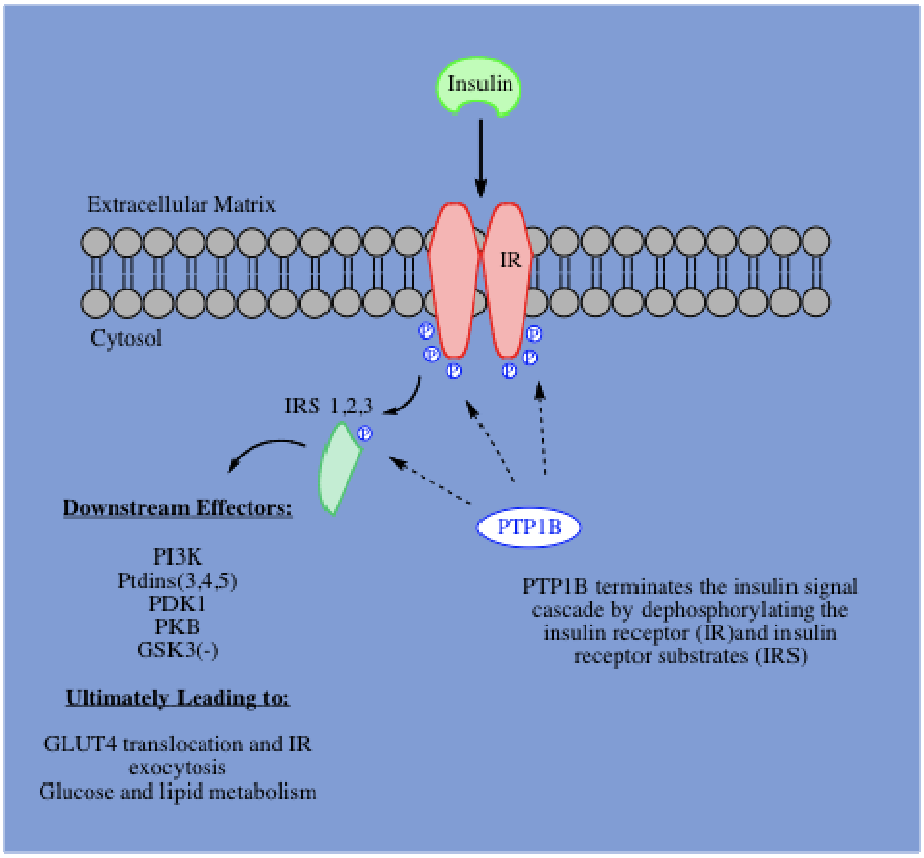

Figure 1.1 A representation of the insulin signal cascade and its negative regulation by PTP1B.

1.2 Protein Tyrosine Phosphatases and the Insulin Signal Cascade

A good example of the expansive role PTPs play in cellular operations can be found in the insulin signal cascade and its role in maintaining glucose homeostasis. The insulin signaling cascade, thus blood glucose homeostasis, is controlled primarily through the action of insulin on insulin receptors (IRs) that are present on the surface of fat and muscle cells (Figure 1.2).[10] Binding of insulin to the IR (which is a heterotetramer of two α and two β subunits) induces a change in secondary structure which leads to autophosphorylation of IR tyrosines 1146, 1162 and 1163.[11] Phosphorylation of these IR β subunit tyrosine residues, in turn, transforms the IR itself into a protein kinase that

subsequently phosphorylates various insulin receptor substrates (IRS). These IRS transmit the insulin signal via a complex and yet-to-be fully elucidated signaling path that eventually leads to cellular uptake of glucose through activation and/or exocytosis of the Glut-4 glucose transporter.[12] While addition of phosphoryl groups to Y1146, 1162 and 1163 activates the IR to phosphorylate various insulin receptor substrates (IRS), removal of these phosphoryl groups by certain PTPs ablates IR kinase activity. In particular, protein tyrosine phosphatase 1B (PTP1B) is the major enzyme responsible for dephosphorylation of the insulin receptor β subunits. Insulin resistance is a major factor in *diabetes mellitus*, a disease of global significance.[13] PTP1B, as the major negative regulator of insulin signal transduction, is therefore a highly sought-after target for anti-diabetes drug development.[14-17]

1.3 Protein Tyrosine Phosphatase Structure and Catalysis

At the time of writing this dissertation, there are approximately 500 kinases known, while 100 phosphatase genes have been identified in the human genome.[18] Members of the phosphatase superfamily are categorized into one of four sub-families: dual-specificity or mixed-function PTPs, CDC-25 phosphatases, low molecular weight PTPs and classical protein tyrosine phosphatases.[19] The following discussion and the studies described herein employed the catalytic subunit of human PTP1B (a.a. 1-322) as an archetypal member of the PTP family of enzymes. While there is little or no sequence homology among the different PTP families, the active sites of PTPs all possess a signature amino acid motif of $C(X)_5R(S/T)$.[19] This motif, in addition to containing residues necessary for catalysis, forms a positively charged phosphate-binding domain known as the phosphate-binding loop, or P-loop (Scheme 1.1). The phosphate-binding

domain is a rigid scaffold that properly positions the substrate using favorable polar and ionic interactions. As is the case with most enzymes, substrate specificity between PTPs is generally imparted by primary, secondary and tertiary structures surrounding the active site.[20, 21]

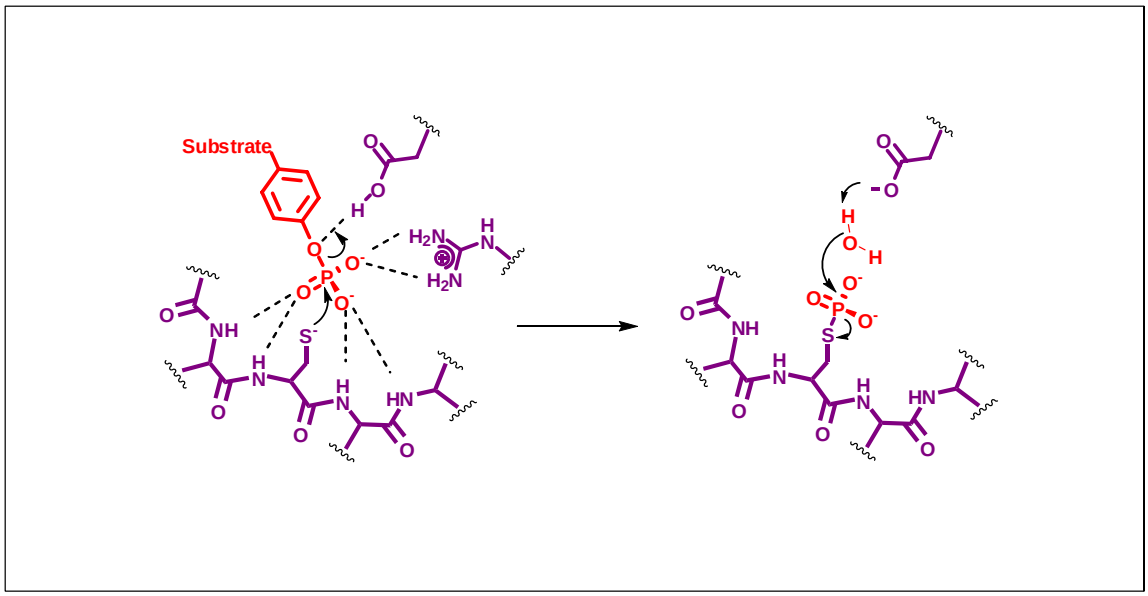

Scheme 1.2 Representation of a general PTP active site and its catalytic action.

Within this PTP active site architecture, there exists a set of highly conserved amino acids that are required for catalytic activity. Perhaps most critical is the cysteine residue positioned within the phosphate binding pocket of the active site (C215 in PTP1B). The thiol moiety of this cysteine functions as a nucleophile, attacking the phosphorus atom of the substrate phosphate group.[19] The pK_a of this cysteine thiol is lowered from ~ 9 to 5.56 through hydrogen bonding to amide NH groups in the P-loop, the helix dipole of a-4, and an invariant arginine residue (R221 in PTP1B).[22, 23] Due to

this shift in pK_a the cysteinyl sulfur exists completely in the reactive thiolate (charged anion) form at physiological pH, which significantly enhances its nucleophilicity. In addition to the cysteine and arginine residues, an aspartic acid that functions as a general acid/base (D181 in PTP1B) is also required for catalysis (Scheme 1.2).

Scheme 1.2 shows a representation of a general PTP catalytic cycle and the amino acid residues that are involved. Catalysis begins with negatively charged phosphorylated substrate binding to the active site via an array of interactions with the P-loop amide functionalities, and the positively charged guanidinium moiety of Arg221. This is followed by nucleophilic attack by the cysteine thiolate on the substrate phosphoryl group to yield a transient phosphorylcysteine enzyme intermediate that is stabilized by Arg221. In PTP1B, this step has been shown to proceed through a dissociative mechanism in which there is minimal bond order between the enzyme and the substrate, which results in a three coordinate meta-phosphate like transition state.[23] This is in contrast to a high bond order associative mechanism that would have a five coordinate phosphorane-type intermediate. The hydroxyl group of the dephosphorylated substrate is protonated via a general acid interaction with Asp 181 as it is released from the active site. Finally, the phosphocysteine enzyme intermediate is hydrolyzed by a water molecule that is activated through a general base interaction with Asp 181. The result is the release of inorganic phosphate and regeneration of the active site cysteine thiolate (active enzyme).

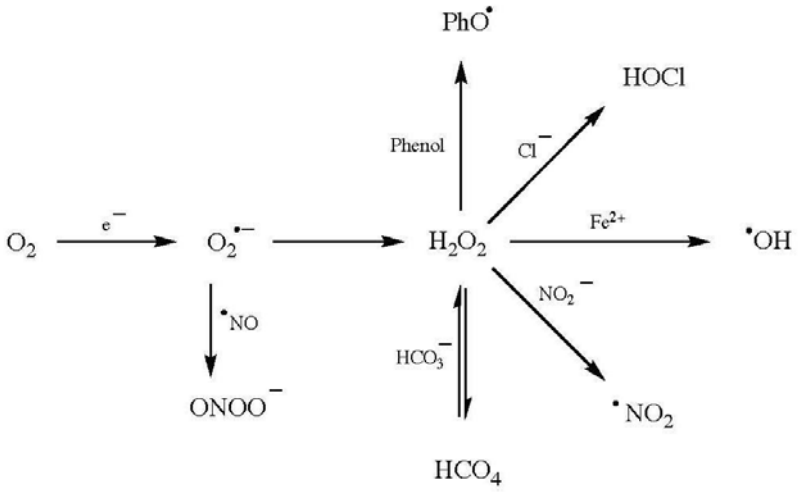

Scheme 1.3 Physiologically-relevant reactive oxygen species (ROS) are typically derived from reduction of oxygen.

1.4 Redox Chemistry of the PTP Active Site

It is becoming clear, from recent studies, that while kinases control the *amplitude* of a signal, endogenous regulation of phosphatase activity can control the *duration* of the response.[9] Given the importance of PTPs in signal transduction, it is not surprising that the activity of these enzymes is regulated during normal cellular processes. An important mechanism for the endogenous regulation of PTPs involves the transient, reversible oxidation of their active site cysteine residue. Due to the fact that PTP catalytic cysteinyl sulfurs exist primarily in the thiolate anion state, they react readily with oxidants to form sulfenic acids. This oxidation renders them catalytically inactive.[7, 24-27] Numerous oxidizing agents have been shown to effect the aforementioned chemistry. From a physiologic perspective these reactive oxygen species (ROS) are normally derived, either spontaneously or enzymatically, from the one-electron reduction of molecular oxygen

(O_2) to superoxide radical anion, $O_2^{\cdot-}$ (Scheme 1.3) Reactive oxygen species such as hydrogen peroxide (H_2O_2) and peroxynitrite (ONOOH) can oxidize a nucleophilic thiolate to the sulfenic oxidation state through a two-electron process (Scheme 1.4).[28] Transition metals such as iron^{II} are also known to oxidize thiolate anions through single electron radical chemistry and recombination with molecular oxygen (also known as Fenton chemistry).[29] [28]

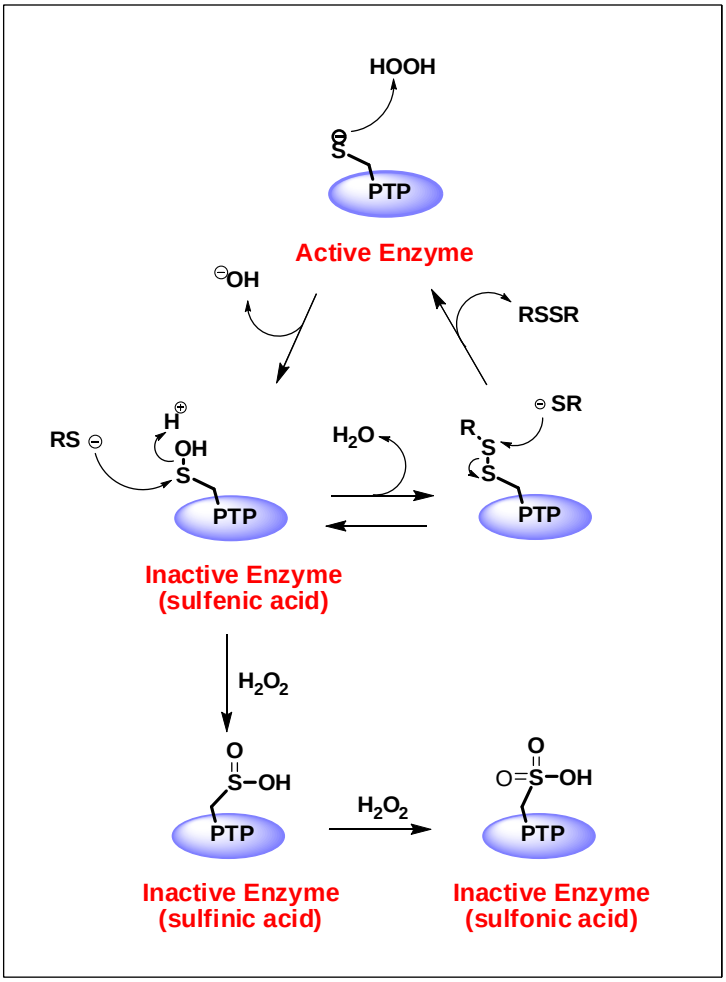

Scheme 1.4 Oxidation of the PTP cysteine thiolate by hydrogen peroxide, and reversal by thiols.

If one considers that the timeframe of cellular responses to insulin stimulation are on the order of minutes,[1] and that it would take hours if not days to replenish permanently

inactivated enzyme, it becomes clear that in addition to switching PTP activity off there need to be provisions for recovering their catalytic activity. This is accomplished by the reducing state of the cytosol. Under normal physiological conditions oxidation of the catalytic cysteine thiolate to the sulfenic oxidation state would be reversed through reaction with ubiquitous cellular reducing equivalents such as glutathione (Scheme 1.5).[30]

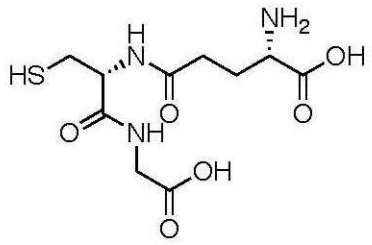

glutathione

Scheme 1.5 Structure of the biological thiol glutathione.

The overall concept of redox regulation is actually more complex than simply the reversible formation of sulfenic acids through oxidation. This is due to the fact that sulfenic acids may be further oxidized to sulfinic and then sulfonic acids (Scheme 1.4). Unlike sulfenic acids these higher oxidation species, if generated in the active site, typically are not reversible by reaction with thiols.[31, 32] Over-oxidation of the PTP catalytic cysteine thiolate to sulfinic and sulfonic acids therefore permanently inactivates the enzyme.

1.5 Hydrogen Peroxide is an Intracellular Signaling Agent that Targets the PTP Active Site

The concept of PTP intracellular redox regulation has only recently been proposed.[25, 27, 33] While H_2O_2 concentrations of 10-100 μM are toxic to cells, it has been determined that biologically relevant (nanomolar to low micromolar) concentrations are produced in response to various stimuli including growth factors, cytokines and insulin.[33, 34] The enzymes responsible for production of hydrogen peroxide during cell signal transduction are the flavin-containing NADPH oxidases (Nox) and dual-cofactor flavin enzymes (Duox).[35, 36] These enzymes, during their catalytic cycle, release superoxide radical anion ($O_2^{\cdot -}$) which very rapidly dismutates to hydrogen peroxide ($k = 5.5\ e^5\ M^{-1}s^{-1}$) (Scheme 1.6).[37, 38] With regard to PTP redox regulation, it has been shown that stimulation of cells with insulin triggers intracellular production of H_2O_2 by the enzyme Nox-4, which leads to inactivation of PTP1B through the previously described reversible oxidation of the catalytic cysteine thiolate.[24, 39] Inactivation of PTP1B effectively preserves phosphorylation of the IR and IRS and prolongs the insulin signal cascade. Endogenous hydrogen peroxide, therefore, acts as a positive regulator of the insulin signal cascade by disabling PTP1B and prolonging cellular uptake of glucose.

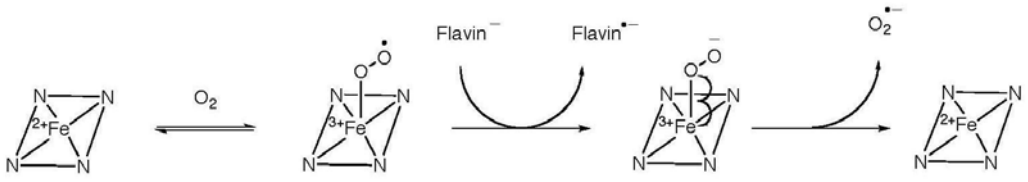

Scheme 1.6 The mechanism of superoxide production by NADPH oxidase (Nox).

1.6 Conclusions and Goals of This Dissertation

Based upon the described chemistry, it is apparent that an oxidation/reduction cycle of PTPs can serve as a molecular switch of sorts, that regulates catalytic activity.[40] This mechanism of intracellular signaling plays a leading role is such critical physiologic processes as the insulin signal cascade. While the concept that PTP redox-regulation is part of normal physiologic intracellular processes, there are many unknowns that have yet to be illuminated. The chemistry by which oxidative species regulate PTPs is relatively well characterized, but the exact mechanism(s) by which these species themselves are produced and regulated remain unclear. Furthermore, ROS remain an elusive target for both detection and quantification due to their transience and high rates of diffusion.[41, 42] Due to these properties, new, specific techniques need to be developed to aid investigators who wish to expand the boundaries of our knowledge about redox regulation.

In the first two chapters of this dissertation, we explore the properties of an oxidizing agent that may be an H_2O_2-derived, biologically accessible endogenous regulator of PTPs. Chapter 2 describes the synthesis, purification and characterization of this agent, known as peroxymonophosphate. We then report the effects of peroxymonophosphate on the catalytic activity of PTP1B in Chapter 3. Chapter 4 describes our development of a new method for selectively detecting peroxymonophosphate by using a fluorescent boronate-based probe. In Chapter 5, we use this agent as a tool to demonstrate enzymatic production of peroxymonophosphate through phosphoryl transfer to hydrogen peroxide. Finally, in Chapter 6, we report a new assay that utilizes the intrinsic fluorescence of PTP1B to monitor the redox state of its active site.

References

1. Saltiel, A. R.; Kahn, C. R., Insulin signalling and the regulation of glucose and lipid metabolism. *Nature* **2001,** *414* (6865), 799-806.

2. Cohen, S., Epidermal growth factor (EGF): historical perspectives. *Horm. Proteins Pept.* **1985,** *12*, 299-304.

3. Ahn, N., Introduction: Protein phosphorylation and signaling. *Chem. Rev.* **2001,** *101* (8), 2207.

4. Stone, R. L.; Dixon, J. E., Protein-tyrosine phosphatases. *J. Biol. Chem.* **1994,** *269* (50), 31323-31326.

5. Abraham, R. T., Cell cycle checkpoint signaling through the ATM and ATR kinases. *Genes Dev.* **2001,** *15*, 2177-2196.

6. Johnson, L. N.; Lewis, R. J., Structural Basis for Control by Phosphorylation. *Chem. Rev.* **2001,** *101* (8), 2209-2242.

7. den Hertog, J.; Groen, A.; van der Wijk, T., Redox regulation of protein-tyrosine phosphatases. *Arch. Biochem. Biophys.* **2005,** *434* (1), 11-15.

8. Majeti, R.; Weiss, A., Regulatory mechanisms for receptor protein tyrosine phosphatases. *Chem. Rev.* **2001,** *101*, 2441-2448.

9. Tonks, N. K., Protein tyrosine phosphatases: from genes, to function, to disease. *Nat Rev Mol Cell Biol* **2006,** *7* (11), 833-846.

10. Ross, S. A.; Gulve, E. A.; Wang, M., Chemistry and Biochemistry of Type 2 Diabetes. *Chem. Rev.* **2004,** *104* (3), 1255-1282.

11. Patti, M. E.; Kahn, C. R., The insulin receptor--a critical link in glucose homeostasis and insulin action. *Journal of basic and clinical physiology and pharmacology* **1998,** *9* (2-4), 89.

12. Liu, M.; Gibbs, E. M.; McCoid, S. C.; Milici, A. J.; Stukenbrok, H. A.; McPherson, R. K.; Treadway, J. L.; Pessin, J. E., Transgenic Mice Expressing the Human GLUT4/Muscle-Fat Facilitative Glucose Transporter Protein Exhibit Efficient Glycemic Control. *PNAS* **1993,** *90* (23), 11346-11350.

13. Zimmet, P.; Alberti, K. G. M.; Shaw, J., Global and societal implications of the diabetes epidemic. *Nature* **2001,** *414* (6865), 782.

14. Cheng, A.; Dube, N.; Gu, F.; Tremblay, M. L., Coordinated action of protein tyrosine phosphatases in insulin signal transduction. *Eur. J. Biochem.* **2002,** *269* (4), 1050-1059.

15. Puius, Y. A.; Zhao, Y.; Sullivan, M.; Lawrence, D. S.; Almo, S. C.; Zhang, Z.-Y., Identification of a second aryl phosphate-binding site in protein-tyrosine phosphatase 1B: A paradigm for inhibitor design. *PNAS* **1997,** *94* (25), 13420-13425.

16. Bridges, A. J., Therapeutic challenges of kinase and phosphatase inhibition and use in anti-diabetic strategy. *Biochem. Soc. Trans.* **2005,** *33* (Pt 2), 343-345.

17. Hooft van Huijsduijnen, R.; Sauer, W. H. B.; Bombrun, A.; Swinnen, D., Prospects for inhibitors of protein tyrosine phosphatase 1B as antidiabetic drugs. *J. Med. Chem.* **2004,** *47*, 4142-4146.

18. Alonso, A.; Sasin, J.; Bottini, N.; Friedberg, I.; Friedberg, I.; Osterman, A.; Godzik, A.; Hunter, T.; Dixon, J.; Mustelin, T., Protein tyrosine phosphatases in the human genome. *Cell* **2004,** *117* (6), 699-711.

19. Jackson, M. D.; Denu, J. M., Molecular Reactions of Protein Phosphatases-Insights from Structure and Chemistry. *Chem. Rev.* **2001,** *101* (8), 2313-2340.

20. Zhang, Z.-Y., Protein tyrosine phosphatases: structure and function, substrate specificity, and inhibitor development. *Ann. Rev. Pharmacol. Toxicol.* **2002,** *42* (42), 209-234.

21. Zongchao Jia, D. B., Andrew J. Flint, Nicholas K. Tonks, Structural Basis for Phosphotyrosine Peptide Recognition by Protein Tyrosine Phosphatase 1B. *Science* **1995,** *268*, 1754-1758.

22. Peters, G. H.; Frimurer, T. M.; Olsen, O. H., Electrostatic Evaluation of the Signature Motif (H/V)CX5R(S/T) in Protein-Tyrosine Phosphatases. *Biochemistry* **1998,** *37* (16), 5383-5393.

23. Lohse, D. L.; Denu, J. M.; Santoro, N.; Dixon, J. E., Roles of Aspartic Acid-181 and Serine-222 in Intermediate Formation and Hydrolysis of the Mammalian Protein-Tyrosine-Phosphatase PTP1. *Biochemistry* **1997,** *36* (15), 4568-4575.

24. Mahadev, K.; Zilbering, A.; Zhu, L.; Goldstein, B. J., Insulin-stimulated Hydrogen Peroxide Reversibly Inhibits Protein-tyrosine Phosphatase 1B in Vivo and Enhances the Early Insulin Action Cascade. *J. Biol. Chem.* **2001,** *276* (24), 21938-21942.

25. Caselli, A.; Marzocchini, R.; Camici, G.; Manao, G.; Moneti, G.; Pieraccini, G.; Ramponi, G., The Inactivation Mechanism of Low Molecular Weight Phosphotyrosine-protein Phosphatase by H2O2. *J. Biol. Chem.* **1998,** *273* (49), 32554-32560.

26. Meng, T.-C.; Fukada, T.; Tonks, N. K., Reversible oxidation and inactivation of protein tyrosine phosphatases in vivo. *Mol. Cell* **2002,** *9*, 387-399.

27. Denu, J. M.; Tanner, K. G., Specific and Reversible Inactivation of Protein Tyrosine Phosphatases by Hydrogen Peroxide: Evidence for a Sulfenic Acid Intermediate and Implications for Redox Regulation. *Biochemistry* **1998,** *37* (16), 5633-5642.

28. Forman, H. J.; Fukuto, J. M.; Torres, M., Redox signaling: thiol chemistry defines which reactive oxygen and nitrogen species can act as second messengers. *Am J Physiol Cell Physiol* **2004,** *287* (2), C246-256.

29. Misra, H. P., Generation of Superoxide Free Radical during the Autoxidation of Thiols. *J. Biol. Chem.* **1974,** *249* (7), 2151-2155.

30. Leslie, N. R.; Lindsay, Y.; Ross, S. H.; Downes, C. P., Redox regulation of phosphatase function. *Biochem. Soc. Trans.* **2004,** *32* (Pt 6), 1018-1020.

31. Sivaramakrishnan, S.; Keerthi, K.; Gates, K. S., A chemical model for the redox regulation of protein tyrosine phosphatase 1B (PTP1B). *J. Am. Chem. Soc.* **2005,** *127*, 10830-10831.

32. Allison, W. S., Formation and reactions of sulfenic acids in proteins. *Accounts Chem. Res.* **1976,** *9*, 293-299.

33. Xu, D.; Rovira, I. I.; Finkel, T., Oxidants Painting the Cysteine Chapel: Redox Regulation of PTPs. *Developmental Cell* **2002,** *2* (3), 251-252.

34. Sundaresan, M.; Yu, Z.-X.; Ferrans, V. J.; Irani, K.; Finkel, T., Requirement for Generation of H(2)O(2) for Platelet-Derived Growth Factor Signal Tran sduction. *Science* **1995,** *270* (5234), 296-299.

35. Lambeth, J. D., NOX enzymes and the biology of reactive oxygen. *Nature Rev. Immunol.* **2004,** *4* (Mar), 181-189.

36. Lambeth, J. D.; Kawahara, T.; Diebold, B., Regulation of Nox and Duox enzymatic activity and expression. *Free Radical Biology and Medicine* **2007,** *43* (3), 319-331.

37. Halliwell, B.; Gutteridge, J. M. C., Role of free radicals and catalytic metal ions in human disease: an overview. *Methods Enzymol.* **1990,** *186*, 1-85.

38. Wilshire, J.; Sawyer, D. T., Redox chemistry of dioxygen species. *Acct. Chem. Res.* **1979,** *12*, 105-110.

39. Goldstein, B. J.; Mahadev, K.; Wu, X., Redox Paradox: Insulin Action Is Facilitated by Insulin-Stimulated Reactive Oxygen Species With Multiple Potential Signaling Targets. *Diabetes* **2005,** *54* (2), 311-321.

40. den Hertog, J.; Groen, A.; van der Wijk, T., Redox regulation of protein-tyrosine phosphatases. *Archives of Biochemistry and Biophysics* **2005,** *434* (1), 11-15.

41. Rhee, S. G., H_2O_2, a necessary evil for cell signaling. *Science* **2006,** *312* (June 30), 1882-1883.

42. Rhee, S. G., Measuring H_2O_2 produced in response to cell surface receptor activation. *Nat Chem Biol* **2007,** *3* (5), 244-246.

Chapter 2

Biologically Relevant Properties of Peroxymonophosphate

2.1 The Redox Paradox

As was described in the introduction, there is extensive evidence supporting the notion that the inactivation of PTP1B during insulin signaling is mediated by the reactive oxygen species hydrogen peroxide. To review: Exposure of cells to insulin activates kinases that add phosphoryl groups to tyrosine residues on target proteins.[1, 2] The resulting downstream activity of this phosphorylation is potentiated by a rapid (2-5 minute onset), transient inactivation of the protein tyrosine phosphatases that are responsible for removal of these phosphoryl groups.[3-5] This involves downstream activation of NADPH oxidases (Nox) that produce an intracellular burst of hydrogen peroxide.[6, 7] Generation of H_2O_2, in turn, leads to inactivation of select PTPs via oxidation of their catalytic cysteine thiol residues to the sulfenic acid oxidation state. Oxidative inactivation of PTPs inside cells is transient because thiol-mediated reduction of the oxidized cysteine residue slowly regenerates the active form of the enzyme (Scheme 2.1).

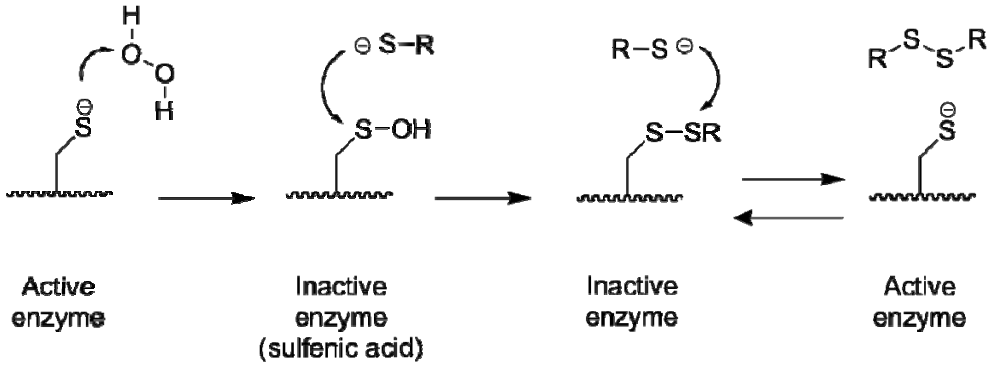

Scheme 2.1 The PTP active site cysteine thiolate redox regulation cycle.

Interestingly, despite clear evidence for its involvement in the intracellular regulation of PTPs, *in vitro* experiments reveal that H_2O_2, at physiologic concentrations, is a rather sluggish PTP inactivator.[3, 8] Specifically, based on the reported rate constants for in vitro inactivation of PTP1B by H_2O_2 (k = 9.8 M-1s-1), one can calculate that the half-life for inactivation of these enzymes by a steady-state concentration of 1 μM H_2O_2 will be approximately 20 h.

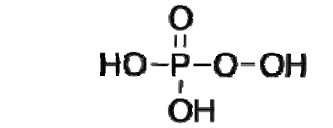

peroxymonophosphate
(1)

Scheme 2.2 Structure of peroxymonophosphate.

In addition to the kinetic conundrum, for some applications, it may be desirable to identify small molecules that mimic the ability of hydrogen peroxide to effect transient, thiol-reversible, oxidative inactivation of PTPs. In general, PTP inactivators have potential both as therapeutic agents and tools for the study of signal transduction pathways.[9] Here, we set out to develop a redox regulator of PTP activity that is more

potent than hydrogen peroxide and may account for the previously described kinetic conundrum. Toward this end, we envisioned that peroxymonophosphate (Scheme 2.2) might be an exceptional PTP inactivator in which noncovalent association of the phosphoryl group with the highly conserved phosphate binding pocket found in the active site of all PTPs would serve to guide the peroxy moiety into position for efficient reaction with the catalytic cysteine residue. To facilitate consideration of the potential role of peroxymonophosphate in biological systems we present studies related to the preparation, characterization, stability and quantitative detection of this agent.

2.2 Preparation of Peroxydiphosphate and Peroxymonophosphate

Peroxymonophosphate is not commercially available, therefore two options were considered for preparation of the material. We first attempted to use a method for peroxymonophosphate synthesis described by Zhu and colleagues in which the bilayer formed between two immiscible solvents (water and carbon tetrachloride) was used to moderate the vigorous reaction between phosphorous pentoxide (P_2O_{10}) and concentrated hydrogen peroxide (70% in water).[10] In this preparation hydrogen peroxide was added dropwise to a stirred suspension of P_2O_{10} in carbon tetrachloride. Due to the extremely exothermic nature of the reaction and the severe oxidizing nature of the concentrated hydrogen peroxide it was necessary to utilize safety measures such as thick safety gloves, full-face protection and a heavy lexan blast shield. The authors warned that the hydrogen peroxide solution had to be added slowly, but not too slowly, because the P_2O_{10} would begin to clump and a violent exotherm would occur. In addition, the authors warned that the hydrogen peroxide could not be added too quickly, as the reaction would rapidly accelerate and a violent exotherm would occur. To say that this reaction was tricky to

perform is an understatement. More often than not, our attempts yielded a loud report and smoking ruins of the vessel contents. Furthermore, and perhaps most important for the purposes of these studies, this reaction yielded a multitude of phosphorous-bearing products which were not easily (if at all) separated (Figure 2.1). This mixture would clearly be unsuitable for careful scientific investigations of the biologically relevant characteristics of peroxymonophosphate.

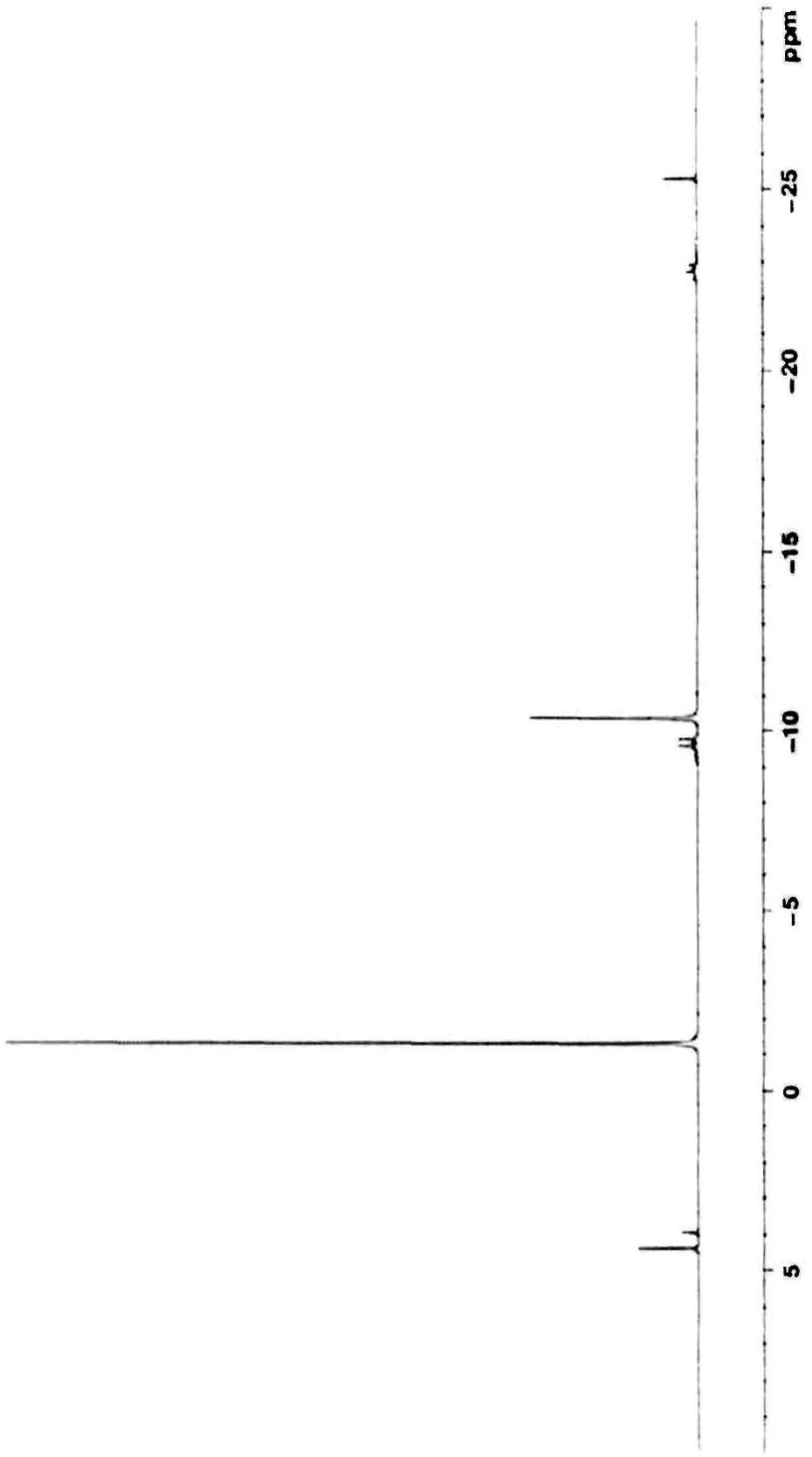

Figure 2.1 ^{31}P NMR scan (uncalibrated) of the complex product profile generated by the Kadla preparation of peroxymonophosphate. A peak corresponding to phosphate is found at – 1.2 ppm.

An alternative to the "hydrogen peroxide prep" (as we called it) was a two-step electrolysis-based preparation. The first step was the synthesis and purification of a peroxydiphosphate potassium salt via electrolysis of an alkaline solution of potassium phosphate and potassium fluoride.[11] The exact nature of the reaction (or reactions) that occurs during electrolysis to produce peroxydiphosphate has not been reported. It is clear, however, due to the destruction of rubber-based materials in the general vicinity of the electrolysis apparatus and a distinctive odor, that the procedure generates a noticeable quantity of ozone. Persons who attempt to duplicate these experiments should take appropriate measures to protect items that may be harmed by this diffusible reaction by-product (perform the reaction in a fume hood).

The potassium salt of peroxydiphosphate was found to be too soluble in water to reliably isolate from phosphate contaminants, therefore a lithium salt of peroxydiphosphate was created via a metathesis process to facilitate recrystallization of pure material.[12] A ^{31}P NMR scan of the product of electrolysis after one round of recrystallization is shown in Figure 2.2.

Peroxydiphosphate is very stable at neutral and alkaline pH. Under acidic conditions, however, peroxymonophosphate readily undergoes hydrolysis to form peroxymonophosphate and inorganic phosphate.[13] Ultimately, peroxymonophosphate was made via acid hydrolysis of a solution of lithium peroxymonophosphate in 1 M perchloric acid at 50^{o}C.[12] It is worth noting that we found commercially available potassium peroxydiphosphate to be unsuitable for this preparation due to the very impure nature of the material.

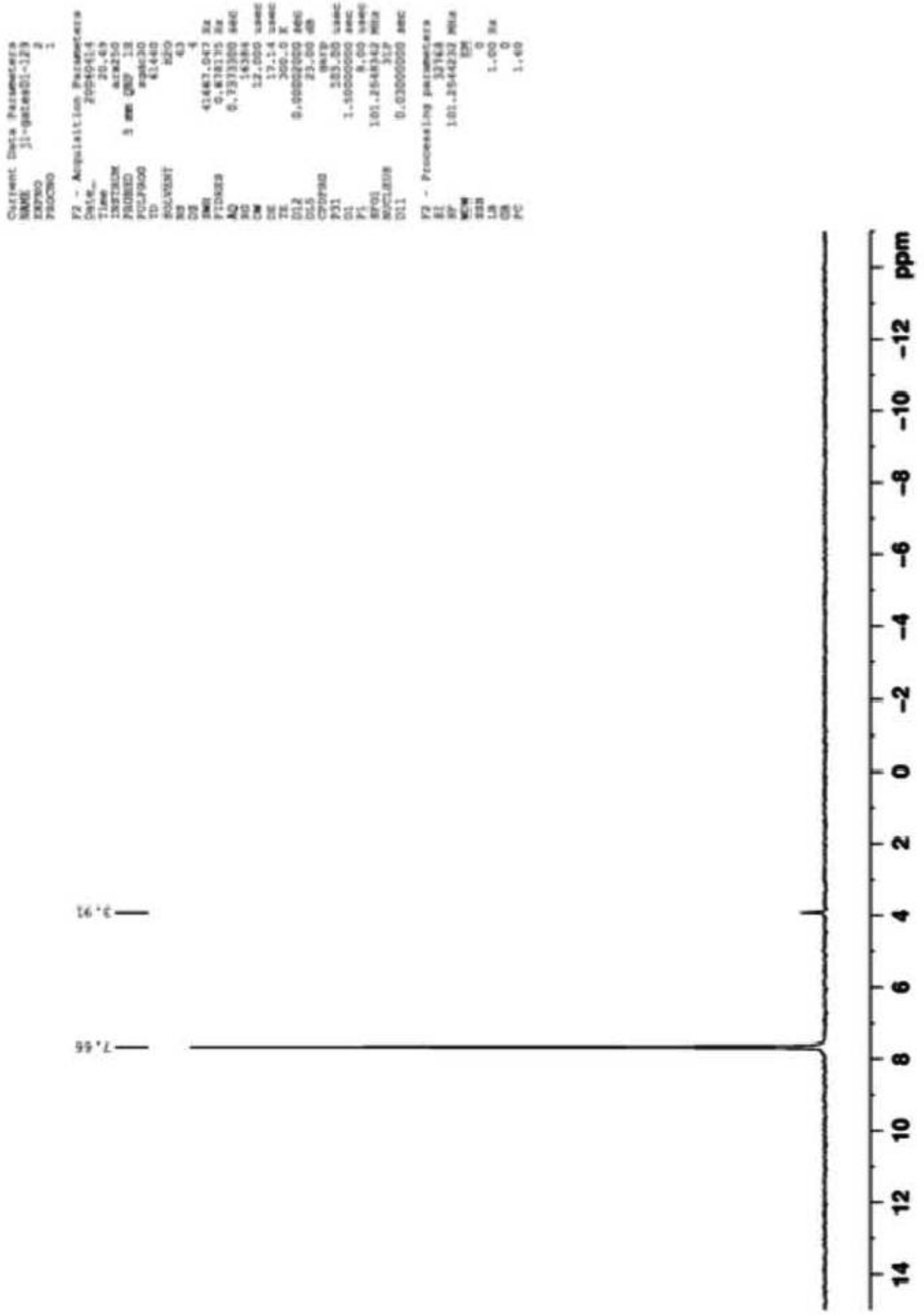

Figure 2.2 ^{31}P NMR of an alkaline (pH ~ 11), aqueous solution of peroxydiphosphate (P_2O_{10}) after one recrysallization from methanol/water. The peaks are assigned as follows: peroxydiphosphate: 7.66 ppm. Phosphate : 3.91 ppm.

2.3 Quantification of Solutions of Peroxydiphosphate and Peroxymonophosphate by ^{31}P NMR

Quantification of reactive oxygen species such as hydrogen peroxide and peroxymonophosphate was typically achieved through lengthy and cumbersome titrations with various indicating agents such as iodide and ferroin.[10] We found that while reaction between a presumed solution of peroxymonophosphate and iodide was useful to provide evidence of a reactive oxygen species, it was neither the easiest nor most accurate way for quantification of peroxymonophosphate itself.

We envisioned that quantitative ^{31}P-NMR would be an ideal technique for analysis of phosphorous-containing species. It was evident from literature precedent, however, that careful consideration of the instrumental parameters under which ^{31}P-NMR spectra were taken was necessary for accurate quatification.[14] The most important, in this case, was the "relaxation time" parameter, or D1 as noted on the Bruker 250 MHz output. Errors of approximately 12-20% were observed when the phosphorous nuclei were not allowed to return to ground state conditions before the cyclical 30^{o} RF excitation pulse. The phosphorous species in which we were interested apparently had a comparatively long relaxation time (~ 12.5 s) compared to "standard" instrumental parameters (~ 1.5 s). In addition to instrument parameters, a proper internal standard was needed for accurate quantification. We chose diphenyl phosphate for the following reasons: (1) it contains one single-resonance phosphorous nuclei (2) it is stable (3) it is commercially available (4) it is inexpensive.

Once the proper NMR parameters were determined, the technique was used to analyze solutions of peroxydiphosphate and peroxymonophosphate. It is important to

note that the chemical shift of each species was highly pH dependent. When diluted 1:2 with a 40 mM solution of diphenyl phosphate in water (0.5 M $HClO_4$ final concentration, pH < 1), and using 85% phosphoric acid as an external instrument zero, peroxymonophosphate shows a ^{31}P-NMR resonance at 4.27 ppm. Figure 2.3.

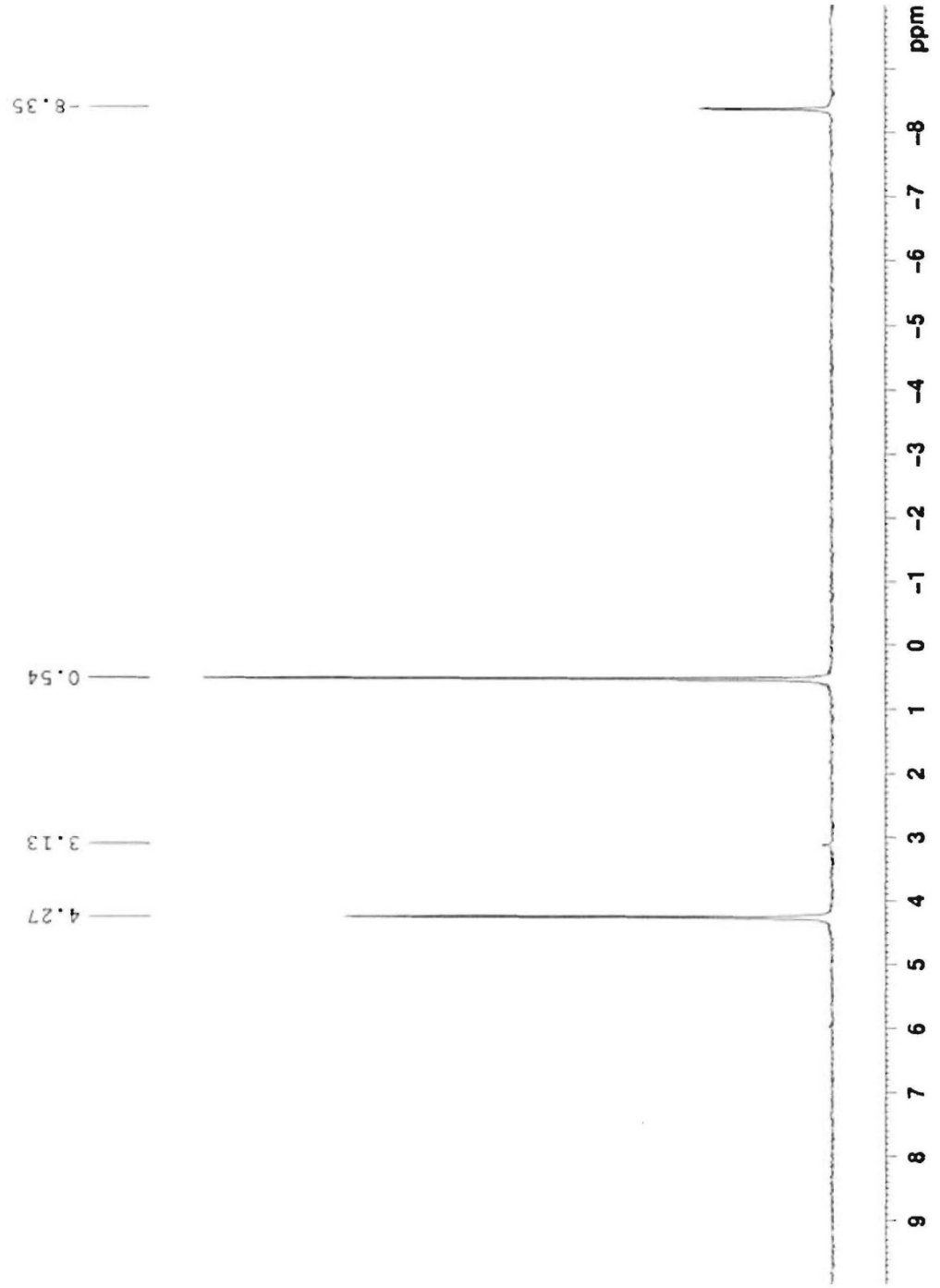

Figure 2.3 ^{31}P NMR of a 200 mM peroxydiphosphate solution treated with 6M $HClO_4$ for 1h at 50^{o}C. Internal standard diphenyl phosphate was added to a concentration of 20 mM. The peaks are assigned as follows: Peroxymonophosphate 4.27 ppm, peroxydiphosphate 3.13 ppm, phosphate 0.54 ppm, diphenylphosphate (internal standard) -8.35 ppm.

2.4 Stability of Peroxymonophosphate in Buffers

Due to the fact that there is little, if any, literature precedent for the use of peroxymonophosphate in life science type experiments we examined its stability in the presence of several commonly used buffers and biologically relevant substrates (Figure 2.4). We find that peroxymonophosphate is quite stable in $HClO_4$ (100 mM) over the course of 1 h at 24°C. Similarly, peroxymonophosphate is stable in sodium phosphate (100 mM, pH 7) and bis-tris buffer (100 mM pH 7) under these conditions. In contrast, under identical conditions, the agent is completely destroyed upon incubation with HEPES buffer. This is not entirely unexpected, for it has been reported that the piperazine moiety of Good's Buffers can be N-oxidized by hydrogen peroxide.[15] Similarly, addition of the biological thiol glutathione (10 mM) to a sodium phosphate buffered solution leads to complete decomposition of the peroxymonophosphate. Again, this is not surprising; the presence of biological thiols such as glutathione in cells is a defense mechanism against oxidative stress.[16, 17] Furthermore, the sulfide-containing amino acid methionine also destroys peroxymonophosphate. Tryptophan and glycine lead to only small amounts of decomposition. Addition of $FeSO_4$ (10 mM) results in a 60% decrease in the concentration of analyte. Neither 1% dimethyl sulfoxide (140 mM) nor the hydrogen peroxide-destroying enzyme catalase had significant effects on the stability of peroxymonophosphate under these conditions.

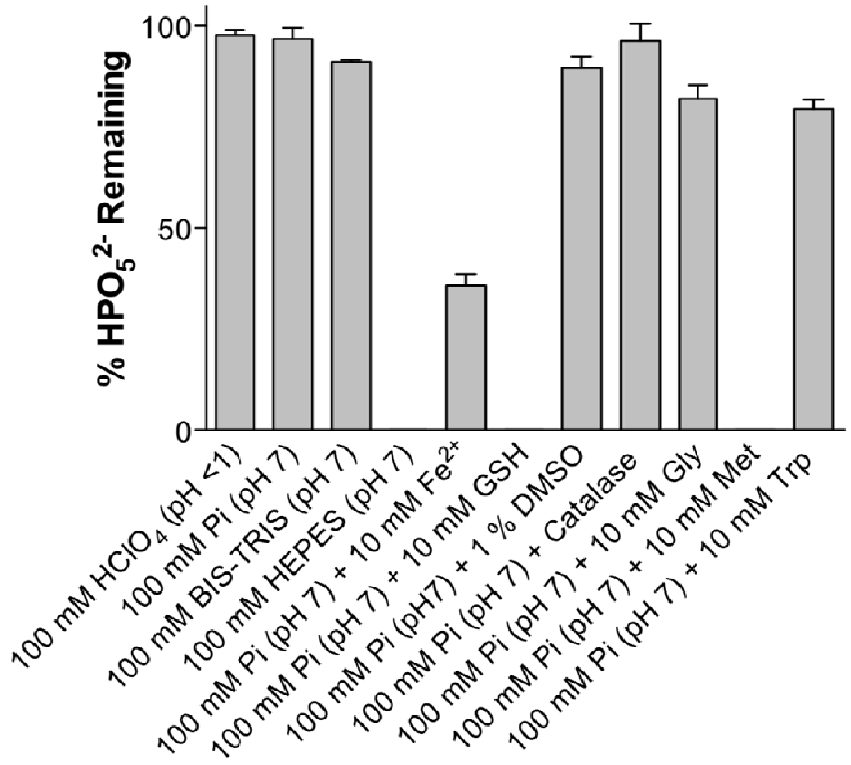

Figure 2.4 The stability of peroxymonophosphate in the presence of biologically relevant additives.

2.5 Conclusions

In summary, we have conducted the first survey of the reactivity of peroxymonophosphate under biologically relevant conditions. Peroxymonophosphate is substantially more reactive than hydrogen peroxide as an oxidant.[18, 19] Nonetheless, we find that the selectivity of peroxymonophosphate towards reactions with various biochemicals, in many regards, mirrors that of H_2O_2. Peroxymonophosphate is stable in perchloric acid, and the commonly used biological buffers sodium phosphate and bis-tris. These results are consistent with those of Battaglia and Edwards who reported the half-life of peroxymonophosphate to be 12.5 h in 4 M $HClO_4$ (rate, k = 1.54 X 10^{-5} s^{-1}).[12]

Peroxymonophosphate is unstable in the presence of iron (II). This breakdown presumably involves a Fenton-type reaction analogous to the well known metal-mediated breakdown of hydrogen peroxide.[20] In addition, we showed that HEPES buffer, the biological thiol glutathione, and the sulfide-containing amino acid methionine all completely decompose peroxymonophosphate. Again, this is analogous to the reactivity of H_2O_2 with HEPES,[15] glutathione,[21] and methionine.[22] Our result with methionine in pH 7 buffer is consistent with previous work showing facile reaction of peroxymonophosphate with aryl sulfides in acetonitrile-water mixtures.[23] We observe that, DMSO, glycine, and the indole-containing amino acid tryptophan do not react substantially with peroxymonophosphate in aqueous pH-neutral solutions. Others have reported reactions of peroxymonophosphate with sulfoxides and indoles.[24, 25] These earlier studies, however, were conducted under conditions where the protonated species H_3PO_5 was predominant. In contrast, with pK_a values of 1.0, 5.5 and 12.8, peroxymonophosphate exists primarily as the dianion under the conditions of our experiments (pH 7).[12, 24] A number of studies show that the reactivity of peroxymonophosphate is pH-dependent, increasing at lower pH values as the oxygen's become increasingly protonated.[23, 25, 26] A most striking difference between H_2O_2 and peroxymonophosphate is revealed by our observation that peroxymonophosphate does not appear to be a substrate for the H_2O_2 destroying enzyme catalase. The inability of catalase to decompose peroxymonophosphate is in agreement with the observation that another bulky hydroperoxide, t-butyl hydroperoxide, is a poor substrate for the enzyme.[27, 28]

2.6 Experimental Procedures

Materials and Methods

Reagents were purchased from the following suppliers: HEPES (#H3375), potassium fluoride (#402931), potassium phosphate (# P0662), diphenyl phosphate (#850608), lithium perchlorate trihydrate (# 205303), phosphorous pentoxide (# 21-470-1), carbon tetrachloride (# 319961), Bis-Tris (#B9754), iron (II) chloride tetrahydrate (# 380024), DMSO (# 276855), glutathione (reduced) (# G4251), tryptophan (# T0254), Methionine (# M9625), Glycine (# G6201), 85% phosphoric acid (# 345245), Potassium hydroxide (# P5958), Sigma-Aldrich (St. Louis, MO). 70% hydrogen peroxide was a kind gift from the Arkema, Inc., Philadelphia, PA. Absolute ethanol was obtained from Pharmco-AAPER, Brookfield, CT.

Lithium Peroxydiphosphate. Lithium peroxydiphosphate was made according to the methods described by Griffith and Battaglia.[11, 12] Sixty mL of distilled deionized water, 33.75 g potassium dihydrogen ortho-phosphate (4.12 M), 22.75 g potassium hydroxide (6.6 M), and 13.5 grams potassium fluoride (3.9 M) was added to a 100 mL three-necked water-jacketed flask. An anode constructed of approximately 30 cm of platinum wire wrapped in a tight spiral, and cathode of approximately 10 cm of straight platinum wire were arranged at opposite sides of the flask. The flask was cooled to 10^{o}C with a recirculating water chiller, flooded with a gentle stream of nitrogen, and subjected to six hour cycles of electrolysis (6V, 325 mA) on three consecutive days, punctuated with 18 h "rest" periods. An image of the electrolysis equipment is shown in Figures 2.5 and 2.6. Rest periods allowed the peroxymonophosphate created during electrolysis to degrade,

leaving the more stable peroxydiphosphate as a fine white precipitate. The resulting solid was collected with vacuum filtration, and re-dissolved in 100 mL of distilled deionized water. An aqueous solution of lithium perchlorate (0.54 g/mL) was slowly added to the filtrate solution dropwise with stirring. A dense white precipitate formed immediately. After about 10 mL was added, the precipitate was removed by vacuum filtration, and a few more drops of lithium perchlorate were added to the filtrate to ensure complete precipitation of the lithium salts. The clear filtrate was warmed to 45^{o}C, and ~ 60 mL methanol was added rapidly with stirring. A fine white precipitate slowly formed. The product was collected by vacuum filtration, subjected to two more water/methanol precipitation steps, then air-dried. An aqueous solution of the product (resulting pH ~ 11) was analyzed with ^{31}P NMR calibrated with 100% phosphoric acid. Two peaks were observed in addition to the diphenylphosphate internal standard: 3.9 ppm corresponding to phosphate and a peak at 7.6 ppm corresponding to peroxydiphosphate (Figure 2.2).

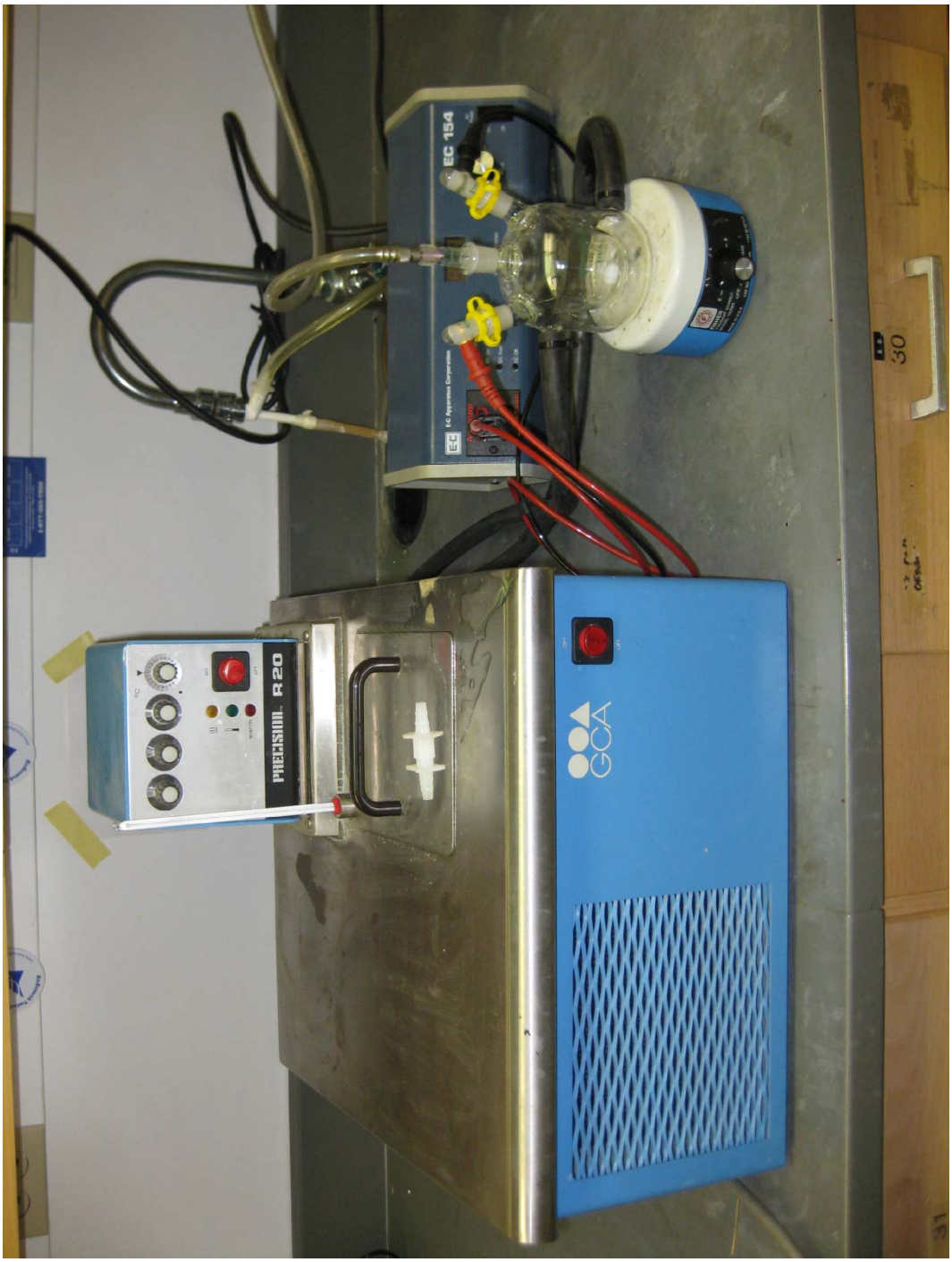

Figure 2.5 The apparatus for electrolytic preparation of potassium peroxydiphosphate consists of a power supply, chiller, and jacketed glass vessel with platinum anode and cathode wires.

Figure 2.6 Close-up of jacketed electrolysis vessel for preparation of peroxymonophosphate.

Peroxymonophosphate (PMP) (1). An aqueous solution of PMP was made according to the method described by Battaglia.[12] One volume of 6 N perchloric acid was combined with 5 volumes of a ~200 mM aqueous solution of lithium peroxydiphosphate, then heated to 50°C for 1 h. Phosphorous NMR of the resulting solution (pH < 1) showed two peaks: one at 0.6 ppm corresponding to phosphate, one at 4.1 ppm corresponding to PMP. A sample removed after 15 min of heating showed three peaks: 0.6 ppp (phosphate), 2.9 ppm (peroxydiphosphate) and 4.3 ppm (PMP). The exact peroxymonophosphate concentration was determined with phosphorous NMR by combining 0.5 mL of product solution with 0.5 mL of an aqueous 40 mM solution of diphenylphosphate internal standard. The molecular mass of peroxymonophosphate, H_3PO_5 $(M+H)^+$ = 114.98 was confirmed with electrospray tandem mass spectroscopy (ESI/MS/MS) (data not shown). Typical concentrations of the peroxymonophosphate solutions prepared with this method were ~130 mM and contained a comparable concentration of phosphate. PMP stock solutions in 1M perchloric acid were stored at -20°C, and are stable for at least four weeks. For enzymatic assays, stock solutions were thawed, diluted with distilled, de-ionized water then used immediately. It is important to note that inorganic phosphate is a known reversible inhibitor of PTPs. At the concentrations present in the assays described here, however, there is no effect on enzyme activity. All of the activity of these solutions can be attributed to peroxymonophosphate.

Stability of Peroxymonophosphate under Biologically Relevant Conditions. To prepare the solutions for quantitative analysis, peroxymonophosphate (~ 120 mM in 1M $HClO_4$) was combined (10 mM final concentration) with various additives and the pH

was adjusted with concentrated NaOH. Stock solutions of $FeSO_4$, GSH, DMSO, Catalase, glycine, methionine and tryptophan were first prepared in water, then added to the peroxymonophosphate solution at the proper ratio for the described final concentration. After standing for 1h at room temperature (22°C), the % HPO_5^{2-} remaining was determined by quantitative ^{31}P NMR (peak area) using a freshly made solution of HPO_5^{2-} in 100 mM $HClO_4$ as a control. Quantitative ^{31}P NMR spectra were collected with a Bruker ARX-250 instrument equipped with a 5mm QMP probe utilizing the following parameters: Inverse gated acquisition-30° pulse, 12.5 s. relaxation delay (D1), 1.47 s. acquisition, 16 scan average. These are similar to previously reported parameters for quantitative analysis of phosphoryl containing molecules.[29] Values shown in Figure 2.4 are averages of three independent experiments and the error bars depict the standard error in the measurements.

References

1. Majeti, R.; Weiss, A., Regulatory mechanisms for receptor protein tyrosine phosphatases. *Chem. Rev.* **2001,** *101*, 2441-2448.

2. Gshwind, A.; Fischer, O. M.; Ullrich, A., The discovery of tyrosine kinases: targets for cancer therapy. *Nature Rev. Cancer* **2004,** *4*, 361-370.

3. Denu, J. M.; Tanner, K. G., Specific and Reversible Inactivation of Protein Tyrosine Phosphatases by Hydrogen Peroxide: Evidence for a Sulfenic Acid Intermediate and Implications for Redox Regulation. *Biochemistry* **1998,** *37* (16), 5633-5642.

4. Mahadev, K.; Zilbering, A.; Zhu, L.; Goldstein, B. J., Insulin-stimulated Hydrogen Peroxide Reversibly Inhibits Protein-tyrosine Phosphatase 1B in Vivo and Enhances the Early Insulin Action Cascade. *J. Biol. Chem.* **2001,** *276* (24), 21938-21942.

5. Tonks, N. K., Redox Redux: Revisiting PTPs and the Control of Cell Signaling. *Cell* **2005,** *121* (5), 667-670.

6. Rhee, S. G., H_2O_2, a necessary evil for cell signaling. *Science* **2006,** *312* (June 30), 1882-1883.

7. Mahadev, K.; Motoshima, H.; Wu, X.; Ruddy, J. M.; Arnold, R. S.; Cheng, G.; Lambeth, J. D.; Goldstein, B. J., The NAD(P)H oxidase homolog Nox4 modulates insulin-stimulated generation of H_2O_2 and plays an integral role in insulin signal transduction. *Mol. Cell Biol.* **2004,** *24* (5), 1844-1854.

8. Ross, S. H.; Lindsay, Y.; Safrany, S. T.; Lorenzo, O.; Villa, F.; Toth, R.; Clague, M. J.; Downes, C. P.; Leslie, N. R., Differential redox regulation within the PTP superfamily. *Cellular Signalling* **2007,** *19* (7), 1521-1530.

9. Johnson, T. O.; Ermolieff, J.; Jirousek, M. R., Protein tyrosine phosphatase 1B inhibitors for diabetes. *Nature Reviews Drug Discovery* **2002,** *1* (9), 696.

10. Tian Zhu, H.-m. C., John F. Kadla, A new method for the preparation of peroxymonophosphoric acid. *Can. J. Chem.* **2003,** *81* (2), 156-160.

11. Griffith, W. P.; Powell, R. D.; Skapski, A. C., Alkali metal and ammonium peroxodiphosphates: Preparation, vibrational and 31P NMR spectra, and the X-ray crystal structure of ammonium peroxodiphosphate dihydrate (NH4)4[P2O8]∑2H2O. *Polyhedron* **1988,** *7* (14), 1305-1310.

12. Battaglia, C. J.; Edwards, J. O., The Dissociation Constants and the Kinetics of Hydrolysis of Peroxymonophosphoric Acid. *Inorg. Chem.* **1965,** *4* (4), 552-558.

13. Crutchfield, M. M.; Edwards, J. O., The Acidity and Complexes of Peroxydiphosphoric Acid. *J. Am. Chem. Soc.* **1960,** *82* (14), 3533-3537.

14. Lerman, L. S., Structural considerations in the interaction of DNA and acridines. *J. Mol. Biol.* **1961,** *3*, 18-30.

15. Zhao, G.; Chasteen, N. D., Oxidation of Good's buffers by hydrogen peroxide. *Analytical Biochemistry* **2006,** *349* (2), 262-267.

16. Meister, A.; Anderson, M. E., Glutathione. *Ann. Rev. Biochem.* **1983,** *52*, 711-760.

17. Chasseaud, L. F., The role of glutathione and glutathione *S*-transferase in the metabolism of chemical carcinogens and other electrophilic agents. *Adv. Cancer Res.* **1979,** ***29***, 175-274.

18. LaButti, J. N.; Chowdhury, G.; Reilly, T. J.; Gates, K. S., Redox Regulation of Protein Tyrosine Phosphatase 1B by Peroxymonophosphate (=O3POOH). *J. Am. Chem. Soc.* **2007,** *129* (17), 5320-5321.

19. Halliwell, B., An attempt to demonstrate a reaction between superoxide and hydrogen peroxide. *FEBS Lett.* **1976,** *72* (1), 8-10.

20. Halliwell, B.; Gutteridge, J. M. C., Role of free radicals and catalytic metal ions in human disease: an overview. *Methods Enzymol.* **1990,** *186*, 1-85.

21. Winterbourn, C. C.; Metodiewa, D., Reactivity of biologically important thiol compounds with superoxide and hydrogen peroxide. *Free Radical Biology and Medicine* **1999,** *27* (3-4), 322-328.

22. Richardson, D. E.; Regino, C. A. S.; Yao, H.; Johnson, J. V., Methionine oxidation by peroxymonocarbonate, a reactive oxygen species formed from CO2/bicarbonate and hydrogen peroxide. *Free Radical Biology and Medicine* **2003,** *35* (12), 1538-1550.

23. Thenraja, D.; Subramaniam, P.; Srinivasan, C., Kinetics and mechanism of oxygenation of aromatic sulfides and arylmercaptoacetic acids by peroxomonophosphoric acid. *Tetrahedron* **2002,** *58* (21), 4283-4290.

24. Suthakaran, R.; Rajagopal, S.; Srinivasan, C., Mechanism of oxygenation of aryl methyl and diaryl sulphoxides by peroxomonophosphoric acid. *Tetrahedron* **2001,** *57* (7), 1369-1374.

25. Raed Ghanem, C. C., Maria A. Munoz, Pilar Guardado, Manuel Balon, Oxidation of 2,3-dimehylindole by peroxyphosphates. *Journal of the Chemical Society, Perkin Transactions 2* **1996,** (10), 2197-2202.

26. Fernando Secco, M. V., Mechanisms of peroxide reactions: kinetics of reduction of peroxo-monosulphuric and peroxomonophosphoric acids by iodide ion. *Journal of the Chemical Society, Dalton Transactions* **1976**, 1410-1414.

27. Hara, I.; Ichise, N.; Kojima, K.; Kondo, H.; Ohgiya, S.; Matsuyama, H.; Yumoto, I., Relationship between the Size of the Bottleneck 15 Å from Iron in the Main Channel and the Reactivity of Catalase Corresponding to the Molecular Size of Substrates. *Biochemistry* **2007,** *46* (1), 11-22.

28. Pichorner, H.; Jessner, G.; Ebermann, R., tBOOH Acts as a Suicide Substrate for Catalase. *Archives of Biochemistry and Biophysics* **1993,** *300* (1), 258-264.

29. Lerman, C. L.; Cohn, M., 31P NMR quantitation of the displacement of equilibria of arginine, creatine, pyruvate, and 3-P-glycerate kinase reactions by substitution of sulfur for oxygen in the beta phosphate of ATP. *J. Biol. Chem.* **1980,** *255* (18), 8756-8760.

Chapter 3

Inactivation of PTPs by Peroxymonophosphate

3.1 Introduction and Objectives

Having successfully synthesized and characterized peroxymonophosphate, our focus turned toward elucidating its effects on protein tyrosine phosphatase enzymatic activity. Our goal was to evaluate whether or not peroxymonophosphate possessed the properties necessary for an intracellular signaling agent. These properties include: rapid active site directed inactivation (rather than inhibition) by low concentrations of agent that is reversible by addition of thiol.

The rationale for this experimentation was introduced in Chapter 1. To recap, if one considers that the expected intracellular concentrations of the known signaling agent hydrogen peroxide are in the high nanomolar to low micromolar range[1], and that measured PTP inactivation kinetics with hydrogen peroxide are slow[2], the time in which PTPs could be inactivated is not consistent with observed time frames for the resulting physiologic effects. For example, when cells are stimulated with insulin, enhanced glucose uptake occurs within 5 minutes, the $t_{½}$ of PTP1B exposed to a 1 μM steady state

concentration of H_2O_2 would be approximately 10-20 h.[3, 4] A possible explanation for this conundrum is that H_2O_2 producing Nox enzymes may be located proximal to PTPs within the cell. This would lead to more rapid PTP inactivation through co-localized areas of high H_2O_2 concentration. Our alternative hypothesis is that H_2O_2 could be converted, either enzymatically or spontaneously, into more potent oxidizing agents. Toward this end, we envisioned peroxymonophosphate as an exceptional PTP inactivator in which noncovalent association of the phosphoryl group with the highly conserved phosphate binding pocket found in the active site of all PTPs would serve to guide the peroxy moiety into position for efficient reaction with the catalytic cysteine residue (Figure 3.1).

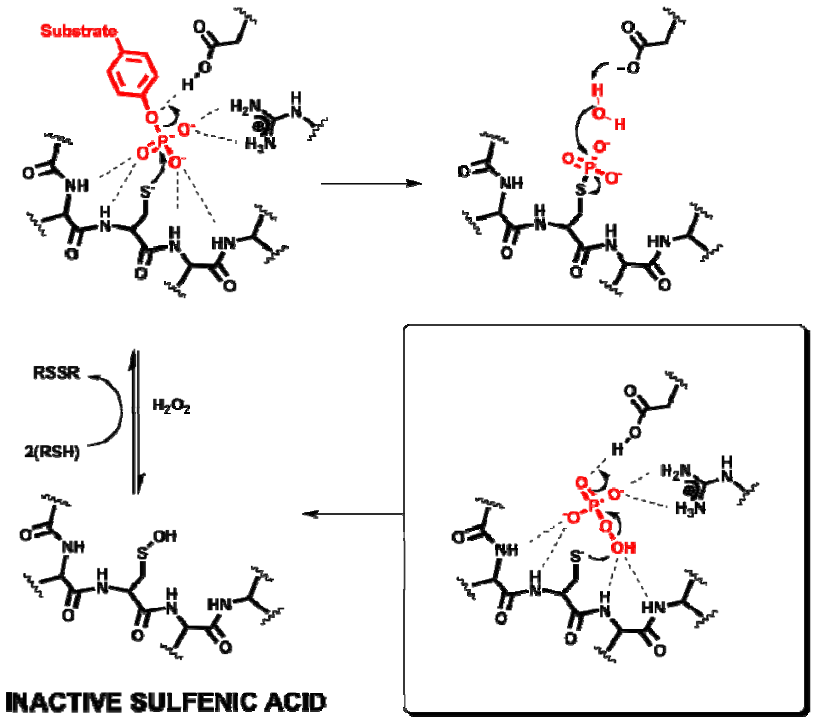

Scheme 3.1 A generalized PTP active site showing substrate interactions with the phosphate binding pocket, oxidation by hydrogen peroxide, recovery of enzyme activity by thiols and the hypothesized mechanism of oxidative inactivation by peroxymonophosphate.

Specifically, we wanted to compare the ability of peroxymonophosphate to inactivate a protein tyrosine phosphatase with that of hydrogen peroxide. In the enzymatic studies described here, we employed the catalytic subunit of human PTP1B (a.a. 1-322) as an archetypal member of the PTP family of enzymes.

3.2 Expression and Purification of PTP1B

PTP1B was one of the first cysteine-dependent protein tyrosine phosphatases isolated, having been characterized in the late 1980's and early 1990's.[5] As such, it is one of the more well-characterized and extensively studied PTPs. In synchronicity with our goals of studying PTP redox regulation, Tanner and Denu reported in 1998 that PTP1B could be reversibly inactivated by hydrogen peroxide.[2] Furthermore, PTP1B had been identified as an anti-diabetic pharmaceutical drug target. Together, these attributes made the enzyme a good candidate for the study of PTP redox-regulation.

(1)MEMEKEFEQI	DKSGSWAAIY	QDIRHEASDF	PCRVAKLPKN	KNRNRYRDVS
PFDHSRIKLH	QEDNDYINAS	LIKMEEAQRS	YILTQGPLPN	TCGHFWEMVW
EQKSRGVVML	NRVMEKGSLK	CAQYWPQKEE	KEMIFEDTNL	KLTLISEDIK
SYYTVRQLEL	ENLTTQETRE	ILHFHYTTWP	DFGVPESPAS	FLNFLFKVRE
SGSLSPEHGP	VVVHCSAGIG	RSGTFCLADT	CLLLMDKRKD	PSSVDIKKVL
LEMRKFRMGL	IQTADQLRFS	YLAVIEGAKF	IMGDSSVQDQ	WKELSHEDLE
PPPEHIPPPP	RPPKRILEPH	NG (322)		

Table 3.1 Amino acid sequence of the PTP1B catalytic subunit employed in these studies. The conserved PTP active site motif of $HCX_5R(S/T)$ is highlighted in red.

While the native human PTP1B gene product is ~ 50 kDa in mass, upon isolation from Escherichia coli it was observed to rapidly degrade to a product of approximately 40 kDa mass.[6] Neither addition of protease inhibitors nor use of protease deficient expression strains halted degradation. In addition, human PTP1B purified from placental tissues was found to have a molecular weight of 37 kDa. Finally, a truncated version of PTP1B has improved solubility over the native version. Taken together, these are the reasons a majority of published experiments carried out with purified PTP1B utilize what is known as the "catalytic subunit" of the enzyme, which corresponds to amino acids 1-322 and has a monoisotopic mass of 37,345.66 Da (Table 3.1). We were fortunate to obtain a clone of the PTP1B catalytic subunit as a generous gift from the lab of Nicholas K. Tonks at the Cold Spring Harbor Laboratory New York.

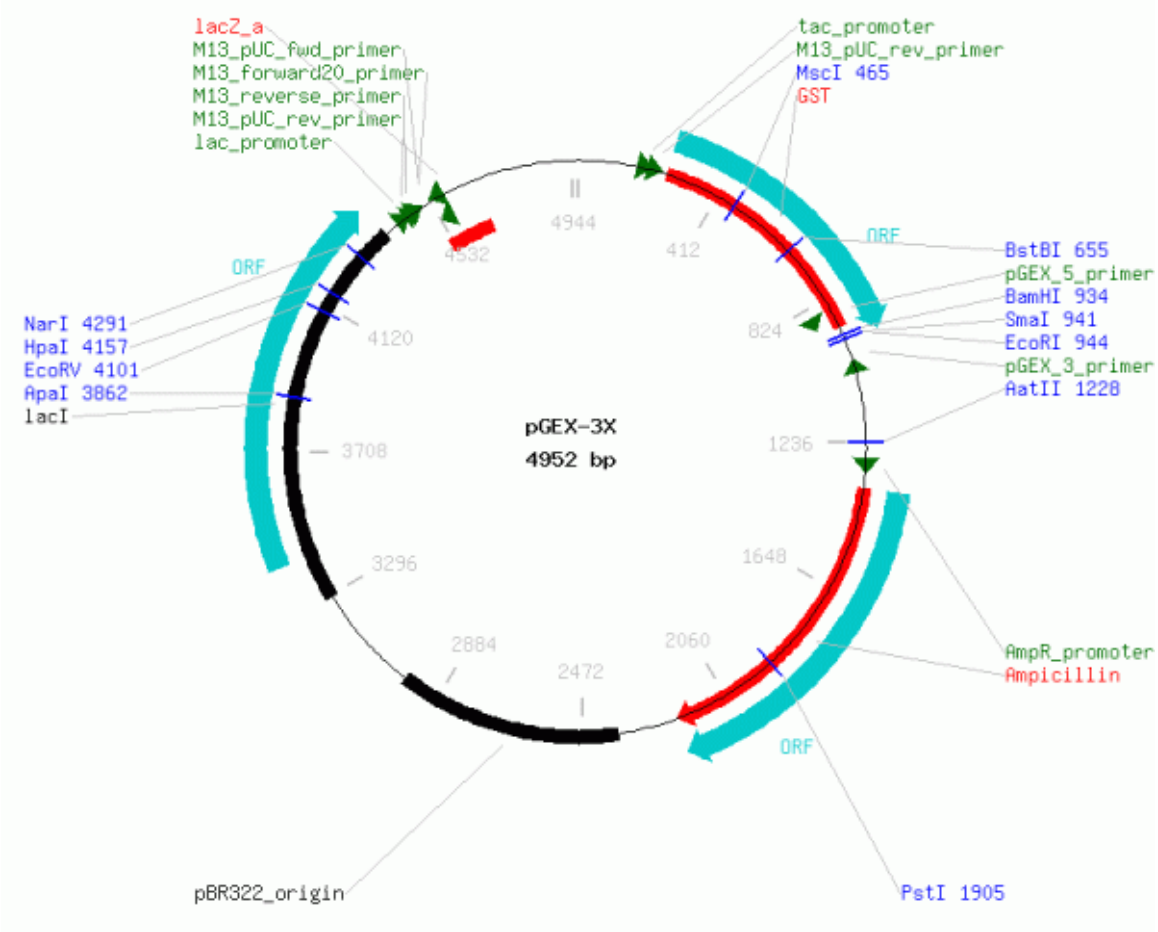

Figure 3.1 Map of pGEX-3X plasmid used to create the pRP261 vector.

We received the DNA coding for PTP1B amino acids 1-322 as a GST-fusion insert in the expression vector pRP261, which was a derivative of the pGEx-3x vector (Figure 3.1). The pGEx-3x vector was designed to express a protein of interest fused with glutathione-S-transferase (GST). Creating GST fusion clones of desired proteins is a common strategy for obtaining pure material with relatively little effort. Briefly, the GST domain has a high affinity for glutathione. After over-expression of the fusion protein in a bacterial system, raw lysate is passed over an affinity column in which glutathione is immobilized on a solid support. GST fusion product is then eluted from the column with increasing concentrations of glutathione. The pRP261 vector was

created by inserting a poly-linker sequence into pGEX-3X immediately after the GST fusion domain. This poly-linker sequence contained several extra restriction endonuclease sites, and a Factor Xa cleavage site for the translated GST fusion protein. The cDNA clone of truncated PTP1B was treated with NcoI/XbaI, and inserted into pRP261 treated with NcoI and SpeI to create the pRP-37k-1B expression vector. With the added poly-linker, the GST domain of purified PTP1B-GST fusion protein could be removed after expression and purification by treatment with the protease Factor Xa.

Gates Lab student Goutham Chowdhury performed the initial purification experiments with the PTP1B/GST fusion protein. Expression of the fusion protein in E. coli was apparently very good, as judged by SDS/PAGE. Purification of protein from lysate went smoothly and yielded a 66 kDa protein of good purity. Unfortunately, repeated attempts at cleaving the GST tag from PTP1B with Factor Xa were unsuccessful. We were reluctant to embark on studies designed to assess PTP1B inactivation kinetics with a fusion protein that may alter our results, so the decision was made to construct a new expression vector without the GST tag.

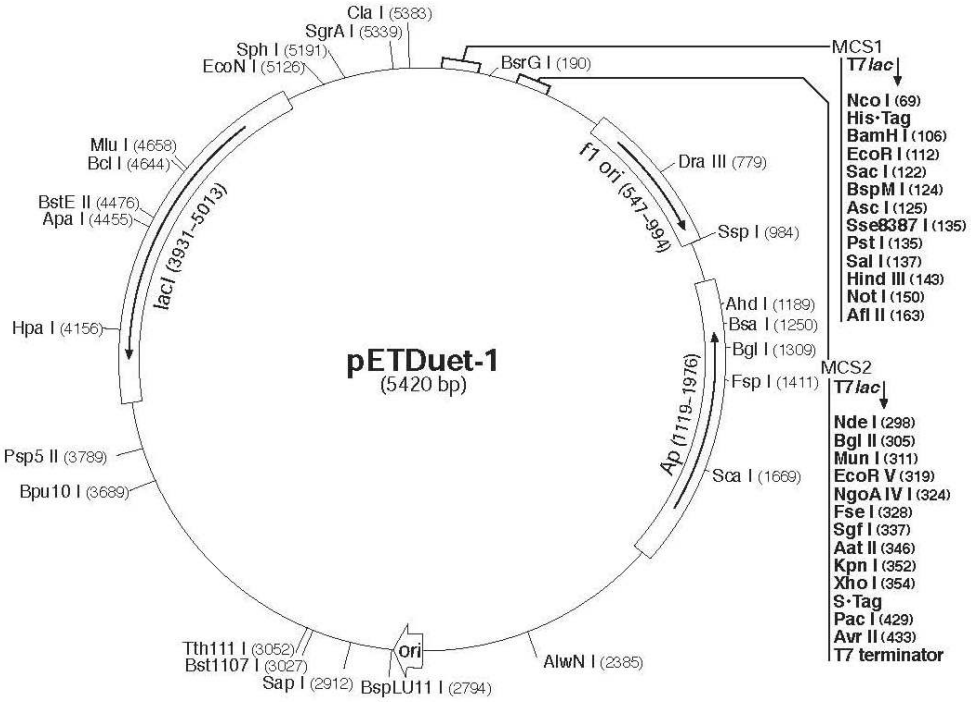

Figure 3.2 Map of the pETDuet-1 vector that was used to express the PTP1B 37 kDa catalytic subunit.

The PTP1B-37kDa domain was excised from the pRP-37k-1B vector with *Eco*R1 and *Nco*1. This liberated a ~ 1 kB DNA fragment was then ligated into similarly digested pETDuet-1 expression vector (Figure 3.2) The rationale for using pETDuet-1 was simple: this particular vector had matching *Eco*RI and *Nco*I restriction sites for the PTP1B insert. Once the PTP1B-37kDa expression vector (without the GST tag) was created, a new clone was selected for expression in Tuner DE3 p-lac I cells. We refer to the 37 kDa product of this system as simply "PTP1B". The expression and purification of the new PTP1B clone was straightforward and followed the protocol described by Puius and

colleagues.[7] This preparation yielded approximately 15 mg of ~95% pure PTP1B with a 3 L bacterial culture (Figure 3.3).

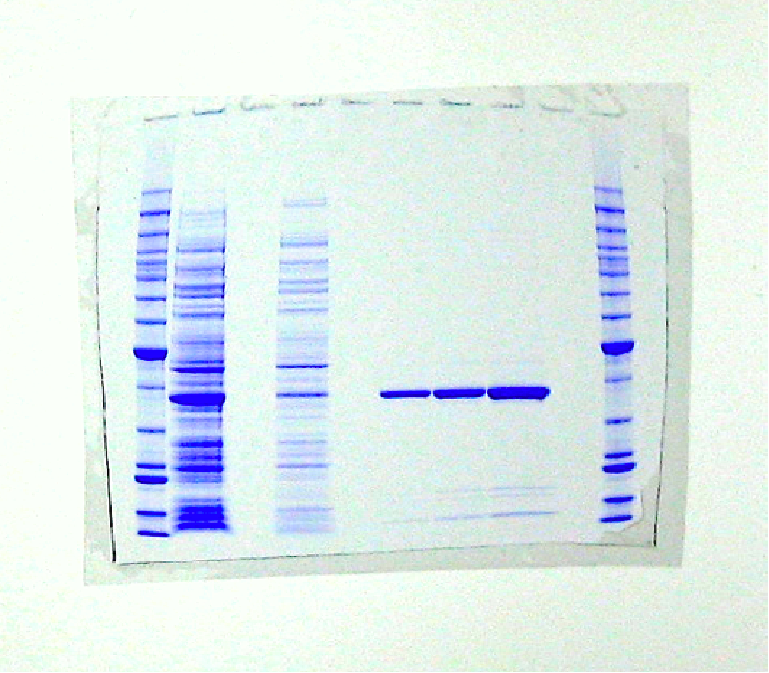

Figure 3.3 SDS-PAGE analysis of a PTP1B protein preparation. Lanes 1,10 = standard. Lane 2 = cell lysate. Lane 4 = column flow through. Lane 6,7,8 = 1, 2, 4 μg of PTP1B.

3.3 Preparation of PTP1B For Inactivation Assays (RSH removal, auto-oxidation chemistry)

PTPs in solution, if not carefully treated, will within minutes lose their catalytic activity even without addition of an oxidizing agent. This is due to the fact that the PTP1B active site cysteine thiol exists primarily in the charged, anionic state it is highly susceptible to auto oxidation. Autooxidation of the active site cysteine thiolate of PTP1B would, naturally, yield inactive enzyme. The mechanism of this reaction is not intuitive, but has been investigated and reported by Misra and colleagues. [8] It is often assumed (incorrectly) that thiolate anions react directly with oxygen gas dissolved in solution to

yield sulfenic acids. The parallel spin states of the unpaired electrons in diradical triplet oxygen, however, do not match with the paired, opposing spin states of the thiolate anion free electrons. Such a reaction, under physiologic-like conditions, would occur very slowly, if at all. In order for oxygen to react with thiolates in solution, either an unpaired electron has to be "moved" to an excited state by irradiation with UV light, or a "redox carrier", such as a transition metal, must be employed. Due to the fact that high intensity UV light is destructive to most components of cellular systems, the logical causative agent for autooxidation of thiolate anions in solution would be dissolved metals. In essence, then, reaction of thiolate anions with molecular oxygen in solution is mediated by transition metals such as iron and copper (Scheme 3.2).

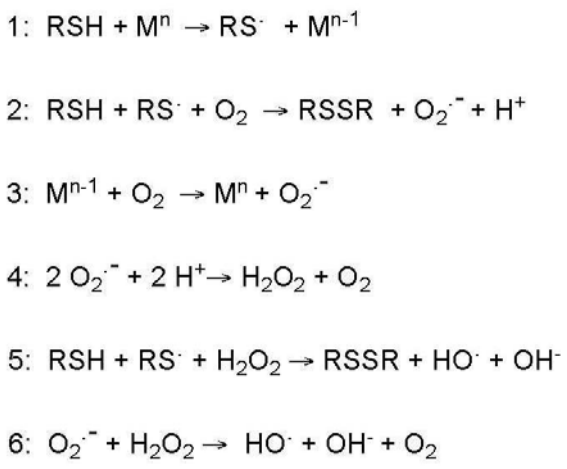

Scheme 3.2 The mechanisms of metal-mediated thiolate autooxidation, adapted from reference 4.

To prevent and/or mitigate oxidation, purified enzyme is stored at -80^{o}C in the presence of metal chelators (either ethylenediaminetetracetic acid or diethylenetriaminepentaacetic acid) and small molecule thiols such as dithiothreitol or B-mercaptoethanol (~1 mM). In order to conduct experiments designed to observe oxidative inactivation of the enzyme by various reactive oxygen species, however, thiol additives must be removed from the enzyme stock solutions. If this is not accomplished, added reactive oxygen species could be quenched by the presence of these thiols, and PTPs active site cysteine sulfenic acids would be readily converted back to the catalytically active cystine thiolate form.

Perhaps the most common method for removing unwanted small molecule components from protein solutions is dialysis. Removal of thiol additives from PTP stock solutions via dialysis presents a challenge in several ways. The extended time required for proper dialysis (~24 h) results in loss of enzyme activity through auto-oxidation. A viable, but cumbersome solution to loss of enzyme activity during dialysis through autooxidation is to perform dialysis in an anaerobic chamber. Another potential issue is that complete recovery of precious enzyme dialysate from dialysis apparatus is difficult, if not impossible, when dealing with the low volumes of enzyme solutions that are typically used during experimentation (10-100 μL of solution at ~ 15 μM).

We felt that the most efficient way, in both in time and resources, to remove small molecule thiols from enzyme stock solutions is using buffer exchange columns. These are small plastic columns filled with either common size-exclusion resin such as Sephadex G-25, or proprietary resins. The volume of gel depends on the size of the column and the size of the column is related to the volume of enzyme solution that can be

used. We typically used Pierce Zeba desalting columns filled with 0.5 mL of their proprietary resin. These columns were rated for use with 10-110 μL of enzyme solution.

An important note for using these columns is that each pass of enzyme solution through a buffer exchange column removes approximately 90-95% of thiol. If only one column is used there is still significant (i.e.: micromolar) thiol remaining, when compared to the concentration of enzyme being used (~ 15 μM). Figure 3.4 shows that to reduce the concentration of thiol to nanomolar levels, three sequential buffer exchange columns had to be employed. With this methodology, a "thiol-free" enzyme solution could be created that proved useful for investigating oxidative reactions of the active site catalytic cysteine residue for several hours before noticeable loss (> 10%) of activity was observed.

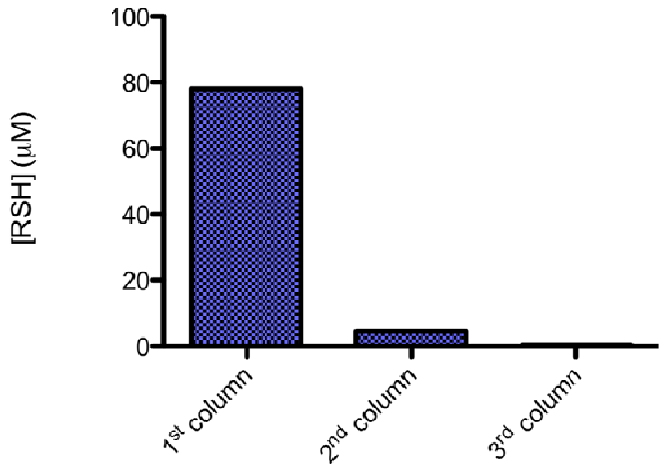

Figure 3.4 Residual thiol present in a 0.1 mL volume of buffer containing 1 mM dithiothreitol after treatment with sequential Pierce Zeba 0.5 mL buffer exchange columns. The concentration of thiol after the third column was approximately 700 nanomolar.

An additional, important component of the thiol removal process is a non-ionic detergent. These molecules are necessary to prevent non-specific adsorption of enzyme to the walls of plastic and glass containers. It is especially important when diluting PTP stock solutions to low-micromolar or nanomolar concentrations. The use of non-ionic detergents is a double-edged sword of sorts. While they prevent loss of enzyme activity from non-specific adsorption, the presence of non-ionic detergents can also lead to destruction of PTP catalytic activity. These detergents invariably contain an ether moiety which is susceptible to oxidation by solvated oxygen, the product of which is peroxides that oxidatively inactivate the enzyme (Scheme 3.3).[9, 10] To prevent this from occurring, only detergents specifically noted to be "low peroxide" should be used. They are typically packed in sealed glass ampules under inert gas. Once opened, auto oxidation begins. While the rates of detergent-peroxide formation were not investigated, we typically used a freshly opened vial of Tween-80 for a few weeks before there was noticeable loss of enzyme activity.

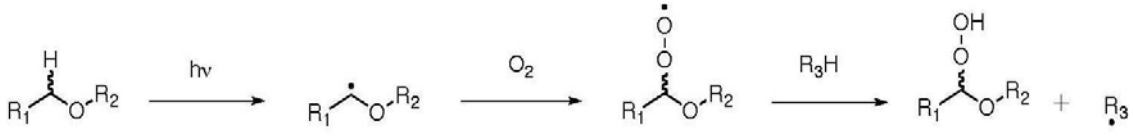

Scheme 3.3 Generation of peroxides from autooxidation of ether-containing non-ionic detergents.

3.4 PTP1B Inactivation Assays

Typically, assays for measuring the kinetics of time-dependent enzyme inactivation are performed by incubating the native enzyme with various concentrations of inactivator in the absence of substrate under pseudo-first order conditions (inactivator concentration is >10 x enzyme concentration).[11] At certain times, aliquots are removed to assess remaining enzyme activity. The aliquots of the enzyme-inactivator mixture are added to a solution containing a suitable concentration of substrate that will saturate the enzyme active site (typically 10 x K_m). The enzyme-inactivator aliquots must be diluted at least by a factor of 50 when added to the substrate solution to effectively stop the inactivation reaction. The remaining enzymatic activity at each time point is then plotted as a function of time, and the apparent rate of inactivation is determined by the slope of each line. These rates are then replotted as a function of inactivator concentration, the slope of which gives the apparent second order rate.

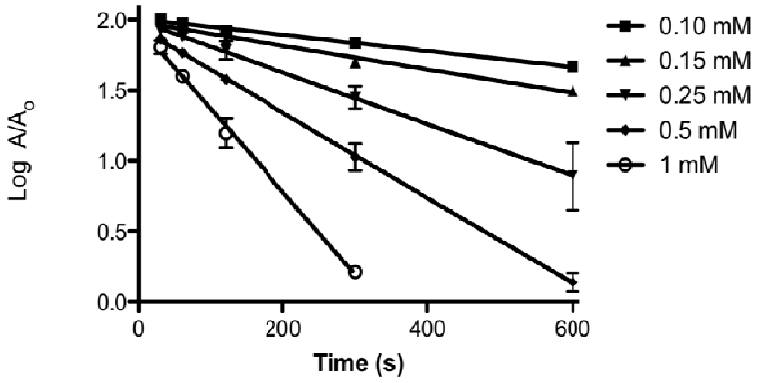

Figure 3.5 Time-dependent inactivation of PTP1B by various concentrations of hydrogen peroxide.

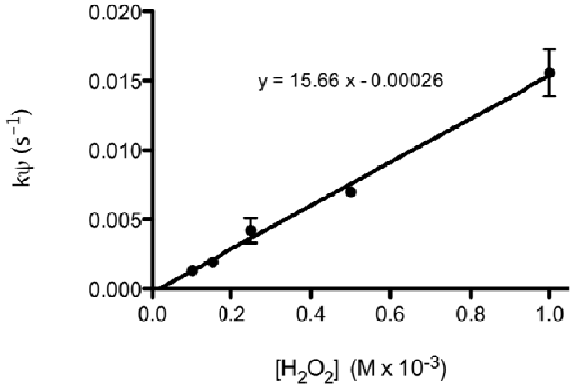

Figure 3.6 Replot of pseudo-first order rates obtained by treating PTP1B with hydrogen peroxide in the absence of substrate. The slope of the line gives the apparent second order rate of 15.66 +/- 0.67 $M^{-1}s^{-1}$.

We employed this type of "time-point" assay (as we called it) to determine the apparent second order rate of PTP1B inactivation by hydrogen peroxide. This measurement would serve as a "benchmark" for our upcoming experiments with peroxymonophosphate, as such numbers had already been reported.[2, 12] Results from the assay are shown in Figures 3.5 and 3.6. Hydrogen peroxide was observed to inactivate PTP1B in a time-dependent manner with an apparent second order rate of 15.7 $M^{-1}s^{-1}$. This is in close agreement with 9.1 $M^{-1}s^{-1}$ as published by Denu. Of worthy note is that replotting the resulting apparent pseudo-first-order rates yields a line that has a y-intercept of approximately zero. This is consistent with a bimolecular reaction in which H_2O_2 does not possess affinity for the PTP1B active site and inactivates the enzyme via a simple second-order reaction process.

It became clear when we attempted to duplicate this experiment with peroxymonophosphate that a different method of data generation would be needed. The time point assay relies on measurement of inactivation rates under pseudo-first-order

conditions. For example, data with hydrogen peroxide was generated using ~ 50 nM enzyme and hydrogen peroxide concentrations that ranged from 0.1 to 1.0 mM. Enzyme activity was assayed at 30 s, 1, 2, 5 and 10 minutes. We found that the rapid rate of PTP1B inactivation by peroxymonophosphate was such that even at nanomolar concentrations all enzyme activity was lost within 20 seconds.

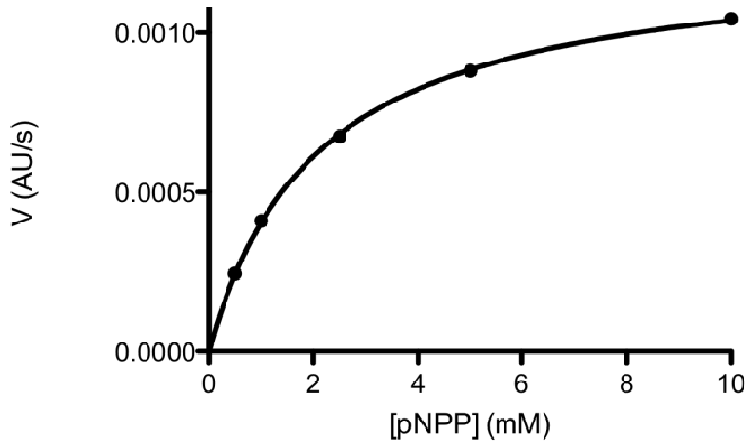

Figure 3.7 Calculation of PTP1B K_m with *p*-nitrophenylphosphate as substrate. K_m is calculated by fitting the data to the Michaeles equation $Y=V_{max}*X/(K_m+X)$ and was found to be 2.11 mM.

Introducing substrate to the PTP1B-peroxymonophosphate mixture is a viable way to slow the reaction.[13, 14] Substrate, in a continuous assay, occupies the enzyme active site for an amount of time, and thereby limits access of the oxidizing agent. Analysis of apparent inactivation rates generated in the presence of substrate requires different mathematical treatment than rates generated without. Due to the fact that the apparent rates of inactivation are reduced, it becomes necessary to apply a correction factor. This correction factor is determined by carefully measuring the substrate K_m and

using this value to determine the actual rates of inactivation. The K_m for PTP1B with *p*-nitrophenylphosphate was determined to be 2.11 mM (Figure 3.7). Analysis also requires making some assumptions about the nature of non-covalent interactions between the protein and the inactivator. For these studies, we assumed that H_2O_2 does not possess affinity for the enzyme active site and analyzed our data accordingly.

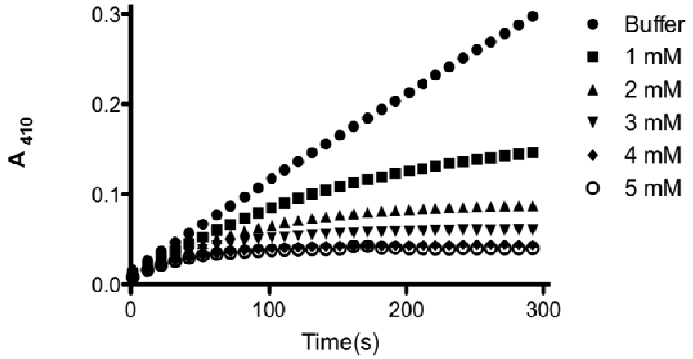

Figure 3.8 Time-dependent inactivation of PTP1B by hydrogen peroxide in the presence of 10 mM substrate. The apparent rate of enzyme inactivation was determined by fitting the data to equation (1).

The inactivator hydrogen peroxide was used as a positive control for analysis of the continuous assay, in a manner similar to the time point assay. This reactive oxygen species showed time-dependent inactivation of PTP1B in the presence of 10 mM substrate (Figure 3.8). These curves were fit with a least-squares method to the following equation given by Voet and colleagues to find the apparent rate of enzyme inactivation, k_{app}.[13, 14]

$$A_{410} = C - \frac{e^{\ln V_o - k_{app} t}}{k_{app}} \quad (1)$$

The equation shown above was used for the sole purpose of measuring the apparent rate of enzyme inactivation. There are many suitable exponential equations that could be used to fit the data. In our case, we chose equation 1 due to the fact that Voet was investigating the inactivation of an enzyme with a competitive inactivator, similar to what we were attempting to do with peroxymonophosphate and PTP1B.

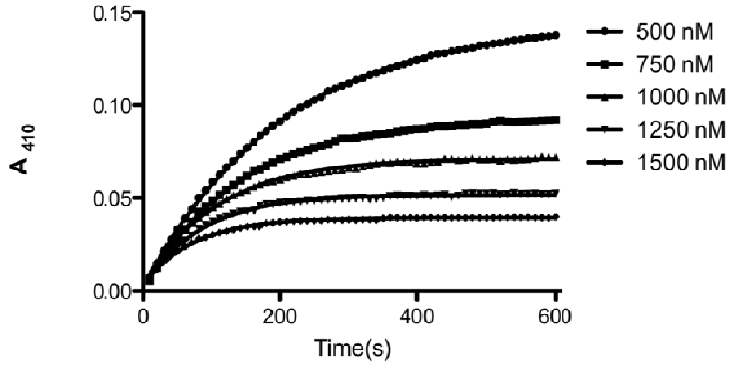

Figure 3.9 Time-dependent inactivation of PTP1B by peroxymonophosphate in the presence of 10 mM substrate (*p*NPP).

PTP1B was rapidly inactivated in a time-dependent manner by nanomolar concentrations of peroxymonophosphate (Figure 3.9). To broaden our understanding of this process, and demonstrate that the inactivation of PTP1B by peroxymonophosphate was not unique, we decided to explore inactivation of the PTP SHP-2. SHP-2, also

known as "Src homology 2 domain phosphatase", has also been identified as a non-receptor type phosphatase that is redox regulated *in vivo*.[15] SHP-2 was, like PTP1B, rapidly inactivated by nanomolar concentrations of peroxymonophospahte (Figure 3.10). Our next task was to determine the kinetic constants of the reactions through careful mathematical analysis of the enzyme inactivation apparent rates.

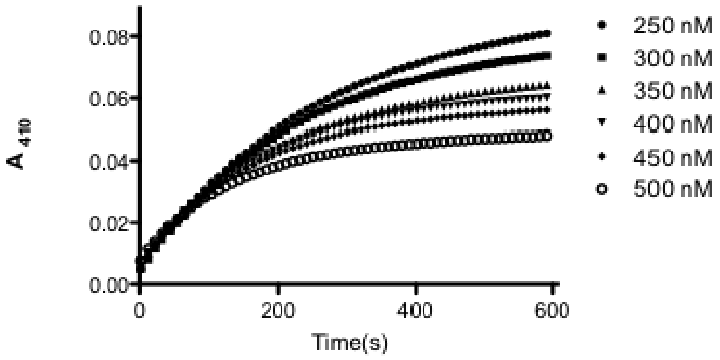

Figure 3.10 Time-dependent inactivation of SHP-2 by peroxymonophosphate in the presence of 10 mM substrate (*p*NPP).

Duranton published a method,[14] based on the work by Tian[16] to correct apparent rates of inactivation for the presence of substrate for a one-step (Scheme 3.4) and two step (Scheme 3.5) inactivation process using the equations (2) and (3) shown below, respectively:

$$k_{app} = \frac{k[I]}{(1+[S]/K_m)} \tag{2}$$

$$k_{app} = \frac{k_{inact}[I]}{[I]+K_I*_{(app)}} \tag{3}$$

where:

$$K_I*_{(app)} = K_I*(1+[S]/K_m)$$

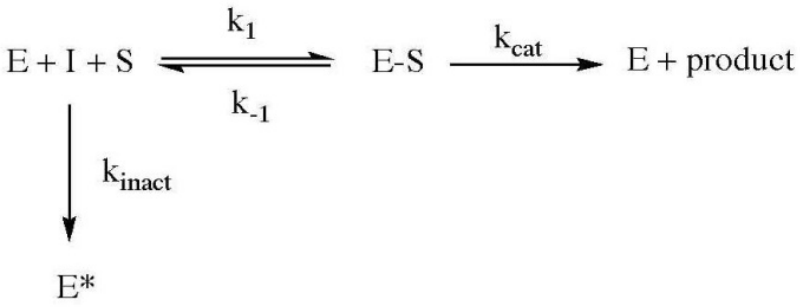

Scheme 3.4 The expected kinetic parameters for a one-step enzyme inactivation (no non-covalent pre-association). The reaction mixture contains enzyme, substrate and inactivator.

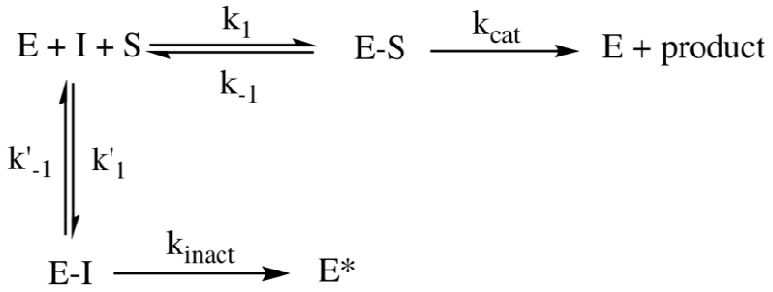

Scheme 3.5 The expected kinetic parameters for a two-step enzyme inactivation (with a non-covalent pre-association, K_I). The reaction mixture contains enzyme, substrate and inactivator.

Equation (2) and Scheme 3.4 have no terms to describe non-covalent affinity of the enzyme for inactivator (K_I). Conversely, equation (3) and Scheme 3.5 assume that non-covalent pre-association occurs. To distinguish between the two situations, i.e., one-step versus two-step, one must construct a plot of inhibitor concentration versus apparent inactivation rates and determine which equation the data fits best. Unfortunately, due to the rapid rate at which these enzymes were inactivated by peroxymonophosphate, we were not able to observe saturation of the reaction (Figures 3.11 and 3.12), thus we could not derive an apparent K_I from equation (3). The lack of observed saturation is not surprising, due to the fact that the measured K_m for inhibition of PTP1B (as well as most PTPs) by inorganic phosphate is in the tens of millimolar range. In fact, Duranton and his colleagues explicitly state that if inhibitor concentration is significantly lower than K_I, the reaction between an enzyme and inactivator that possesses non-covalent affinity for its active site will behave as if it were bimolecular and not show saturation.

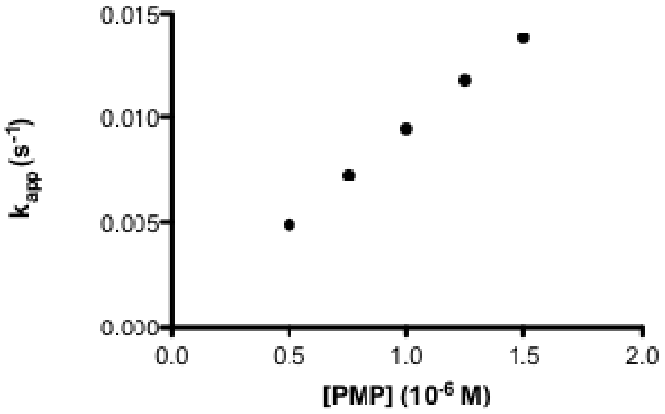

Figure 3.11 A plot of peroxymonophosphate concentration versus the apparent rate of PTP1B inactivation. These data are derived from Figure 3.10 and appears to describe a bimolecular reaction.

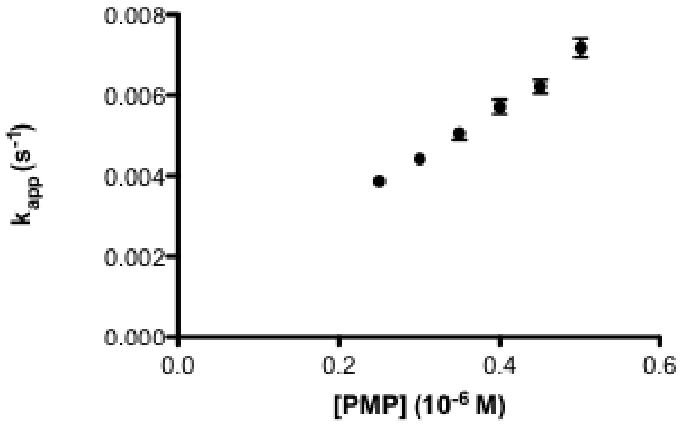

Figure 3.12 A plot of peroxymonophosphate concentration versus the apparent rate of SHP-2 inactivation. These data are derived from Figure 3.11, and appears to describe a bimolecular reaction.

Due to the fact that our assays used concentrations of peroxymonophosphate in the nanomolar range, rather than millimolar, we chose to simplify analysis and attempt to treat the data as if they were indeed describing a bimolecular reaction and utilized equation three. By moving k from the numerator of equation (3) one can plot the apparent rates of inactivation as a straight line by using the known values for substrate K_m, starting concentration of substrate and concentrations of inactivator:

$$k_{app} = k * \frac{[I]}{(1 + [S]/K_m)} \tag{4}$$

$$y = mx$$

From equation 4, data can be plotted as a straight line with the slope equal to the apparent second order rate of reaction between PTP1B and hydrogen peroxide. When plotting, x values are equal to the ratio of inhibitor concentration to the value of $(1+[S]/K_m)$. For this experiment, the apparent second order rate of PTP1B inactivation by hydrogen peroxide was calculated to be 29.8 +/- 1.4 M-1s-1 (Figure 3.13). This value is in agreement with previously published work and our own data (~ 10-20 $M^{-1}s^{-1}$).[12]

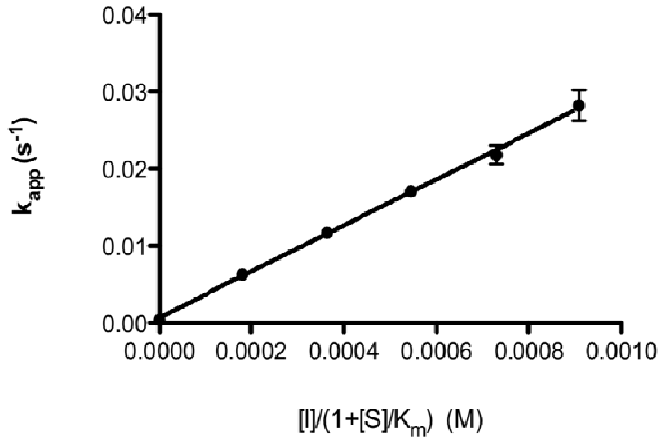

Figure 3.13 Analysis of the observed rates of PTP1B inactivation by hydrogen peroxide in the presence of 10 mM substrate. The slope of the line corresponds to the apparent second order rate of inactivation. This was measured to be 29.8 +/- 1.4 $M^{-1}s^{-1}$

When the data for inactivation of PTP1B by peroxymonophosphate is fit to equation 1 (Figure 3.9) and the resulting apparent rates plotted according to equation 4 (Figure 3.14) we find, indeed, that peroxymonophosphate is a superior inactivator of PTP1B with an apparent second order inactivation rate of 46710 +/- 940 $M^{-1}s^{-1}$. Thus, peroxymonophosphate is approximately 5000 times more potent than H_2O_2 as a PTP1B inactivator. Identical analysis of the rates of SHP-2 inactivation by peroxymonophosphate is shown in Figure 3.15 and gives a slightly lower apparent second order inactivation rate of 25,930 +/- 1435 $M^{-1}s^{-1}$. The dissociation constant for SHP-2 with *p*NPP was determined to be 5.47 mM (data not shown).

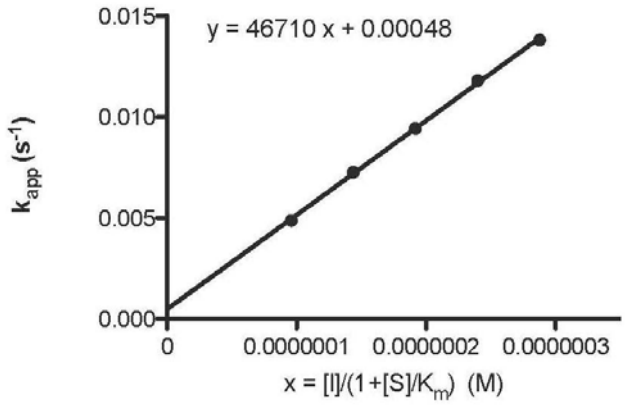

Figure 3.14 Replot of peroxymonophosphate inactivation data for PTP1B using the "Duranton" analysis. The apparent second order rate of inactivation is 46710 +/- 940 M-1s-1.

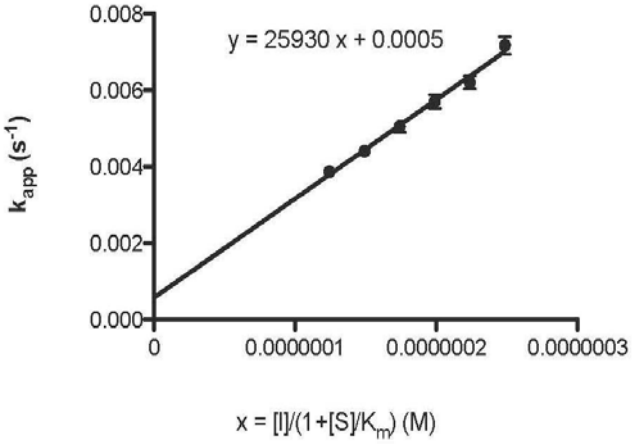

Figure 3.15 Replot of peroxymonophosphate inactivation data for SHP-2 using the "Duranton" analysis. The apparent second order rate of inactivation is 25930 +/- 1435 M-1s-1.

We thought it would be prudent to use another method to analyze our inactivation data in an attempt to measure the dissociation constant (K_I) and k_{inact} for PTP1B and SHP-2 inactivation by peroxymonophosphate. The method described by Voet appeared ideal for this task, and is based on the following equation:

$$\frac{1}{[I]} = \frac{k_{inact}(1-\alpha)}{K_I} * \frac{1}{k_{app}} - \frac{1-\alpha}{K_I} \qquad (4)$$

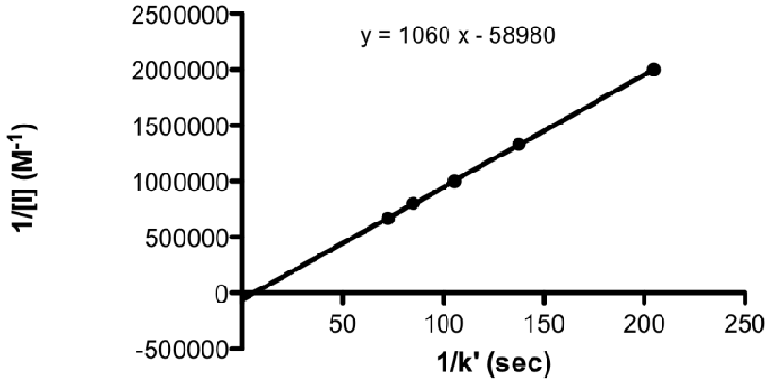

Figure 3.16 Replot of peroxymonophosphate inactivation data for PTP1B using the "Voet" analysis. The apparent second order rate of inactivation is 58,000 +/- 2200 $M^{-1}s^{-1}$.

Equation 4 expresses a straight line with a slope of $k_{inact}(1-\alpha)/K_I$ and a y-intercept of $-(1-\alpha)/K_I$. When 1/[I] is plotted against $1/k_{app}$ values for k_{inact} and K_I can be determined (Figure 3.16).

The apparent second order inactivation rate of PTP1B by peroxymonophosphate, using the Voet method of analysis was 58,000 +/- 2000 $M^{-1}s^{-1}$ (K_I = 3.4 +/- 1.6 x 10^{-6} M;

k_{inact} = 0.2 +/- 0.09 s^{-1}). Similarly, the apparent second order inactivation rate of SHP-2 by peroxymonophosphate using the Voet method was 48,050 +/- 2118 $M^{-1}s^{-1}$ (K_I = 7.6 +/- 2.7 x 10^{-7} M; k_{inact} = 0.037 +/- 0.002 s^{-1}). The negative y-intercept of the lines shown in Figures 3.16 and 3.17 suggest saturation kinetics are observed for the inactivation of PTP1B by peroxymonophosphate and that the phosphoryl group does, indeed, provide noncovalent binding affinity for the enzyme active site. Very large values of K_I essentially result in a y-intercept of zero (see equation 4). This could be interpreted as there being little or no non-covalent affinity for the active site. Complete lack of affinity for the active site renders equation 4 invalid.

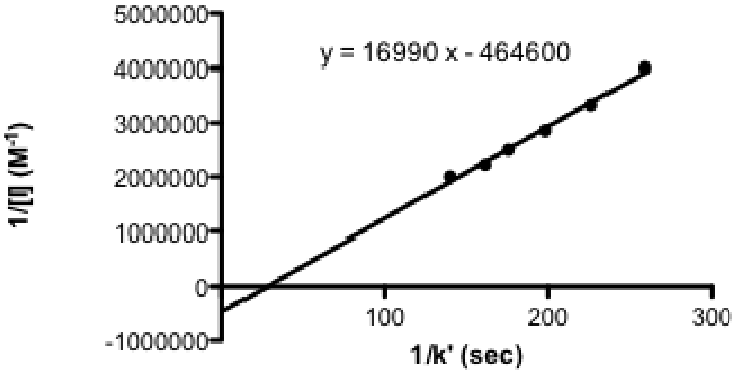

Figure 3.17 Replot of peroxymonophosphate inactivation data for SHP-2 using the "Voet" analysis. The apparent second order rate of inactivation is 48,050 +/- 2118 $M^{-1}s^{-1}$ (K_I = 800 +/- 270 nM, k_{inact} = 0.037 +/- 0.002 s^{-1}).

The affinity of the negatively charged phosphoryl moiety toward the PTP1B active site is likely derived from interactions with positive charges present in the phosphate-binding loop. In fact, competitive inhibitors with two net negative charges have been shown to have higher affinity than those with only one net negative charge. At physiologic pH (~7), peroxymonophosphate is expected to exist predominantly with two negative charges due to lower second pK_a values than phosphate (5.5 vs. 7.1).[17] Thus, one would expect peroxymonophosphate to have a higher apparent affinity for the active site than phosphate.

To provide more evidence to support our contention that peroxymonophosphate shows affinity for the PTP1B active site, we performed inactivation assays with increasing ionic strength. If the dual negative charges of peroxymonophosphate are conferring affinity, then increasing ionic strength would, in effect, neutralize those charges and reduce the apparent rate of inactivation. Figure 3.18 shows that, indeed, increasing ionic strength reduces the apparent rate of PTP1B inactivation by peroxymonophosphate. In contrast, increasing ionic strength did not decrease the rate of PTP1B inactivation by hydrogen peroxide (Figure 3.19). This is to be expected, for hydrogen peroxide and PTP1B were shown to react in a bimolecular fashion.

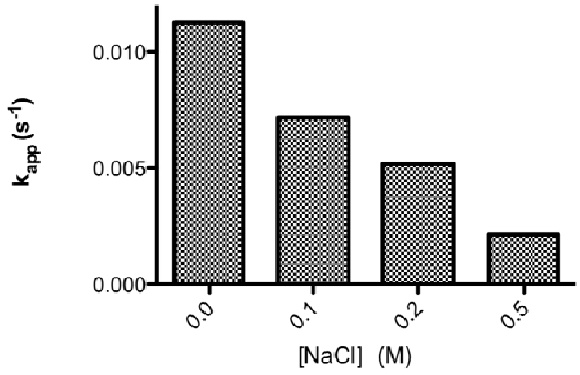

Figure 3.18 Increasing ionic strength decreases the rate of PTP1B inactivation by 1 μM peroxymonophosphate.

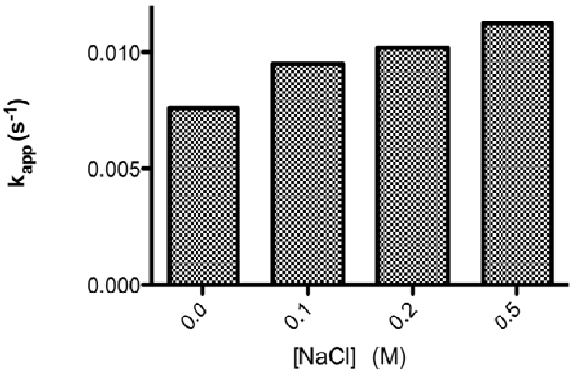

Figure 3.19 Increasing ionic strength does not decrease the rate of PTP1B inactivation by 1 mM H_2O_2

Consistent with a process that involves covalent modification of the enzyme, inactivation of PT1B by peroxymonophosphate is time-dependent and is not reversed by gel filtration of the inactivated enzyme. Furthermore, addition of the competitive PTP1B inhibitor phosphate[18] markedly slows inactivation by peroxymonophosphate, indicating that the process is active-site directed (Figure 3.20).

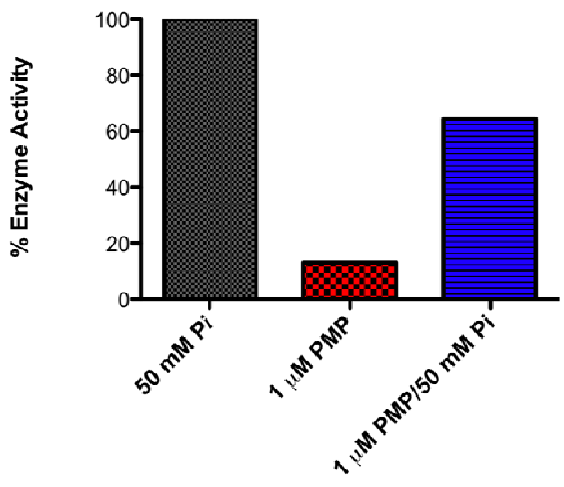

Figure 3.20 The competitive PTP inhibitor phosphate protects PTP1B from inactivation by peroxymonophosphate.

Significantly, inactivation of PTP1B by peroxymonophosphate (1 eq) is readily reversed by treatment of the inactivated enzyme with dithiothreitol (Figure 3.21). This indicates that peroxymonophosphate is able to inactivate PTP1B through the sulfenic oxidation state. It is interesting to note that if the reaction shown in Figure 3.21 is allowed to proceed for much longer than 120 s., recovery of PTP activity is compromised. This suggests that peroxymonophosphate is capable of "over oxidizing" the enzyme to sulfinic and sulfonic states. High-resolution tandem mass spectrometric analysis confirmed that treatment of the enzyme with excess inactivator (1 μM, 10 minutes) indeed causes conversion of the active site cysteine-215 to the sulfinic and sulfonic acid oxidation states (data not shown). Together these results suggest that low concentrations of peroxymonophosphate are able to reversibly inactivate PTPB via conversion of the active site cysteine residue to the sulfenic acid oxidation state.

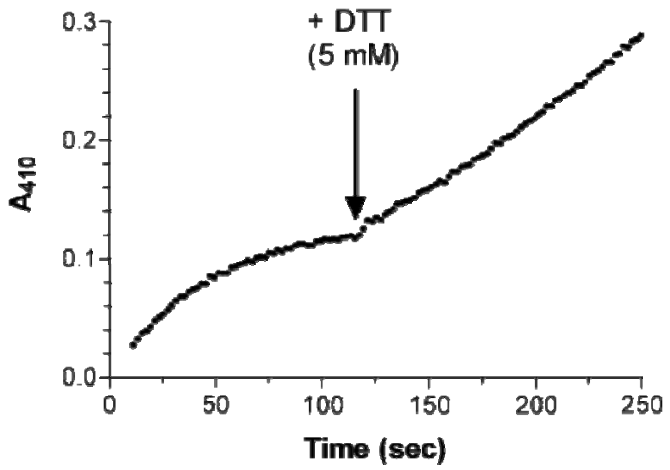

Figure 3.21 Addition of thiol at 120 s to a reaction containing PTP1B (~ 50 nM) and peroxymonophosphate (1 μM) reverses inactivation of the enzyme.

In principle, PTP1B could catalyze the hydrolysis of peroxymonophosphate to H_2O_2 and inorganic phosphate. Two lines of evidence, however, suggest that such an enzyme-catalyzed decomposition does not occur. First, addition of the H_2O_2-destroying enzyme catalase has no effect on the inactivation of PTP1B by peroxymonophosphate. Second, titration of the enzyme with peroxymonophosphate reveals a turnover number of approximately one (Figure 3.22) indicating that a single equivalent of peroxymonophosphate is sufficient to inactivate the enzyme.

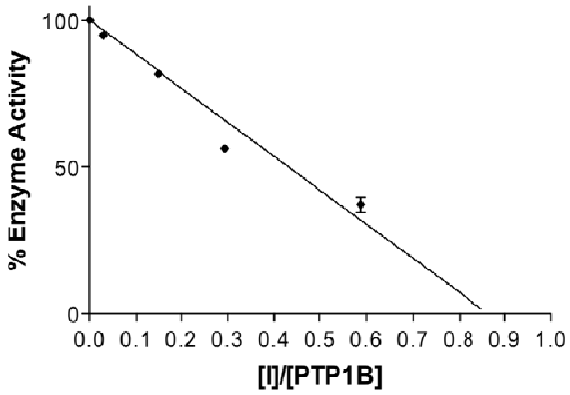

Figure 3.22 Determination of peroxymonophosphate partition ratio with PTP1B

Mammalian cells contain millimolar concentrations of thiols that have the potential to decompose peroxides.[19, 20] Therefore, we investigated whether peroxymonophosphate retains the ability to inactivate PTP1B in the presence of the biological thiol glutathione. We find that peroxymonophosphate (100 nM) causes substantial inactivation of PTP1B (21% +/- 3% remaining activity) within 5 minutes even in the presence of physiologically relevant concentrations of glutathione (1 mM). This result shows that peroxymonophosphate reacts selectively with the active site cysteine thiolate of PTP1B over solution thiols.

3.5 Discussion and Conclusions

In conclusion, we find that peroxymonophosphate is a potent oxidative inactivator of both protein tyrosine phosphatases PTP1B and SHP-2. In this regard, peroxymonophosphate is far more potent than H_2O_2. It appears that the potency of this agent is likely due to both its intrinsic reactivity as well as its affinity for the PTP1B active site. Increasing the ionic strength of the reaction medium decreased the rate of

time dependent PTP1B inactivation by peroxymonophospahte, while similar conditions did not reduce the rate of inactivation by hydrogen peroxide. This supports our hypothesis that the negative charges of the peroxymonophosphate phosphoryl moiety confer non-covalent affinity for the PTP1B active site.

As part of this study, we have generated rates of inactivation for peracetic acid and hydrogen peroxide, both oxidative agents that have no measurable affinity for the PTP1B active site. If one compares the apparent second order rates of PTP1B inactivation for peracetic acid, peroxymonophosphate and hydrogen peroxide, it is clear that peroxymonophosphate is much more potent than one would predict based on its leaving group pK_a (Figure 3.23). This, too, suggests that the phosphate moiety confers active site affinity to peroxymonophosphate.

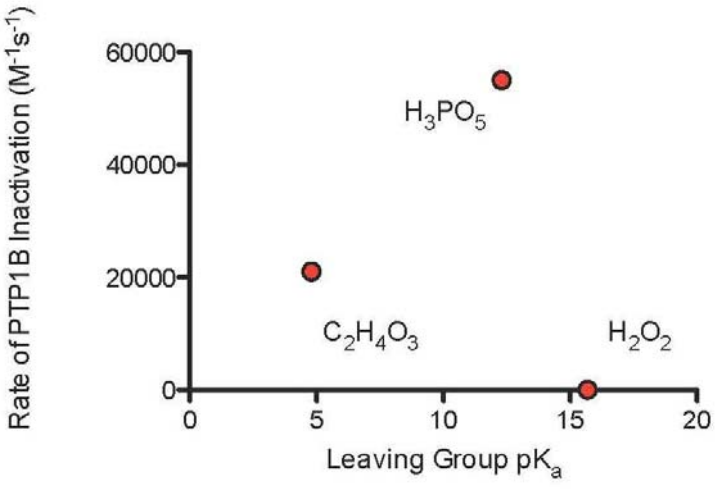

Figure 3.23 A plot of leaving group pK_a vs. the apparent rate of PTP1B inactivation for three compounds: Peracetic acid ($C_2H_4O_3$), peroxymonophosphate (H_3PO_5) and hydrogen peroxide (H_2O_2).

Inactivation of PTP1B by peroxymonophosphate, like that by H_2O_2, is readily reversed by treatment of the inactivated enzyme with thiol. A few other oxidative PTP inactivators are known[21] but none (other than the endogenous signaling agents H_2O_2 and nitric oxide) have been shown to yield thiol-reversible inactivation.[2, 22] Importantly, the inactivation of PTP1B by nanomolar concentrations of peroxymonophosphate proceeds effectively in the presence of physiologically-relevant concentrations of the biological thiol glutathione. Collectively, these properties may make peroxymonophosphate a useful tool for probing the role of cysteine-dependent PTPs in various signal transduction pathways. Finally, another interesting facet of peroxymonophosphate is that this molecule could be biologically accessible via phosphorylation of H_2O_2.

In addition to its aforementioned role as an intracellular signaling agent, H_2O_2 is produced in cells as a byproduct of aerobic metabolism and as a result of various disease states.[23, 24] Phosphoryl transfer to oxygen nucleophiles is a ubiquitous reaction in biology[25] and H_2O_2, though present at relatively low concentrations, is a substantially better nucleophile than water.[26] Subsequent chapters show that peroxymonophosphate can be generated through spontaneous or enzyme-catalyzed reactions of H_2O_2 with phosphoryl donors under physiological conditions. The results reported here suggest that nanomolar concentrations of peroxymonophosphate could affect reversible down-regulation of cellular PTP activity within minutes. In conclusion, peroxymonophosphate possesses key properties expected for an endogenous signaling molecule involved in the redox-regulation of PTP activity.

3.6 Experimental Procedures

Materials and Methods

Reagents were purchased from the following suppliers: Buffers, salts, *p*-nitrophenylphosphate (*p*NPP), *5*,5'-dithiobis(2-nitrobenzoicacid) (DTNB), thiols, ampicillin (# A9518)), chloramphenicol (# C0378) LB media (# L3522) and yellow-86 agarose (# R2382s) were obtained from Sigma-Aldrich (St. Louis, MO). Q-Sepharose High Performance IEX chromatography media (# 17-1014-1) and P1 chromatography pumps were obtained from GE Healthcare (Piscataway, NJ). Restriction endonucleases EcoRI (# R0101) and SmaI (# R0141) were obtained from New England Biolabs (Ipswich, MA). DH5α competent cells (# 18258-012) were obtained from Invitrogen (Carlsbad, CA). Wizard Plus Plasmid Minipreps (# A7100) were obtained from Promega (Madison, WI). Novagen pETDuet1 vector (# 71146) and Tuner DE3 pLacI competent cells (# 70625) were obtained from EMD-Biosciences (San Diego, CA). Catalase (# 106 810) and Compleat® Free Protease Inhibitor (# 11-873-580-001) was purchased from Roche Bioscience. Zeba mini and micro centrifugal buffer exchange columns (#89882) and high-purity 10% solution of Tween 80 (Surfact-Amps® 80 # 28328) were purchased from Pierce Biotechnology (Rockford, IL). Amicon Ultra centrifugal filter devices (# UFC901008) were purchased from Millipore (Milford, MA).

PTP1B Expression, Purification and Characterization. *Preparation of PTP1B constructs:* The DNA sequence coding for amino acids 1-322 of PTP1B was amplified from a plasmid kindly provided by Dr. Nicholas Tonks. Truncated PTP1B DNA was cloned into a pETDUET vector with *EcoRI* and *NcoI* restriction sites at each end. The

resulting construct was purified on a 0.8% agarose gel, and extracted from the gel with Promega Wizard Plus Plasmid DNA isolation columns. DNA sequencing confirmed the correct PTP1B coding sequence in the open reading frame.

Recombinant PTP1B protein expression: *E. coli* DH5α competent cells were transformed according to manufacturer protocol with purified pETDUET plamids containing the truncated PTP1B gene. Plasmid DNA extracted from a 5 mL clonal DH5α culture was then used to transform Tuner (DE3) placI cells according to manufacturer protocol. Cells from both transformations were selected on LB agar supplemented with ampicillin to 100 μg/mL. A sixty μL aliquot from a 5 mL overnight culture of transformed Tuner DE3 cells in LB (LB/Amp^{50}/$Chlor^{34}$) fortified with ampicillin (50 μg/ml) and chloramphenicol (34 μg/ml) was diluted 1:500 in identical media fortified with 0.2% glucose and grown at 37°C to an A_{600} of approximately 0.6. The cells were then harvested by centrifugation at 5000 x *g* for 10 min, and resuspended in 6 mL of fresh LB/Amp^{50}/$Chlor^{34}$ media. One mL of the resulting suspension was used to inoculate each of six 500 mL volumes of LB/Amp^{50}/$Chlor^{34}$ containing 0.2% glucose. Cultures were grown at 37°C with rapid shaking (250 rpm) until an A_{600} of approximately 0.6 was measured. Expression was then induced with the addition to each culture of 5 mL of a 40 mM isopropyl-1-thio-beta-D-galctopyranoside (IPTG) solution in water. Following IPTG addition, the cultures were incubated with reduced shaking (175 rpm) at 37°C for 3 h. Cells were harvested as previously described, and the PTP1B catalytic subunit was purified essentially as described by Puius and colleagues.[7] Briefly, the cell pellets were resuspended in 50 mL buffer A (100 mM 2-(4-morpholino)-ethane sulfonic acid (MES), pH 6.5 with 1mM EDTA and 1 mM dithiothreitol) containing Compleat®

Free Protease Inhibitor cocktail, and lysed with three passes through a French Press. The resulting lysate was clarified by centrifugation at 37000 x *g* for 15 min. Clarified lysate was combined with 50 mL of CM-sephadex C50 resin pre-equilibrated with buffer A and shaken gently for 45 min. The resin was then loaded onto a 25 X 100 mm column and washed with 10 column volumes of buffer A. PTP1B was eluted with a linear NaCl gradient from 0⇨0.5 M in buffer A @ 2 ml/min. Fractions containing activity against *p*NPP were pooled, and concentrated with Amicon Ultra-15 centrifugal filter devices (10,000 MW cut off) to approximately 0.5 mg/mL total protein. A typical preparation yielded 15-20 mg of 95% pure PTP1B. The concentrated enzyme was divided into 100 μL aliquots, immediately frozen on dry ice and stored at -70^{o}C. Protein concentration, purity and identity were confirmed with UV absorbance (ε_{280} ~ 46410-46785 $M^{-1}cm^{-1}$) SDS-PAGE (NuPAGE Novex Bis-Tris polyacrylamide gel with MOPS running buffer) and MALDI-TOF mass spectrometry (data not shown).

Determination of PTP1B Active Site Concentration with 5,5'-dithiobis(2-nitrobenzoic acid) (DTNB): The concentration of PTP1B active sites was determined by measuring thiol concentration with DTNB in the presence or absence of the PTP transition state mimic vanadate as described by Pregel et al.[27] Thiol additives (β-mercaptoethanol or dithiothreitol) were completely removed from a 100 μL aliquot of concentrated PTP1B stock solution (~ 10 mg/ml) with three sequential Zeba mini centrifugal buffer exchange columns according to manufacturer protocol. Exchange buffer contained 100 mM Tris-HCl, 10 mM NaCl, 10 mM diethylenetriaminepentaacetic acid (DTPA), 0.05% Tween-80, pH 7.4. Four reactions were prepared in 2.0 mL polypropylene snap-top microcentrifuge tubes. Reactions # 1 and 2 were a blank and test for total PTP1B thiols,

respectively. To reaction tubes #1 and 2 was added 0.97 mL of assay buffer (200 mM Tris-HCl, pH 8.0, 1 mM EDTA). To reaction tubes #3 and 4 were added 0.96 mL of assay buffer. To reaction tubes # 2 and 4 was added a sufficient volume of PTP1B to obtain approximately 2.5 μM enzyme in what would be a 1.0 mL final volume (for example, 10 μL of a 250 μM stock). To tubes #3 and 4 was added 20 μL of a 100 mM solution of sodium orthovanadate (final concentration of 2 mM). To tubes # 1 and #2 was added an equivalent amount of assay buffer. The cuvettes were mixed and to each was added 20 μL of a 10 mM solution of DTNB dissolved in DMSO. After allowing the reaction tubes to stand for 10 min, the absorbance at 410 nm of tubes #2 and #4 were carefully measured by blanking the instrument with tubes # 1 and #3, respectively. Absorbance values were converted to thiol concentration (μM) using the TNB extinction coefficient (ε= 14150 $M^{-1}cm^{-1}$ at pH 8.0). The concentration of enzyme active sites was then calculated by determining the difference in thiol concentration between reactions #2 and #4.

Continuous Phosphatase Assay for Time-Dependent Inactivation of PTP1B by Peroxymonophosphate. Prior to running assays, free thiols were removed from stock enzyme aliquots with Zeba mini centrifugal buffer exchange columns (one column per aliquot) according to manufacturer protocol, yielding "thiol-free enzyme". Exchange buffer contained 100 mM Tris-HCl, 50 mM Bis-Tris, 50 mM Na^+ Acetate, 10 mM DTPA, 0.05% Tween-80, pH 7. For assay of either enzyme activity or time-dependent inactivation of enzyme activity by peroxymonophosphate, 10 μL of enzyme (25-50 pmol) diluted in exchange buffer was added to a cuvette containing a three component assay

buffer (100 mM NaOAc, 50 mM Bis-Tris, and 50 mM Tris pH 7.0) with substrate (*p*NPP, 10 mM) and various concentrations of peroxymonophosphate in a total volume of 1 mL. Immediately following addition of enzyme to the cuvette, the reaction was mixed by repeated inversion, and enzyme-catalyzed release of *p*-nitrophenol was monitored with a Hewlett Packard model 8453 spectrophotometer at 410 nm, and 25°C. Data points were taken every 2 s. The kinetic constants k_{inact} and K_I were obtained from inactivation time course data using the methods described by Hart et al. and Kraut et al.[13, 28]

Inactivation of PTP1B by (1) Is Not Reversed by Gel Filtration. PTP1B treated with peroxymonophosphate was subjected to gel filtration to determine if removal of residual peroxymonophosphate would result in the return enzyme activity. An aliquot of thiol free enzyme solution (100 nM final concentration) diluted in buffer (100 mM NaOAc, 50 mM Bis-Tris, and 50 mM Tris, 0.05% NP-40, 10 mM DTPA, pH 7.0) was combined with an equal volume of peroxymonophosphate (1 μM final concentration) in water and incubated at 25°C for 2 min. A 10 μL aliquot was removed and tested for activity with the continuous phosphatase assay as described above. Twelve μL of the remaining solution was then subjected to buffer exchange via centrifugal gel filtration in a Zeba micro spin column according to manufacturer protocol. Exchange buffer contained 100 mM Tris-HCl, 10 mM NaCl, 10 mM DTPA, 0.05 % NP-40, pH 7.4. Following buffer exchange, 10 μL of the resulting enzyme filtrate was tested for residual activity in the continuous phosphatase assay as described above.

Restoration of PTP1B Enzyme Activity by Thiol. To determine whether inactivation could be reversed by the addition of thiol, thiol-free PTP1B (100 pmol) was first

inactivated by treatment with peroxymonophosphate (2 μM) in 1 mL assay buffer (100 mM NaOAc, 50 mM Bis-Tris, and 50 mM Tris pH 7.0) containing *p*NPP (10 mM). Progress of inactivation was monitored at 410 nm according to the continuous phosphatase assay procedure described above. When enzyme activity was observed to be at or near zero, 5 μL of a 1 M solution of dithiothreitol (DTT) in H_2O was added to the cuvette to yield a final concentration of 5 mM. Progress of enzyme reactivation was monitored until no further increase in activity was observed. Approximately 88% of original enzyme activity returns within 5 min.

Inactivation of PTP1B in the Presence of Glutathione (GSH). For assay of time-dependent inactivation in the presence of thiol, PTP1B was diluted (5 nM final concentration) in assay buffer (100 mM NaOAc, 50 mM Bis-TRIS, and 50 mM Tris, 0.05% NP-40, 10 mM DTPA, pH 7.0) supplemented with GSH (1mM final concentration) and combined with an equal volume of water containing various concentrations of **1** at 25°C. At 0.5, 1.0, 1.5, 3 and 5 minutes, a 20 μL aliquot was removed from the mixture, and added to 0.5 mL of buffer containing substrate (0.1 M NaOAc, 20 mM *p*NPP, pH 5.5) at 30°C. After 10 min, the reaction was quenched by adding 0.5 mL of 2 N NaOH, and A_{410} measured to determine residual enzyme activity.

Inactivation of PTP1B in the Presence of Catalase. Assays were performed to determine if catalase could affect the ability of peroxymonophosphate to inactivate PTP1B. Ten μL of thiol-free PTP1B (100 pmol) diluted in exchange buffer (100 mM Tris-HCl, 10 mM NaCl, 10 mM DTPA, 0.05 % NP-40, pH 7.4) was added to a cuvette containing buffer (100 mM NaOAc, 50 mM Bis-Tris, and 50 mM Tris pH 7.0), *p*NPP

substrate (10 mM), peroxymonophosphate (1 μM) and 2000 U of catalase in a total volume of 1 mL. Enzyme activity was measured with the continuous phosphatase assay as described above.

Inactivation of PTP1B in the Presence of Reversible Enzyme Inhibitors. To demonstrate that the target of enzyme inactivation by peroxymonophosphate was the active site, inactivation assays were performed in the presence of the known competitive phosphatase inhibitors phosphate or vanadate. To verify protection against inactivation by peroxymonophosphate, an aliquot of thiol-free enzyme (100 nM final concentration) in buffer (100 mM NaOAc, 50 mM Bis-Tris, and 50 mM Tris, 0.05 % NP-40, 10 mM DTPA, pH 7.0) was combined with an equal volume of peroxymonophosphate (1 μM final concentration) in buffer (100 mM NaOAc, 50 mM Bis-Tris, and 50 mM Tris pH 7.0) containing either phosphate (50 mM final concentration) or vanadate (1 mM final concentration) at 25^{o}C. After 30 s, a 10 μL aliquot was removed and assayed for activity with the continuous phosphatase assay as described above.

Determination of the Turnover Number for Inactivation of PTP1B by Peroxymonophosphate. Ten μL of thiol-free PTP1B (35 pmol) diluted in exchange buffer (100 mM Tris-HCl, 10 mM NaCl, 10 mM DTPA, 0.05 % NP-40, pH 7.4) was added to a cuvette containing buffer (100 mM NaOAc, 50 mM Bis-Tris, and 50 mM Tris pH 7.0), *p*NPP substrate (10 mM), and various amounts of peroxymonophosphate (10-40 pmol) in a total volume of 1 mL and allowed to incubate at 25^{o}C. After 10 min, 50 μL of 210 mM *p*NPP substrate was added and residual enzyme activity immediately monitored at 410 nm. Residual activity was plotted against the molar ratio of enzyme to

peroxymonophosphate, the resulting data fitted to a linear regression, and the turnover number was extrapolated to the x-axis.

Measurement of PTP1B K_m for *p*-nitrophenylphosphate (*p*NPP). PTP1B (5 μL @ 0.5 mg/ml) was added to 0.95 mL of assay buffer (100 mM Tris-HCl, 50 mM Bis-Tris, 50 mM Na^+ Acetate, 10 mM DTPA, 0.05% Tween 80, pH 7) containing various concentrations of *p*NPP in a 1.0 mL cuvette in triplicate. The cuvette was quickly inverted three times to mix the contents, and the absorbance at 410 nm was recorded every 10s for 1min. The resulting data were fit to an equation depicting a straight line. The slope of each line (at each concentration) was then plotted as a function of substrate concentration, and the data analyzed to determine K_m with the graphing software Prism.

References

1. Stone, J. R., An assessment of proposed mechanisms for sensing hydrogen peroxide in mammalian systems. *Archives of Biochemistry and Biophysics* **2004,** *422* (2), 119-124.

2. Denu, J. M.; Tanner, K. G., Specific and Reversible Inactivation of Protein Tyrosine Phosphatases by Hydrogen Peroxide: Evidence for a Sulfenic Acid Intermediate and Implications for Redox Regulation. *Biochemistry* **1998,** *37* (16), 5633-5642.

3. Tonks, N. K., Redox Redux: Revisiting PTPs and the Control of Cell Signaling. *Cell* **2005,** *121* (5), 667-670.

4. Mahadev, K.; Zilbering, A.; Zhu, L.; Goldstein, B. J., Insulin-stimulated Hydrogen Peroxide Reversibly Inhibits Protein-tyrosine Phosphatase 1B in Vivo and Enhances the Early Insulin Action Cascade. *J. Biol. Chem.* **2001,** *276* (24), 21938-21942.

5. Tonks, N. K.; Diltz, C. D.; Fischer, E. H., Characterization of the major protein-tyrosine-phosphatases of human placenta. *J. Biol. Chem.* **1988,** *263* (14), 6731-6737.

6. Hoppe, E.; Berne, P.-F.; Stock, D.; Rasmussen, J. S.; Miller, N. P. H.; Ullrich, A.; Huber, R., Expression, purification and crystallization of human phosphotyrosine phosphatase 1B. *European Journal of Biochemistry* **1994,** *223* (3), 1069-1077.

7. Puius, Y. A.; Zhao, Y.; Sullivan, M.; Lawrence, D. S.; Almo, S. C.; Zhang, Z.-Y., Identification of a second aryl phosphate-binding site in protein-tyrosine phosphatase 1B: A paradigm for inhibitor design. *PNAS* **1997,** *94* (25), 13420-13425.

8. Misra, H. P., Generation of Superoxide Free Radical during the Autoxidation of Thiols. *J. Biol. Chem.* **1974,** *249* (7), 2151-2155.

9. Lever, M., Peroxides in detergents as interfering factors in biochemical analysis. *Analytical Biochemistry* **1977,** *83* (1), 274-284.

10. Clover, A. M., Auto-oxidation of ethers. *Journal of the American Chemical Society* **1924,** *46* (2), 419-430.

11. Silverman, R. B., *Mechanism-Based Enzyme Inactivation: Chemistry and Enzymology*. CRC Press: Boca Raton, 1988; Vol. I.

12. Barrett, W. C.; DeGnore, J. P.; Keng, Y.-F.; Zhang, Z.-Y.; Yim, M. B.; Chock, P. B., Roles of Superoxide Radical Anion in Signal Transduction Mediated by Reversible Regulation of Protein-tyrosine Phosphatase 1B. *J. Biol. Chem.* **1999,** *274* (49), 34543-34546.

13. Kraut, D.; Goff, H.; Pai, R. K.; Hosea, N. A.; Silman, I.; Sussman, J. L.; Taylor, P.; Voet, J. G., Inactivation Studies of Acetylcholinesterase with Phenylmethylsulfonyl Fluoride. *Mol Pharmacol* **2000,** *57* (6), 1243-1248.

14. Duranton, J.; Adam, C.; Bieth, J. G., Kinetic Mechanism of the Inhibition of Cathepsin G by α1-Antichymotrypsin and α1-Proteinase Inhibitor. *Biochemistry* **1998,** *37* (32), 11239-11245.

15. Jaeyul Kwon, C.-K. Q., Jin-Soo Maeng, Rustom Falahati, Chunghee Lee and Mark S Williams, Receptor-stimulated oxidation of SHP-2 promotes T-cell adhesion through SLP-76–ADAP. *The EMBO Journal* **2005,** *24*, 2331-2341.

16. Tian, W. X.; Tsou, C. L., Determination of the rate constant of enzyme modification by measuring the substrate reaction in the presence of the modifier. *Biochemistry* **1982,** *21* (5), 1028-1032.

17. Battaglia, C. J.; Edwards, J. O., The Dissociation Constants and the Kinetics of Hydrolysis of Peroxymonophosphoric Acid. *Inorg. Chem.* **1965,** *4* (4), 552-558.

18. Montalibet, J.; Skorey, K. I.; Kennedy, B. P., Protein tyrosine phosphatase: enzymatic assays. *Methods* **2005,** *35*, 2-8.

19. Meister, A.; Anderson, M. E., Glutathione. *Ann. Rev. Biochem.* **1983,** *52*, 711-760.

20. Winterbourn, C. C.; Metodiewa, D., Reactivity of biologically important thiol compounds with superoxide and hydrogen peroxide. *Free Rad. Biol. Med.* **1999,** *27* (3/4), 322-328.

21. Lueng, K. W. K.; Posner, B. I.; Just, G., Periodinates: a new class of protein tyrosine phosphatase inhibitors. *Bioorg. Med. Chem. Lett.* **1999,** *9*, 353-356.

22. Li, S.; Whorton, R., Regulation of protein tyrosine phosphorylation 1B in intact cells by S-nitrosothiols. *Arch. Biochem. Biophys.* **2003,** *410*, 269-279.

23. Balaban, R. S.; Nemoto, S.; Finkel, T., Mitochondria, oxidants, and aging. *Cell* **2005,** *120* (Feb 25), 483-495.

24. Rhee, S. G., H_2O_2, a necessary evil for cell signaling. *Science* **2006,** *312* (June 30), 1882-1883.

25. Knowles, J. R., Enzyme-catalyzed phosphoryl transfer reactions. *Ann. Rev. Biochem.* **1980,** *49*, 877-919.

26. Hershlag, D.; Jencks, W. P., Nucleophiles of high reactivity in phosphoryl transfer reactions: alpha-effect compounds and fluoride ion. *J. Am. Chem. Soc.* **1990,** *112*, 1951-1956.

27. Pregel, M. J.; Storer, A. C., Active Site Titration of the Tyrosine Phosphatases SHP-1 and PTP1B Using Aromatic Disulfides. REACTION WITH THE ESSENTIAL CYSTEINE RESIDUE IN THE ACTIVE SITE. *J. Biol. Chem.* **1997,** *272* (38), 23552-23558.

28. Hart, G. J.; O'Brien, R. D., Recording spectrophotometric method for determination of dissociation and phosphorylation constants for the inhibition of acetylcholinesterase by organophosphates in the presence of substrate. *Biochemistry* **1973,** *12* (15), 2940-2945.

Chapter 4

Synthesis and Use of PC-1 as a Selective Detector of Peroxymonophosphate

4.1 Introduction and Objectives

Reactive oxygen species (ROS) are produced in cells by a number of mechanisms, including exposure to UV/ionizing radiation, metabolism of xenobiotics[1], mitochondrial respiration[2] and immune system responses[3]. Uncontrolled or excessive generation of ROS in these situations, naturally, has negative toxicological consequences. There is growing evidence, however, that these molecules are released under normal physiologic conditions and play important roles in tightly controlled processes such as cardiovascular regulation and intracellular signal transduction.[4, 5] A specific example of such action is the role of hydrogen peroxide (produced by NADPH oxidase) in the insulin signal cascade.[6]

While it is clear that ROS such as hydrogen peroxide are so-called second messengers involved in intracellular signaling pathways, detailed knowledge of the mechanisms by which ROS exert their action is incomplete, at best.[7, 8] Some aspects of

hydrogen peroxide mediated intracellular signaling are in fact at odds with observed physiology. J. Stone, in fact, proposes that hydrogen peroxide is merely a carrier of oxidative equivalents, much like the ubiquitous biological thiol glutathione is a carrier of reductive equivalents.[7] In this scenario, H_2O_2 would transfer its oxidative action to another agent, either spontaneously or by the actions of an unknown enzyme. These "higher order" oxidative species have yet to be discovered. Furthermore, many if not all of the molecules that possess the characteristics expected for an intracellular redox-signaling agent also have characteristics that make detection and analysis difficult. They are small, diffuse rapidly and are highly reactive. A major obstacle, therefore, in this field is the facile, selective detection of ROS over other cellular agents. Traditional indicators of ROS, such as 2',7'-dichlorodihydrofluorescein and Pentafluorobenzenesulfonyl fluorescein lack selectivity and sensitivity, respectively (Scheme 4.1).[9] Herein we set out to develop a new method to selectively detect higher-order ROS, such as peroxymonophosphate, over others such as hydrogen peroxide, and/or nitric oxide.

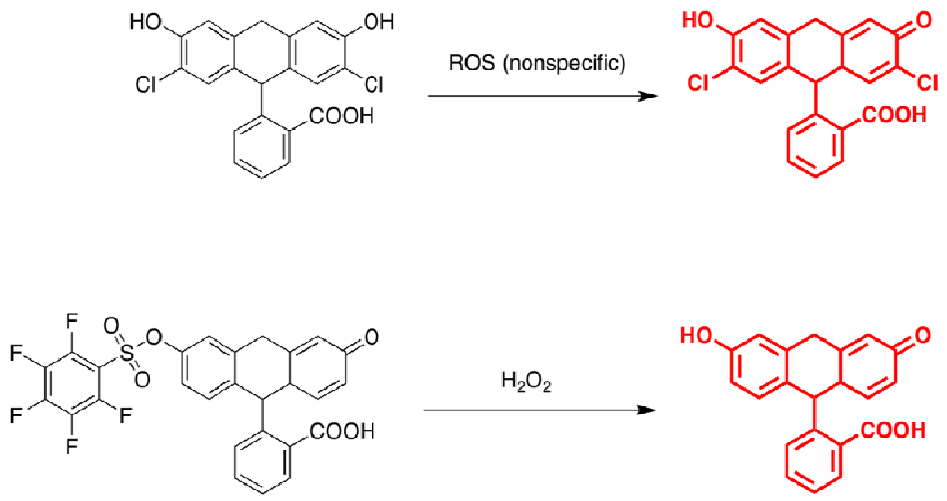

Scheme 4.1 Examples of ROS indicators that lack either selectivity or sensitivity

4.2 Oxidative Deboronation

C. Chang recently reported use of boronate based fluorescent probes to selectively detect hydrogen peroxide over other physiologically relevant ROS.[10, 11] We were particularly interested in this mechanistic approach toward ROS detection due to this author's knowledge of oxidative reactions with boron containing xenobiotics.[12, 13]

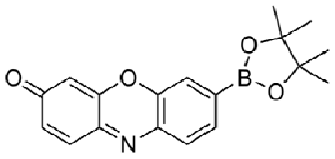

PC-1
(1)

Scheme 4.2 The boronate-containing ROS indicator PC-1

The fluorescent, boronate containing ROS probe PC-1 (Scheme 4.2) takes advantage of the stereoselective oxidative deboronation reactions that have been reported by H.C. Brown.[14] The presence of the pinacol-borane moiety on the resorufin scaffold of PC-1 effectively quenches its intrinsic fluorescence. In the presence of a reactive oxygen species such as hydrogen peroxide, PC-1 will undergo oxidative deboronation to yield resorufin (Scheme 4.3). Interestingly, PC-1 reacts very slowly (or not at all) with other known physiologically relevant ROS species such as nitric oxide. This is a very desirable characteristic, and as such we wanted to determine whether or not PC-1 would react with the potential intracellular redox-regulator peroxymonophosphate.

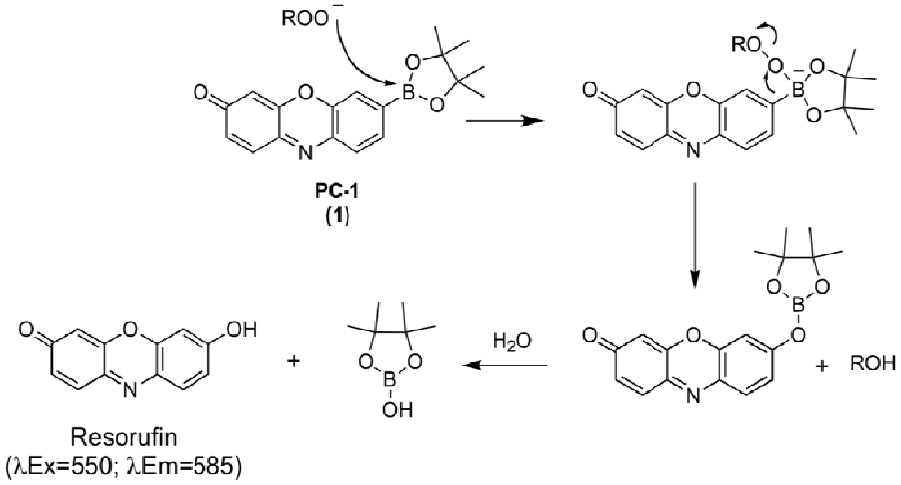

Scheme 4.3 Oxidative deboronation of PC-1 yields highly fluorescent resorufin.

4.3 Preparation of PC-1

Synthesis of PC-1 was straightforward and was accomplished by closely following the protocol described in the supplemental information of Chang's

publication.[10, 11] This two-step preparation was initiated by combining resorufin sodium salt with N-phenyl bis(trifluoromethanesulfonamide) and Hünig's base in dry dimethylformamide. The resulting triflate was then converted into the borane-containing PC-1 via Suzuki-Miyura-like cross-coupling with bis(pinacolato)diboron in a dry inert atmosphere glove box (Scheme 4.4). The bright orange product was stable as a dry powder. Once it was dissolved in a protic solvent, however, slow but steady hydrolysis of the boronate group occurred resulting in an increase in background fluorescence. A successful way to prepare and store stock solutions of PC-1 was to dissolve it in dry acetonitrile to a concentration of ~ 1 mM. When a solution of PC-1 prepared in this manner was kept dry and stored at -20°C it was stable for at least six months.

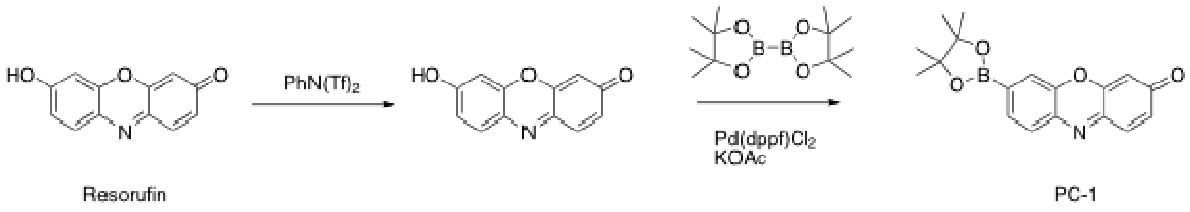

Scheme 4.4 Preparation of PC-1 as described by Chang.

4.4 Fluorescence Measurements

Our initial experiments with PC-1 determined the proper parameters for fluorescent detection. To achieve this, a matrix of excitation versus emission wavelengths was created using a 1 μM solution of resorufin in 50 mM Bis-Tris buffer, pH 7.0. Figure 4.1 shows the results of scanning the excitation wavelength from 500 to 570 nm, and observing the resulting emission intensity from 570 to 600 nm. The

emission maximum was found to be at or around 585 nm. For the purposes of our experiments, we chose an excitation wavelength of 550 nm. This gave good fluorescent emission intensity, and was far enough away from the emission wavelength of 585 nm to avoid Raleigh scattering at the detector.

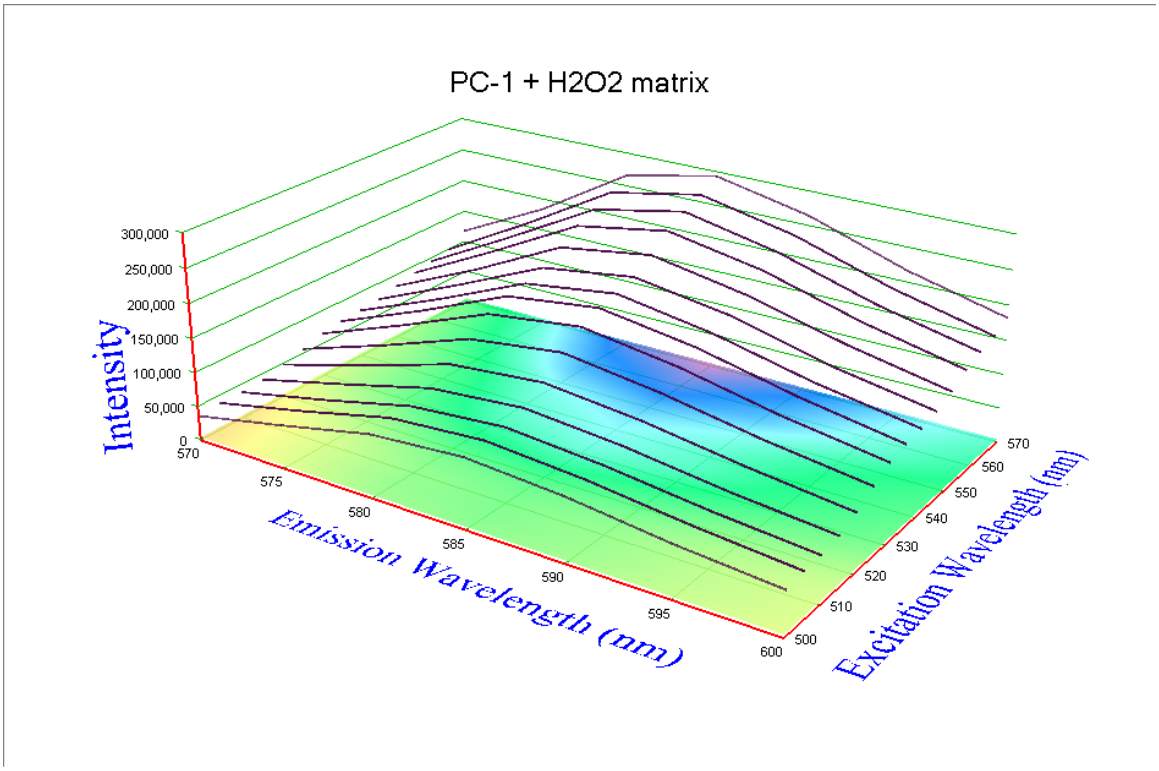

Figure 4.1 Plot of fluorescent intensity versus excitation and emission wavelength for deboronated PC-1.

Chang reported that treatment of PC-1 with 100 μM hydrogen peroxide for 1 h resulted in a roughly 40-fold increase in fluorescence intensity. To determine the absolute fluorescence increase possible by deboronating PC-1, we treated the compound with 10 mM H_2O_2 for 45 min, at which point the slope of fluorescence intensity versus time became zero. Figure 4.2 shows that there was an approximately 150-fold increase in fluorescent response between native PC-1 and PC-1 treated as described. This is a significant delta, and the anticipated high rate of reaction between PC-1 and

peroxymonophosphate makes it a promising reagent for detection. In addition to the change in fluorescent intensity, there was a marked difference in the color of the native and oxidized compound (Figure 4.3). This proved useful in assessing the gross stability of PC-1 stock solutions. From this point on, our goal was to quantify the differences in reactivity between PC-1 and the two reactive oxygen species peroxymonophosphate and hydrogen peroxide.

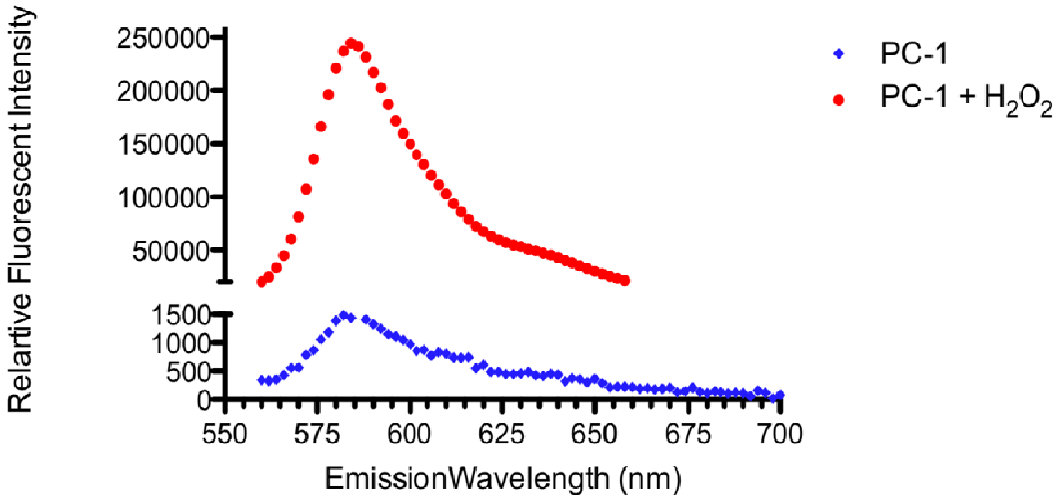

Figure 4.2 Increase in fluorescent intensity caused by oxidative deboronation of PC-1.

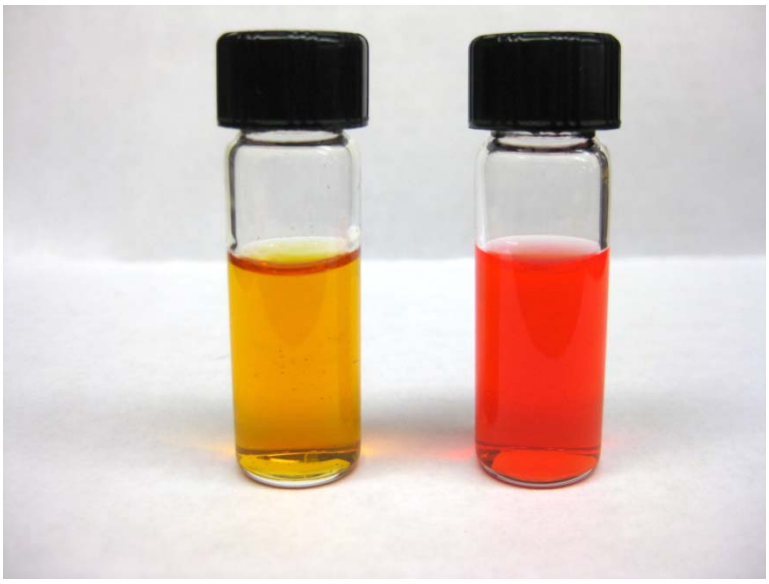

Figure 4.3 Color change resulting from treatment of PC-1 with hydrogen peroxide. Left: 1 mM solution of PC-1 in 50 mM Bis-Tris pH 7.0. Right: 1 mM solution of PC-1 in 50 mM Bis-Tris pH 7.0 treated with 10 mM H_2O_2 for 1h.

While the fluorescence intensity of PC-1 did increase upon addition of hydrogen peroxide, the rate of this reaction was obviously slow, even when compared to the sluggish reaction of H_2O_2 with PTP1B. Measurement of the rate of reaction between PC-1 and hydrogen peroxide under pseudo-first order conditions confirmed this observation. The apparent second order rate was determined to be 1.2 M-1s-1, which is consistent with what was reported by Chang (~ 1 $M^{-1}s^{-1}$) (Figures 4.4 and 4.5).[11]

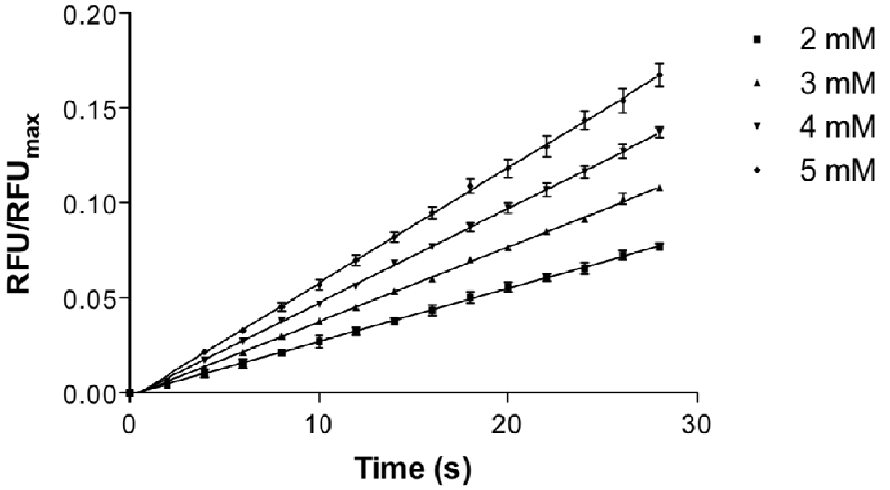

Figure 4.4 The apparent pseudo-first order rates of PC-1 deboronation by hydrogen peroxide.

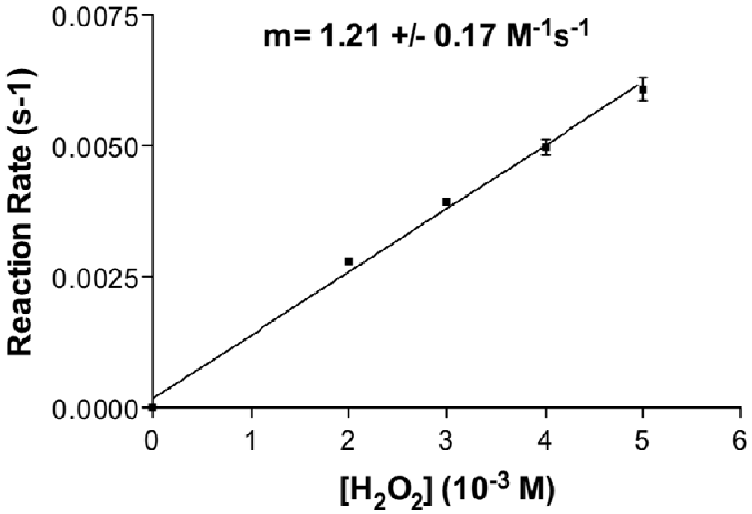

Figure 4.5 The apparent second order rate of the reaction between PC-1 and hydrogen peroxide is 1.2 +/- 0.17 $M^{-1}s^{-1}$.

It was immediately clear that peroxymonophosphate caused rapid deboronation of PC-1 when combined in equimolar ratios. In fact, addition of 10 μM peroxymonophosphate to a 1 μM solution of PC-1 resulted in complete deprotection of the resorufin core and maximum fluorescent intensity in less than 30 seconds. To facilitate measurement of reaction kinetics under pseudo-first order conditions it was necessary, therefore, to reduce the concentration of PC-1 to 100 nM from the original concentration of 1 μM. This allowed us to treat PC-1 with concentrations of peroxymonophosphate that allowed visualization of reaction the in a more reasonable time frame of minutes, instead of seconds.

When analyzed with pseudo-first order conditions, we found that PC-1 was indeed selective for peroxymonophosphate over hydrogen peroxide, with an apparent second order reaction rate of 1447 ± 52 $M^{-1}s^{-1}$ (Figures 4.6 and 4.7).[15]

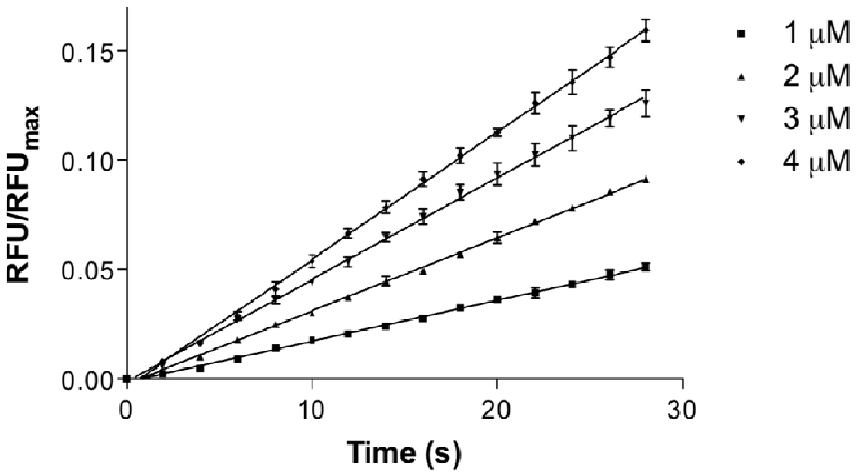

Figure 4.6 The apparent pseudo-first order rates of PC-1 deboronation by peroxymonophosphate.

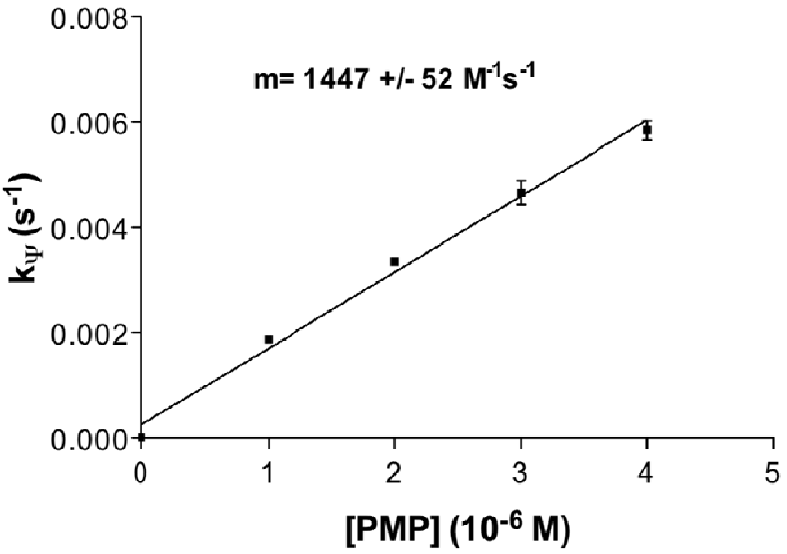

Figure 4.7 The apparent second order rate of the reaction between PC-1 and peroxymonophosphate is 1447 +/- 52 $M^{-1}s^{-1}$.

4.5 Conclusions

Peroxymonophosphate readily "lights up" the fluorescent peroxide indicator PC-1. The reaction of PC-1 with peroxymonophosphate is approximately 1200 times faster than with H_2O_2. This finding highlights the possibility that boronate ester probes might preferentially detect a secondary H_2O_2-derived oxidant such as peroxymonophosphate if this species is generated inside cells. Taken together, elements of the work described here provide a foundation for the development of assays designed to detect spontaneous or enzyme-catalyzed conversion of H_2O_2 to peroxymonophosphate in biochemical or biological systems. After incubation of H_2O_2 with a phosphoryl donor substrate (perhaps in the presence of a putative enzymatic catalyst), catalase can be used to destroy excess H_2O_2. Catalase treatment leaves peroxymonophosphate intact and addition of the peroxide indicator PC-1 provides a means for its highly sensitive detection under a given

set of reaction conditions. This general approach might be amenable to either a high-throughput micro plate reader or in-gel assays that search for peroxymonophosphate-producing enzymes in a proteome. Such tools will help explore the possibility that peroxymonophosphate participates in the regulation (or dysregulation) of cell signaling processes under physiological or pathophysiological conditions.

4.6 Experimental Procedures

Materials and Methods

Reagents were purchased from the following suppliers: Bis-Tris (#B9754), resorufin sodium salt (#R3257), anhydrous dimethylformamide (#227056) N-phenyl bis(trifluoromethanesulfonamide) (#295973), N,N-diisopropylamine (Hunigs base, #386464), bis(pinacolato)diboron (#473294), diphenyl, 1,1′-Bis(diphenylphosphino)ferrocene] dichloropalladium(II), complex with dichloromethane (#379670), 1,1′-Bis(diphenylphosphino)ferrocene (#177261), potassium acetate (#236497), anhydrous 1,4 dioxane (#296309), anhydrous Na_2SO_4 (#239313) were obtained from Sigma-Aldrich (St. Louis, MO). CDCl3 was obtained from Cambridge Isotope Labs, Cambridge, Massachusetts. Hydrogen peroxide (#H325-500) was obtained from Fisher Scientific, Fairlawn, New Jersey.

Preparation of 3-Oxo-3*H*-phenoxazin-7-yl trifluoromethanesulfonate (2). The fluorescent boronate-containing ROS indicator PC-1 was prepared exactly as described by Chang and coworkers. To recap: Resorufin sodium salt (500 mg/2.2 mmol) was dissolved in a round-bottom flask (using Schlenk apparatus and dry nitrogen) in 40 mL of dry dimethylformamide (dried over 4 Å molecular sieves) with an equimolar ratio of *N*-

phenyl bis(trifluoromethanesulfonamide) (786 mg). Hünig's base (1.1 mL, 6.6 mmol) was then added via syringe and the reaction mixture was stirred in the dark, under dry nitrogen (low positive pressure), for 24 hours. The reaction mixture was concentrated via rotary evaporation (high-vacuum, dry ice/acetone traps) to ~ 5 mL volume and diluted with 200 mL ethyl acetate. The organic layer was washed three times with 200 mL of water, dried over anhydrous magnesium sulfate, and dried with rotary evaporation. Flash column chromatography with 100g silica gel (1:1, ethyl acetate:hexanes) gave the product 3-Oxo-3*H*-phenoxazin-7-yl trifluoromethanesulfonate as an orange-yellow solid that eluted between bright red and bright yellow bands. (568 mg, 74% yield). ^{1}H NMR ($CDCl_3$, 300 MHz) δ 7.89 (1H, d, J=), 7.45 (1H, d, J=), 7.29 (3H, m), 6.9 (1H, dd, J=), 6.35 (1H, d, J=) (Figure 4.8). ^{19}F NMR ($CDCl_3$, 250 MHz) δ -72 (s) (Figure 4.10). Crude ^{13}C NMR is shown in Figure 4.9.

Preparation of 3-Oxo-3*H*-phenoxazin-7-yl pinacolatoboron (PC-1, (1)). In a dry inert atmosphere glove box to a 25 mL round bottom flask was added 3-Oxo-3*H*-phenoxazin-7-yl trifluoromethanesulfonate (166 mg, 0.50 mmol), bis(pinacolato)diboron (186 mg, 0.73 mmol), [1,1′-Bis(diphenylphosphino)ferrocene]dichloropalladium(II) complexed with dichloromethane ($PdCl_2(dppf)•CH_2Cl_2$, 40 mg, 0.05 mmol), and 1,1′-Bis(diphenylphosphino)ferrocene (dppf, 26 mg, 0.05 mmol). To this mixture was added 6 mL of a suspension of potassium acetate (32 mg, 0.33 mmol) in anhydrous 1,4 dioxane. The flask was then sealed in the glove box with a 15 cm reflux condenser topped with an "L" shaped glass stopcock equipped with a tubing nipple. The entire system was then removed from the glove box, attached to dry nitrogen purged Schlenk apparatus, and heated at 80^{o}C for 3 h. All ground glass joints were treated with minimal silicone sealant

to prevent air intrusion during transfer to the Schlenk apparatus. After heating, the reaction was allowed to cool to room temperature, diluted with ~ 20 mL toluene, and any precipitates were removed by filtering with a sintered glass funnel (medium pore size). The filtrate was washed three times with 25 mL of brine, and dried over anhydrous sodium sulfate. Solvent was removed with rotary evaporation followed by high vacuum for several hours. The resulting reddish-brown solid was washed several times on a sintered glass funnel (medium pore size) with small volumes of ethanol (~ 10 mL) to give the product, PC-1 as a bright orange solid (20 mg, 12% yield). ^{1}H NMR ($CDCl_3$, 300 MHz) δ 7.77 (3H, m), 7.45 (1H, d, J = 9.98 Hz), 6.87 (1H, dd, J1 = 2.07 Hz, J2 = 9.9 Hz), 6.33 (1H, d, J = 1.9 Hz), 1.32 (12H, s) (Figure 4.11). ^{13}C NMR ($CDCl_3$, 300 MHz) δ 186, 149.8, 149.5, 135.36, 134.73, 131.3, 129.46, 122.18, 106.9, 84.54, 24.84 (Figure 4.12).

Measurement of Fluorescent Parameters for Detection of PC-1. All fluorescent spectra were taken with an SLM-AMINCO 8100 spectrofluorimeter equipped with a temperature controlled cell holder. Slit widths were set at 4 nm at both excitation and emission optics. For measurement of fluorescence excitation and emission spectra, a 1 μM solution of PC-1 was prepared by adding 1 μL of 1 mM stock PC-1 dissolved in dry acetonitrile to 0.99 mL 50 mM Bis-Tris buffer, pH 7.0. This solution proved very stable when kept from moisture and stored at -20^{o}C. If the solution was contaminated with water, slow but steady deboronation of PC-1 occurred. Excitation wavelengths were scanned from 500 to 570 nm in 10 nm steps, and emission intensity was observed from 570 to 600 nm in 5 nm steps. While emission intensity peaked at 585 nm, there was a broad range of good excitation wavelengths that ranged from 540 to 570 nm (Figure 4.1).

There was minimal signal gain from 540 to 570 nm, so 550 nm was chosen for excitation to prevent Raleigh scatter from occurring. This combination, excitation at 550 nm, emission at 585 nm with 4 nm slit widths yielded approximately 200,000 relative fluorescence units of intensity with a 1 μM solution of PC-1 in 50 mM Bis-Tris buffer pH 7.0.

Measurement of the Rate of Reaction between PC-1 and Hydrogen Peroxide. The rate of reaction between PC-1 and hydrogen peroxide was measured under pseudo-first order conditions. For measurement of the apparent rate of fluorescence increase catalyzed by hydrogen peroxide, in a fluorescence cuvette to 1 mL of a 1 μM solution of PC-1 (1 μL of a 1 mM stock solution dissolved in dry acetonitrile) in 50 mM Bis-Tris buffer pH 7.0 was added varying amounts of hydrogen peroxide (2, 3, 4, 5 mM final concentration, from an 1 mM stock). The cuvette was quickly stoppered, inverted three times to mix, and fluorescence intensity was observed for 30 s. at 2 s. intervals using an SLM-AMINCO 8100 spectrofluorimeter with the parameters described in the previous section. Each measurement was performed in triplicate. The apparent rate of reaction was determined by plotting relative fluorescence intensity (% of maximum fluorescence of a 1 μM solution of fully deboronated PC-1) as a function of time and fitting the data to the equation ($y = m*x + b$) where $y = RFU/RFU_{max}$, x = time in seconds (Figure 4.4). The slope of each line was equal to k_Ψ (units = s^{-1}), the apparent pseudo-first order reaction rate. When the various values of k_Ψ were then replotted as a function of H_2O_2 concentration, the slope of the resulting line was equal to the apparent second order rate of reaction (1.21 +/- 0.17 $M^{-1}s^{-1}$, (Figure 4.5).

Measurement of the Rate of Reaction between PC-1 and Peroxymonophosphate. Due to the rapid rate of reaction between PC-1 and peroxymonophosphate, to preserve pseudo-first order conditions it was necessary to reduce the concentration of PC-1 to 100 nM from 1 μM. The reactions and data analysis were carried out as previously described, the differences being PC-1 concentration (100 nM), and peroxymonophosphate concentrations (1, 2, 3, 4 μM from a 1 mM solution in water) (Figure 4.6). Replotting the pseudo-first order rates of reaction gave the apparent second order rate of reaction between PC-1 and peroxymonophosphate (1447 +/- 52 $M^{-1}s^{-1}$, (Figure 4.7).

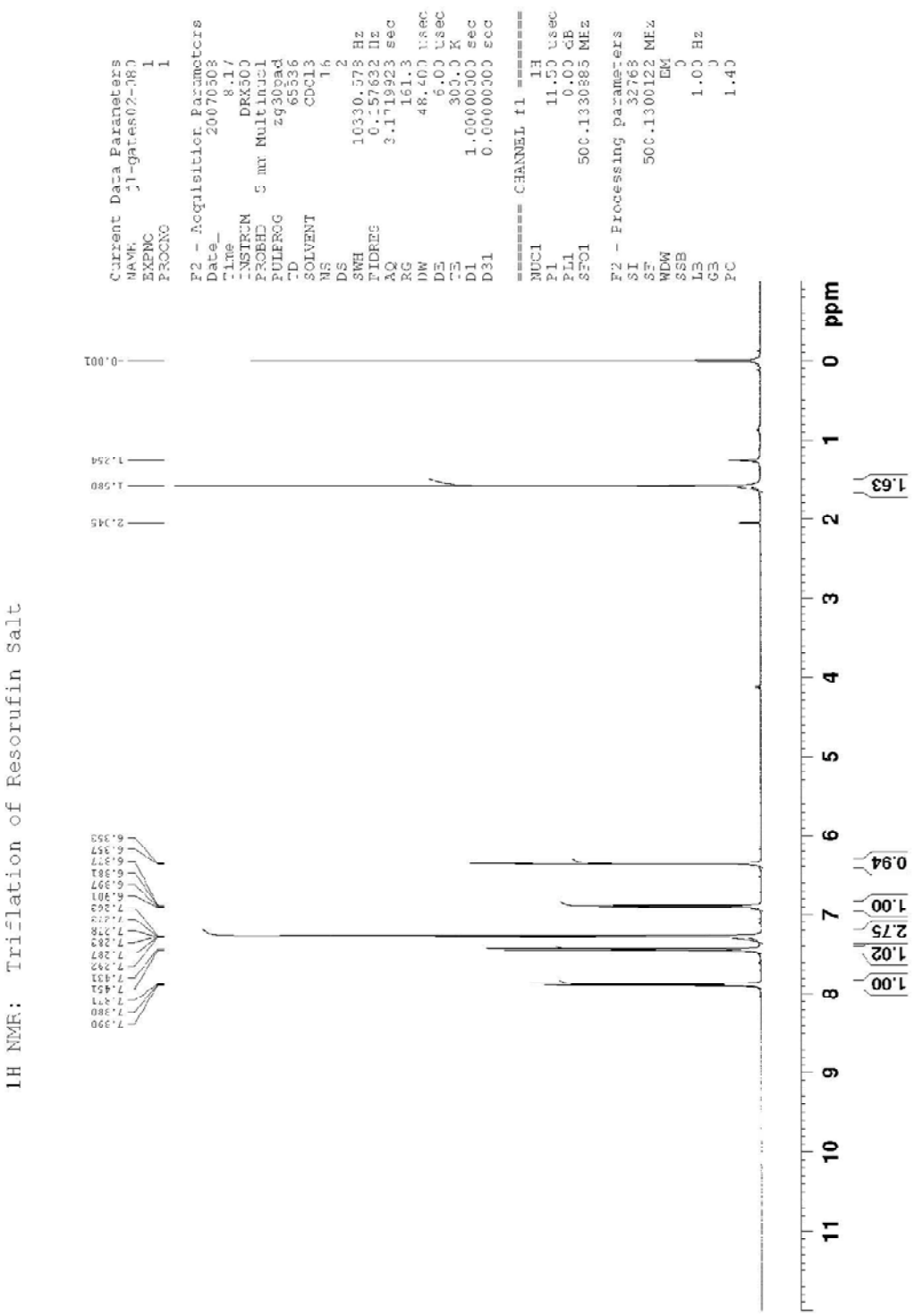

Figure 4.8 ^{1}H NMR of (2).

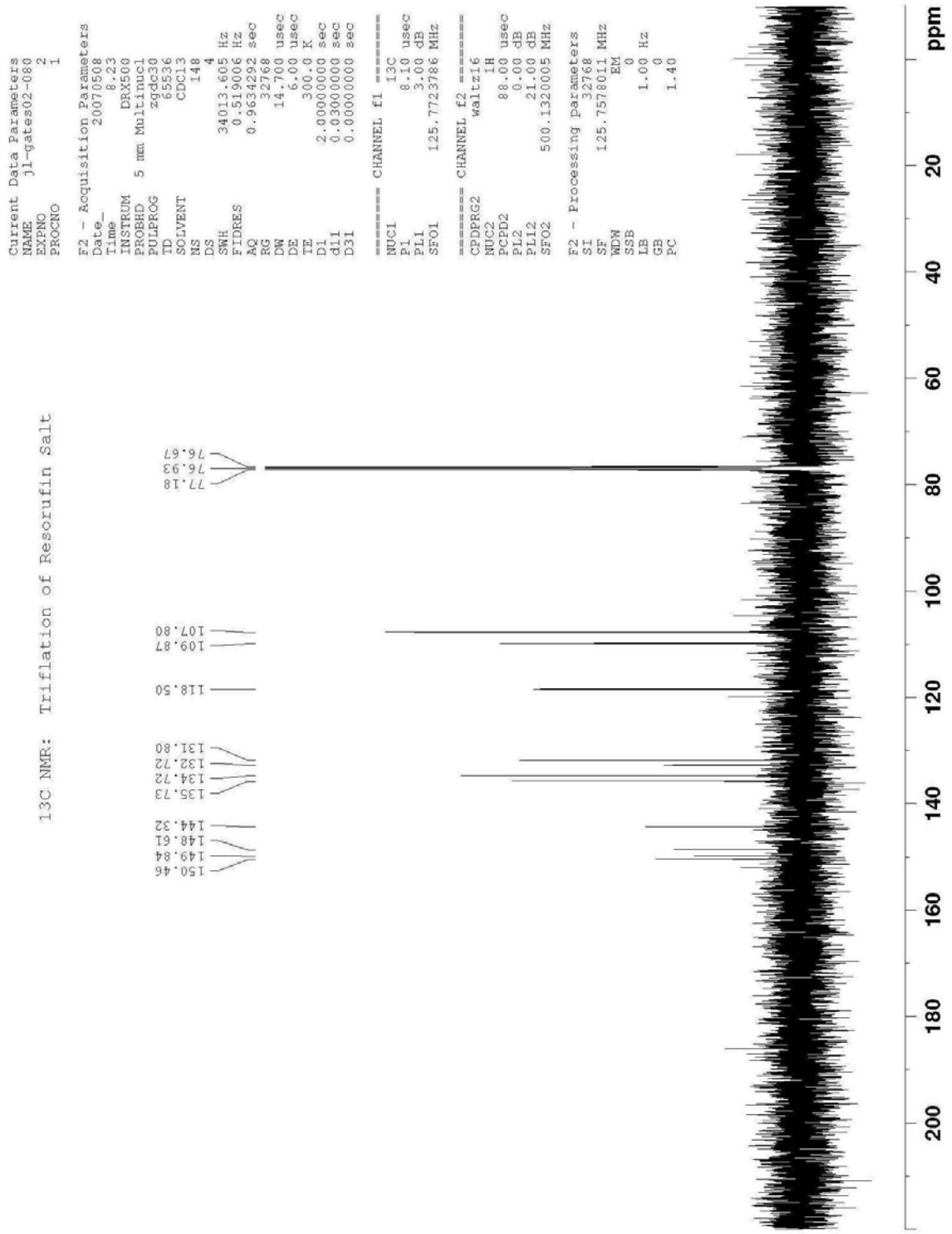

Figure 4.9 ^{13}C NMR of (2).

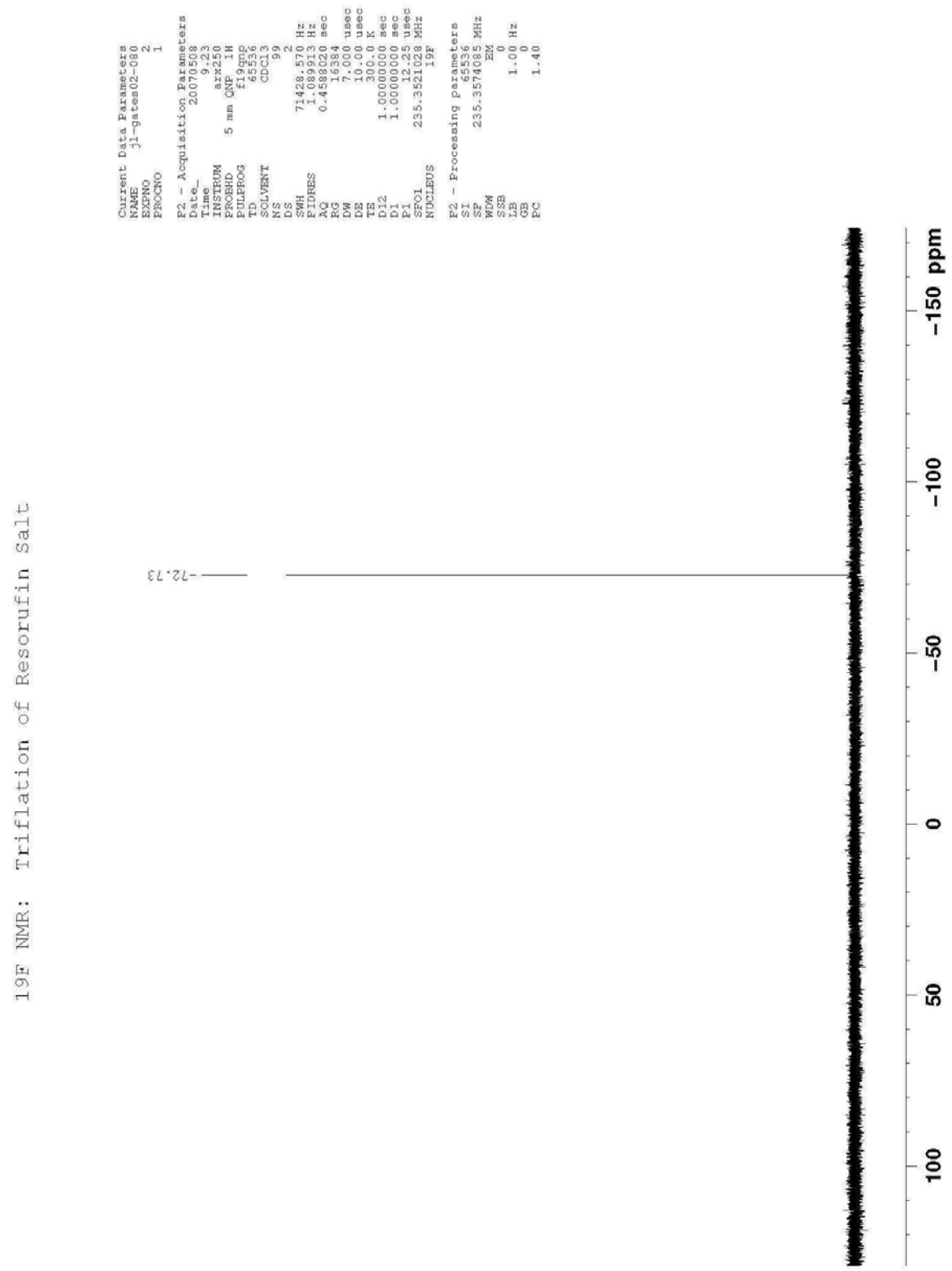

Figure 4.10 ^{19}F NMR OF (2)

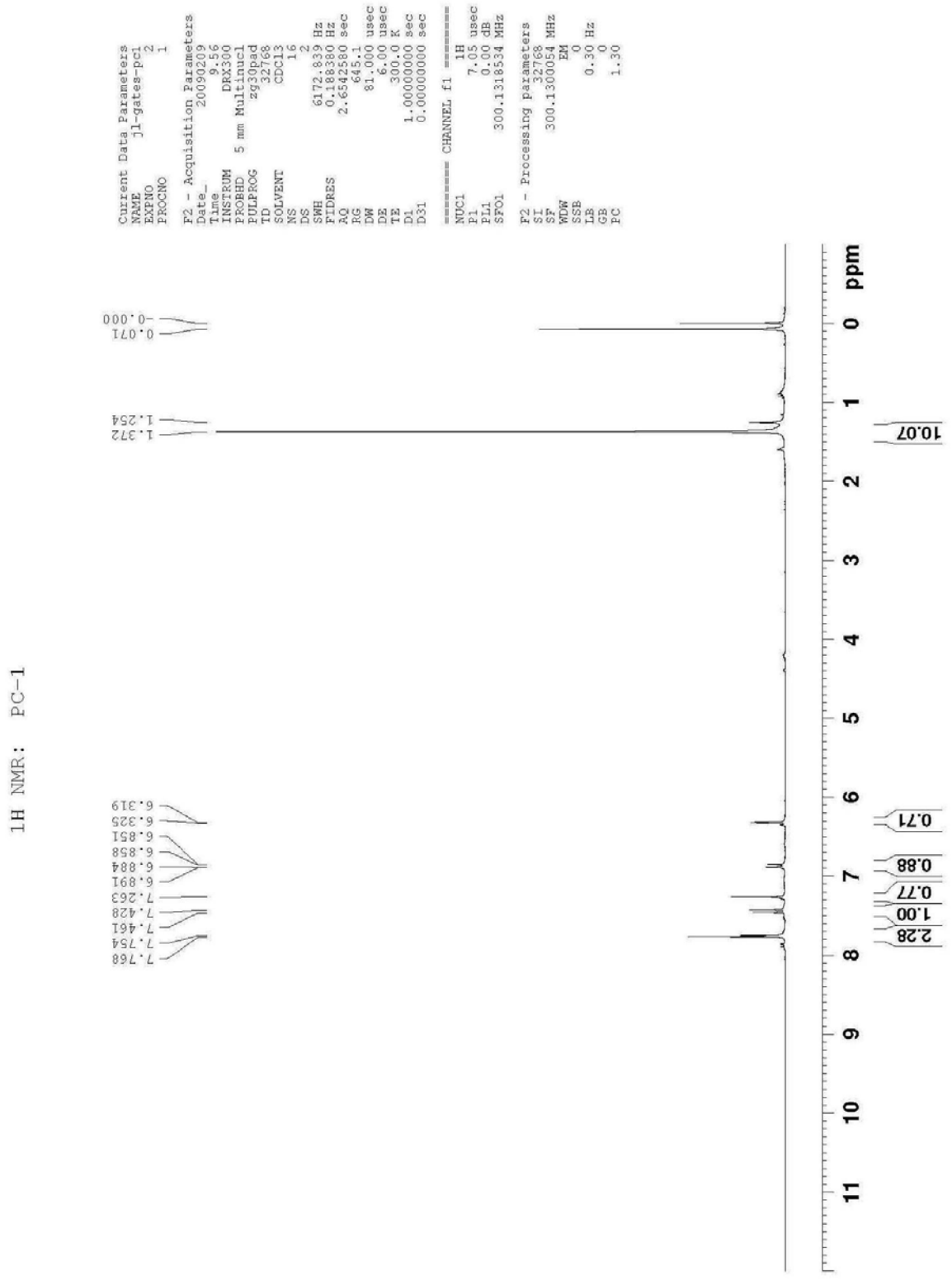

Figure 4.11 ^{1}H NMR of PC-1 (1)

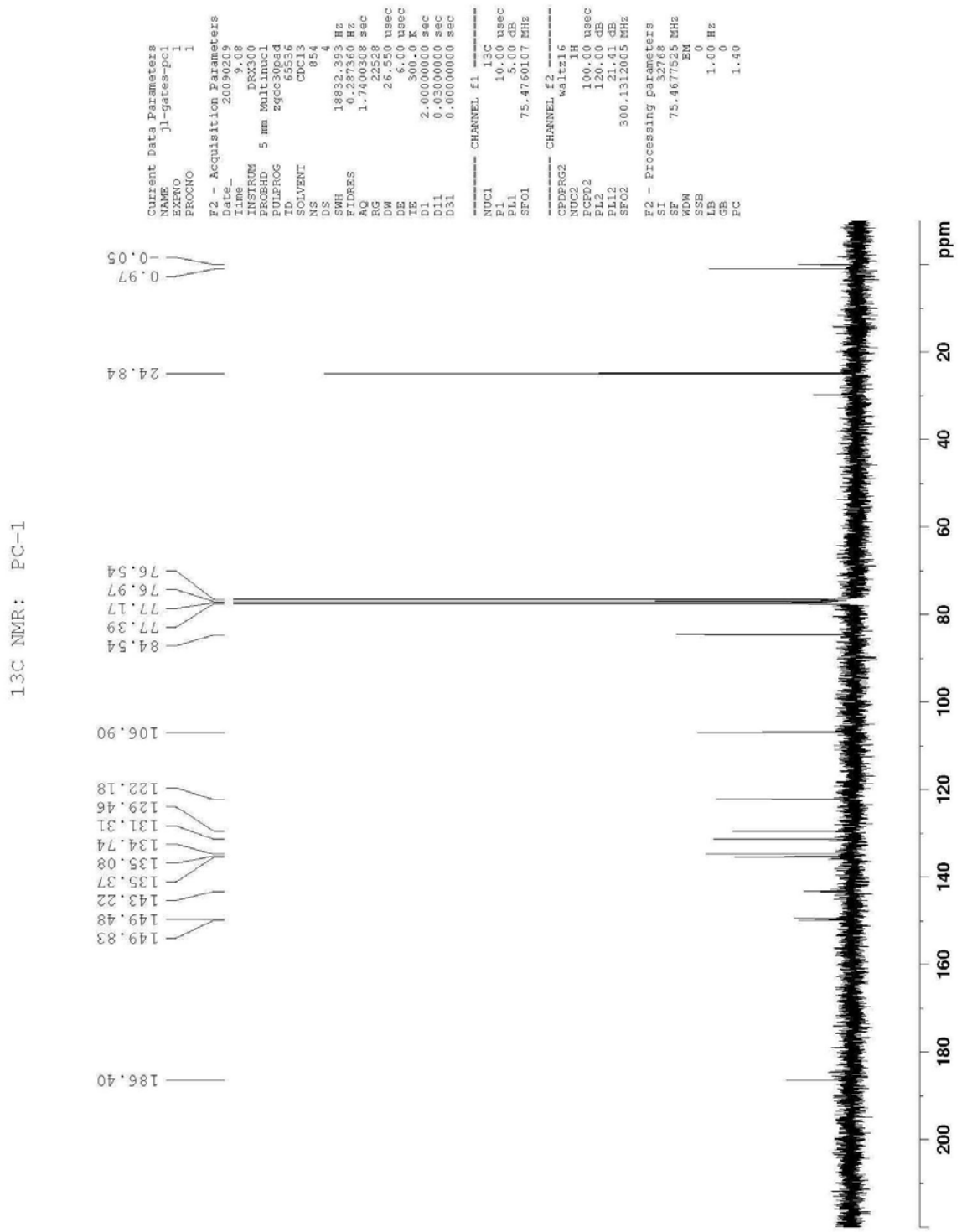

Figure 4. 4.12 ^{13}C NMR of PC-1 (1).

References

1. O'Brien, P. J., Radical formation during the peroxidase catalyzed metabolism of carcinogens and xenobiotics: The reactivity of these radicals with GSH, DNA, and unsaturated lipid. *Free Radical Biology and Medicine* **1988,** *4* (3), 169-183.

2. Staniek, K.; Nohl, H., Are mitochondria a permanent source of reactive oxygen species? *Biochimica et Biophysica Acta (BBA) - Bioenergetics* **2000,** *1460* (2-3), 268-275.

3. Nauseef, W. M., How human neutrophils kill and degrade microbes: an integrated view. *Immunological Reviews* **2007,** *219* (1), 88-102.

4. Forman, H. J.; Fukuto, J. M.; Torres, M., Redox signaling: thiol chemistry defines which reactive oxygen and nitrogen species can act as second messengers. *Am J Physiol Cell Physiol* **2004,** *287* (2), C246-256.

5. Sundaresan, M.; Yu, Z.-X.; Ferrans, V. J.; Irani, K.; Finkel, T., Requirement for Generation of H_2O_2 for Platelet-Derived Growth Factor Signal Transduction. *Science* **1995,** *270* (5234), 296-299.

6. Goldstein, B. J.; Mahadev, K.; Wu, X.; Zhu, L.; Motoshima, H., Role of Insulin-Induced Reactive Oxygen Species in the Insulin Signaling Pathway. *Antioxidants & Redox Signaling* **2005,** *7* (7-8), 1021-1031.

7. Stone, J. R., An assessment of proposed mechanisms for sensing hydrogen peroxide in mammalian systems. *Archives of Biochemistry and Biophysics* **2004,** *422* (2), 119-124.

8. Stone, J. R.; Yang, S., Hydrogen Peroxide: A Signaling Messenger. *Antioxidants & Redox Signaling* **2006,** *8* (3-4), 243-270.

9. Rhee, S. G., Measuring H_2O_2 produced in response to cell surface receptor activation. *Nat. Chem. Biol.* **2007,** *3* (5), 244-246.

10. Miller, E. W.; Tulyathan, O.; Isacoff, E. Y.; Chang, C. J., Molecular imaging of hydrogen peroxide produced for cell signaling. *Nat Chem Biol* **2007,** *3* (5), 263-267.

11. Miller, E. W.; Albers, A. E.; Pralle, A.; Isacoff, E. Y.; Chang, C. J., Boronate-Based Fluorescent Probes for Imaging Cellular Hydrogen Peroxide. *J. Am. Chem. Soc.* **2005,** *127* (47), 16652-16659.

12. Labutti, J.; Parsons, I.; Huang, R.; Miwa, G.; Gan, L. S.; Daniels, J. S., Oxidative Deboronation of the Peptide Boronic Acid Proteasome Inhibitor Bortezomib: Contributions from Reactive Oxygen Species in This Novel Cytochrome P450 Reaction. *Chem. Res. Toxicol.* **2006,** *19* (4), 539-546.

13. Pekol, T.; Daniels, J. S.; Labutti, J.; Parsons, I.; Nix, D.; Baronas, E.; Hsieh, F.; Gan, L.-S.; Miwa, G., Human metabolism of the proteasome inhibitor bortezomib: Identification of circulating metabolites. *Drug. Metab. Dispos.* **2005,** *33* (6), 771-777.

14. Brown, H. C.; Midland, M. M.; Kabalka, G. W., Stoichiometrically controlled reaction of organoboranes with oxygen under very mild conditions to achieve essentially quantitative conversion into alcohols. *JACS* **1971,** *93* (4), 1024-1025.

15. LaButti, J. N.; Gates, K. S., Biologically relevant chemical properties of peroxymonophosphate (O3POOH). *Bioorg. Med. Chem. Lett.* **2009,** *19* (1), 218-221.

Chapter 5

Enzymatic Production of Peroxymonophosphate

5.1 Introduction and objectives

We have thus far synthesized, characterized, and observed the redox effects of peroxymonophosphate on the archetypal protein tyrosine phosphatase PTP1B and SHP-2. It is clear from the results of these experiments that peroxymonophosphate possesses properties expected for an endogenous redox-regulator of protein tyrosine phosphatase activity. These properties include, but are not limited to: Active site directed, thiol-reversible oxidative inactivation of a PTP that is orders of magnitude faster than hydrogen peroxide. A critical property that remains to be investigated is that of biological accessibility. While the enzymatic processes that lead to generation of hydrogen peroxide by NADPH oxidases during intracellular signaling are relatively well characterized, we have yet to uncover evidence for production of peroxymonophosphate by enzymatic processes.

Conceptually, our hypothesis for enzymatic production of peroxymonophosphate is straightforward and is based upon two well-accepted concepts:

1. Enzyme mediated phosphoryl transfer (also known as "phosphotransferase" activity) is a ubiquitous process in cellular systems.[1]
2. Hydrogen peroxide is a much more potent nucleophile than water due to both its intrinsic reactivity ($k_{HOO^-}/k_{HO^-} \sim 100$) and its greater anionic fraction at physiologic pH ($pK_a\ H_2O_2 = 11.6$; $pK_a\ H_2O = 15.7$).[2]

In this scenario, hydrogen peroxide would compete with water during the catalytic cycle of an enzyme and release peroxymonophosphate instead of inorganic phosphate. We have coined a term for enzymes that would accomplish this process: *peroxykinases*.

The concept of phosphotransferase activity by phosphohydrolases has been well characterized in the literature.[3, 4] When considering a feasible peroxykinase scenario, one would therefore envision that an enzyme of the phosphohydrolase class (EC 3.1.3 superfamily) would utilize an alternative nucleophile to water when cleaving a phosphoenzyme intermediate (Scheme 5.1). This class of enzymes, given the formal term "phosphoric monoester hydrolases" by the IUPAC-IUBMB Joint Commission on Biochemical Nomenclature (JCBN) and Nomenclature Committee of IUBMB (NC-IUBMB) includes a diverse group ranging from prototypical phosphatases such as alkaline phosphatase and protein tyrosine phosphatases to metallo-enzymes such as purple acid phosphatase.[5]

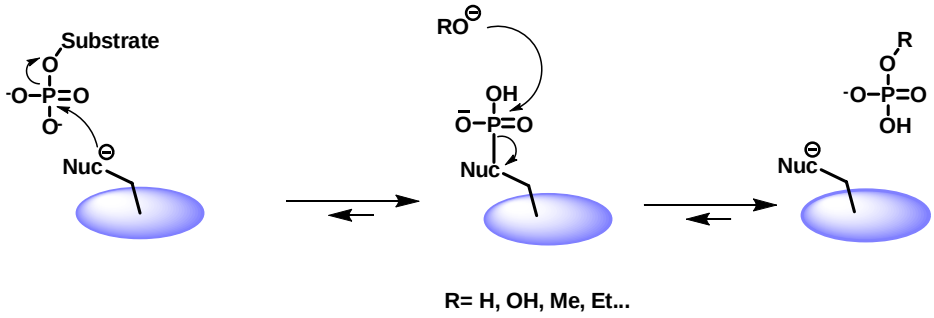

Scheme 5.1 A general mechanistic view of enzyme mediated phosphotransferase activity by a phosphatase. In the specific case of peroxykinase activity to generate peroxymonophosphate, R = OH.

In the studies described in herein, we investigate whether or not phosphoryl transfer to hydrogen peroxide, i.e., peroxykinase, can be accomplished through enzymatic processes thereby producing peroxymonophosphate. We initially used the redox-regulated protein tyrosine phosphatase PTP1B to test for peroxykinase activity, due to its high sensitivity towards peroxymonophosphate (~ 55,000 $M^{-1}s^{-1}$). We then employed the peroxymonophosphate-selective redox indictor PC-1 in combination with a variety of EC 3.1.3 class enzymes to screen for peroxykinase activity across the enzyme superfamily. Finally, we confirmed the enzymatic production of peroxymonophosphate via quantitative ^{31}P NMR in conjunction with authentic standards.

5.2 Utilizing PTP1B to Detect Peroxykinase Activity

It is clear, from the experiments described in Chapter 3, that peroxymonophosphate rapidly inactivates PTP1B through oxidation of its active site catalytic cysteine thiolate. The rate of inactivation with peroxymonophosphate is in fact orders of magnitude greater than that observed with hydrogen peroxide (~55,000 versus ~20 M-1s-1). This makes PTP1B an ideal candidate to identify peroxykinase activity, because of its ability to respond (lose activity) to very low concentrations of peroxymonophosphate. Scheme 5.2 depicts the general protocol for detection of peroxykinase activity with PTP1B. The first step is to combine putative peroxykinase with an appropriate mono-phosphorylated substrate in the presence of hydrogen peroxide. After allowing the enzyme to act upon substrate for a certain amount of time, excess hydrogen peroxide is quenched by adding catalase. This is a crucial step due to the fact that in the early, proof of concept phase these experiments were carried out under "forcing conditions": High substrate and very high H_2O_2 concentrations. Following H_2O_2 quenching, both peroxykinase and catalase are removed via centrifugal filtration. This is a crucial step, because the presence of other phosphohydrolase enzymes would negate the probative value of PTP1B for peroxymonophoshate by creating a large background of substrate turnover. Thus, a viable assay must to include a step that removes the putative peroxykinase enzyme prior to addition of PTP1B. Finally, to the centrifugal filtrate is added PTP1B and *p*NPP, and the activity of the enzyme is monitored at 410 nm.

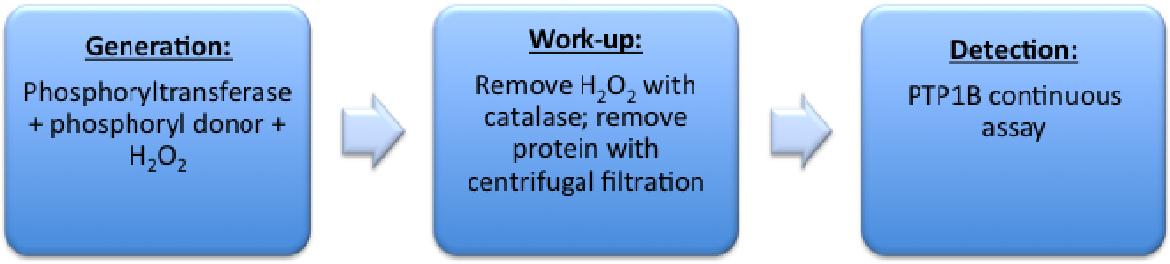

Scheme 5.2 General protocol for detection of peroxykinase activity with PTP1B.

The first enzyme chosen for our proof of concept studies was AcpA. This acid phosphatase class enzyme (Acp) was first isolated from the pathogen *Francisella tulerensis* by Reilly and colleagues.[6] AcpA was chosen for three main reasons:

1. Acid phosphatases, including AcpA, have been shown to exhibit phosphotransferase activity with alternate nucleophiles such as methanol and ethanol.[6-8]
2. AcpA was well characterized and possessed low K_m and high V_{max} for readily available reasonably priced substrates such as 5' adenosine monophosphate.[6]
3. Professor Reilly kindly offered to give us purified enzyme for our experiments.

The results of initial studies carried out with AcpA in the presence of 10 mM 5'-adenosine monophosphate and 1, 10 or 100 mM H_2O_2 are shown in Figure 5.1. It is clear that there is a reactive oxygen species produced during the incubation of AcpA, with 5'AMP and hydrogen peroxide that causes time-dependent inactivation of PTP1B at all three concentrations of hydrogen peroxide. Importantly, the produced ROS is not a substrate for catalase. Furthermore, controls that combined AcpA and 5' AMP *without* hydrogen peroxide had little or no effect on PTP1B activity. Finally, the procedure for

quenching hydrogen peroxide was shown to be valid by fortifying a buffer blank with 1M H_2O_2. This control, after processing it in way identical to other samples, showed minimal inactivation of PTP1B. This, overall, was a significant step towards identifying peroxykinase activity and was, thus, a very exciting result.

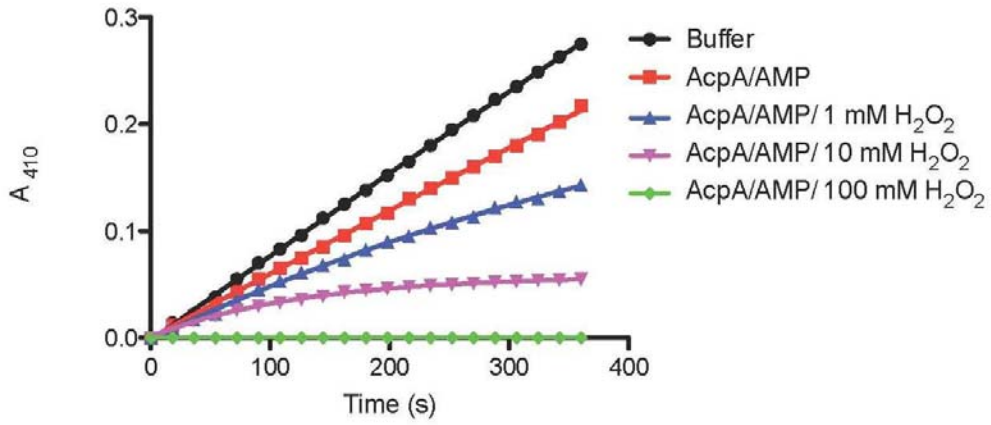

Figure 5.1 Time-dependent inactivation of PTP1B by the product of a phosphatase enzymatic reaction in the presence of various concentrations of hydrogen peroxide.

5.3 Use of PC-1 to Probe for Enzymatic Production of Peroxymonophosphate

While it may initially appear desirable to utilize PTP1B activity to probe a wide variety of enzymes for peroxykinase activity, close examination of the technical details of the assay indicate otherwise. The prototypical procedure for the assays, as shown in Scheme 5.1, includes a step dedicated to removal of the putative peroxykinase from the incubation volume with centrifugal filtration. While this step is not technically challenging it does not lend itself to rapid analysis of multiple samples due to the length of time required for centrifugal filtration (~ 45 min.). Furthermore, it adds significant

expense to the assay; at the time of the study the filters cost roughly ten dollars each. It is more economical, in both time and resources, therefore to utilize the peroxymonophosphate-selective redox detector PC-1 instead of PTP1B to screen for enzymatic production of peroxymonophosphate. A depiction of the new assay is shown in Scheme 5.3. For reasons elaborated in the previous section, the acid phosphatase AcpA was chosen for initial experiments with PC-1.

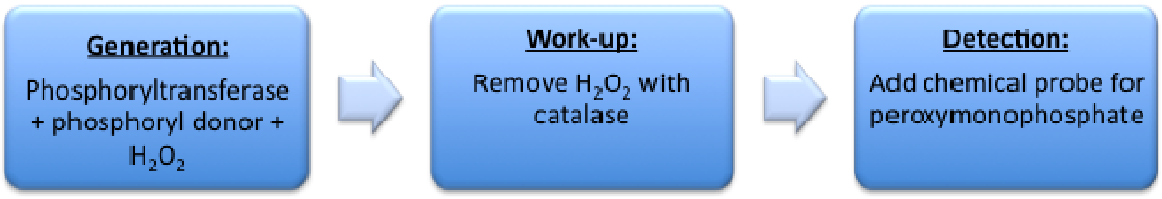

Scheme 5.3 General procedure for detection of peroxykinase activity. In the detection phase, the chemical probe may be either a fluorescent redox indicator, or a redox-regulated protein.

In the presence of 5' adenosine monophosphate and hydrogen peroxide we find that AcpA produces a reactive oxygen species that causes elevated PC-1 deboronation rates (Figure 5.2). Importantly, this reactive oxygen species is it not a substrate for catalase. Furthermore, the rate of PC-1 deboronation is concentration-dependent with respect to the initial concentrations of hydrogen peroxide. Finally, the presence of hydrogen peroxide, phosphorylated substrate and enzyme are necessary to achieve elevated rates of PC-1 deboronation. This provides good, albeit indirect, evidence for peroxykinase activity by AcpA.

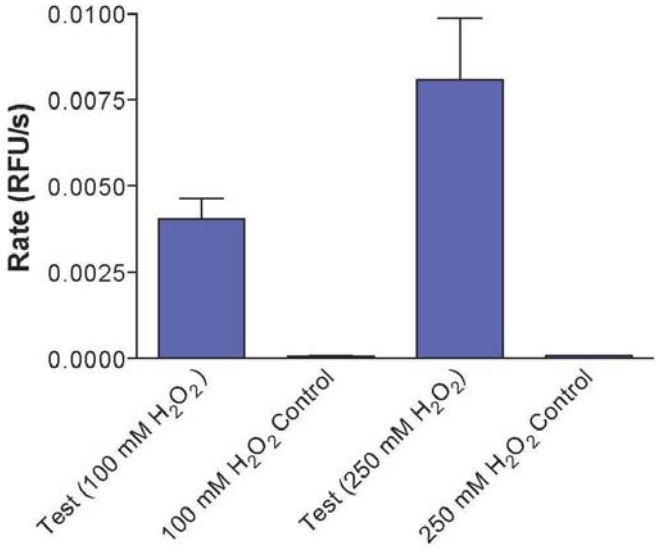

Figure 5.2 Deboronation rates of PC-1 by the product of reaction mixture of AcpA combined with 5' adenosine monophosphate and hydrogen peroxide.

5.4 Confirmation of Enzyme-produced Peroxymonophosphate With ^{31}P NMR

We recognized that while our data supported the notion of peroxykinase activity, direct evidence of enzyme-generated peroxymonophosphate was needed. We accomplished this through the careful use of quantitative ^{31}P NMR. The limit of detection for peroxymonophosphate with the 250 mHz instrument to which we had access was determined to be at or around 2 mM with a ten minute quantitative scan. To facilitate detection of peroxymonophosphate with ^{31}P NMR we therefore decided to try to enhance its production by increasing the concentrations of both substrate and hydrogen peroxide from 10 mM/1-100mM to 100mM/1M, respectively.

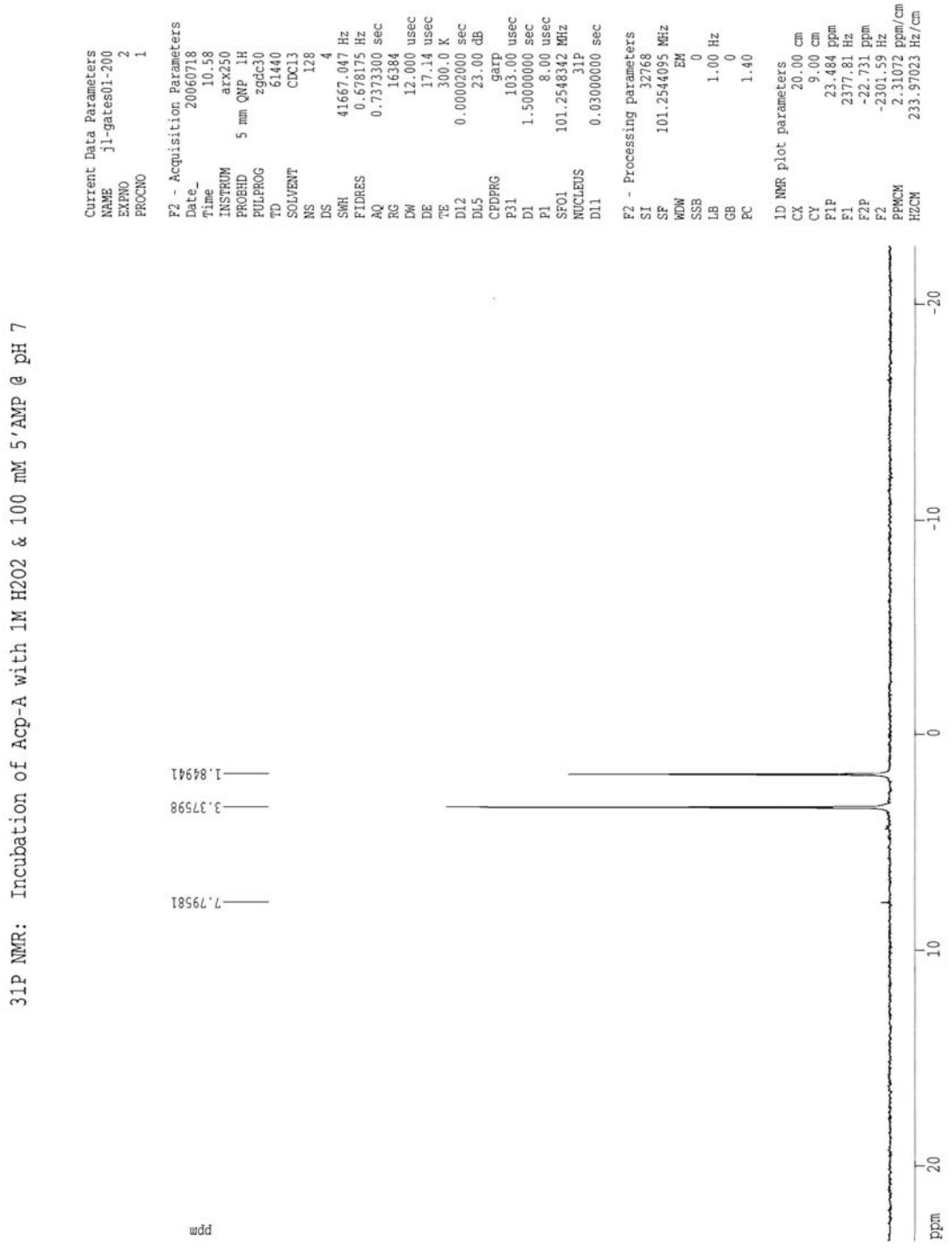

Figure 5.3 ^{31}P NMR of a test for peroxykinase activity that contained AcpA, 1M H_2O_2 and 100 mM 5'-AMP @ pH 7.0. Peaks are assigned as follows: peroxymonophosphate: 7.8 ppm; 5'-AMP: 3.4 ppm and inorganic phosphate at 1.9 ppm.

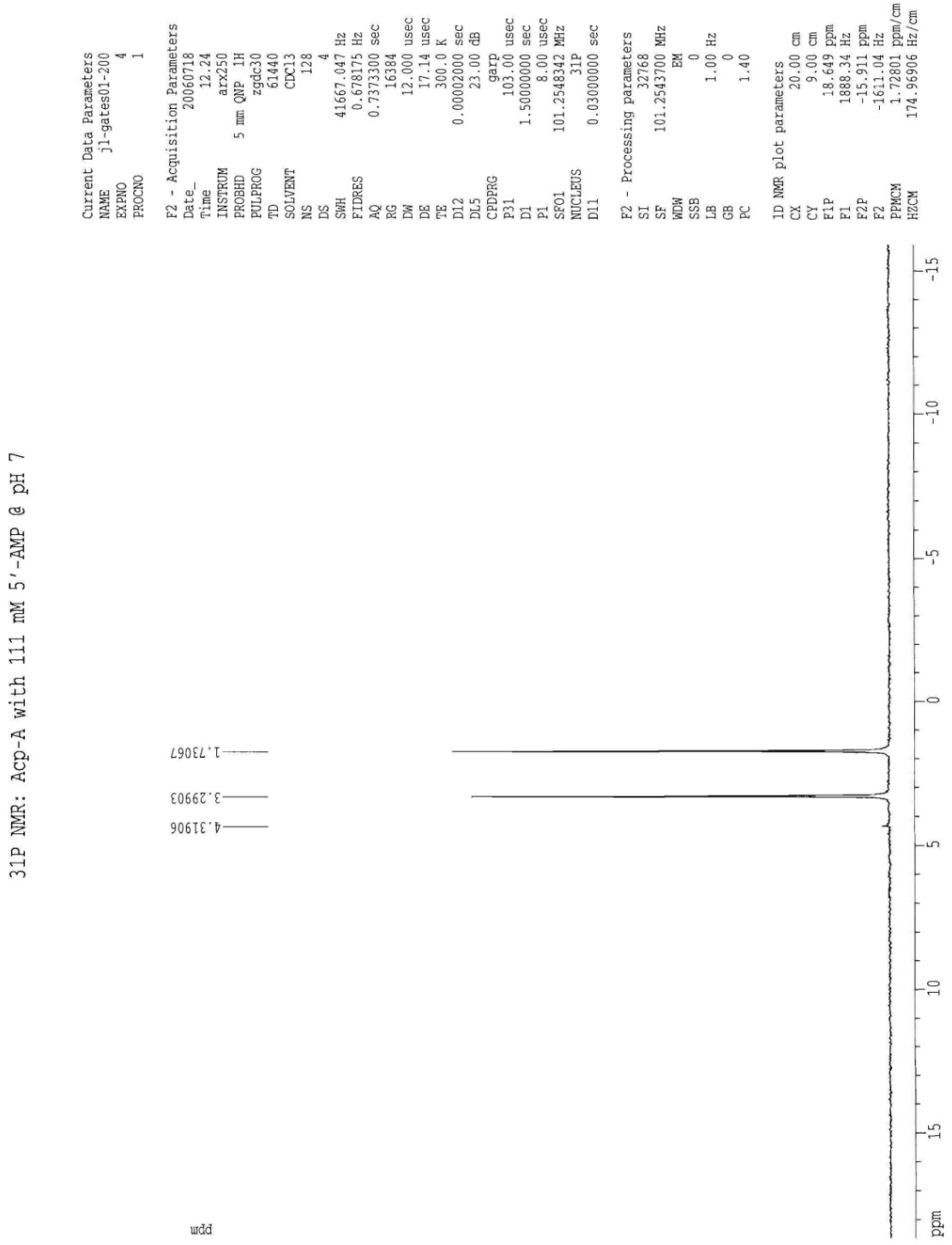

Figure 5.4 ^{31}P NMR of a control sample for peroxykinase activity that contained AcpA and 100 mM 5'-AMP. Peaks are assigned as follows: 5'-AMP: 3.3 ppm; inorganic phosphate: 1.7 ppm.

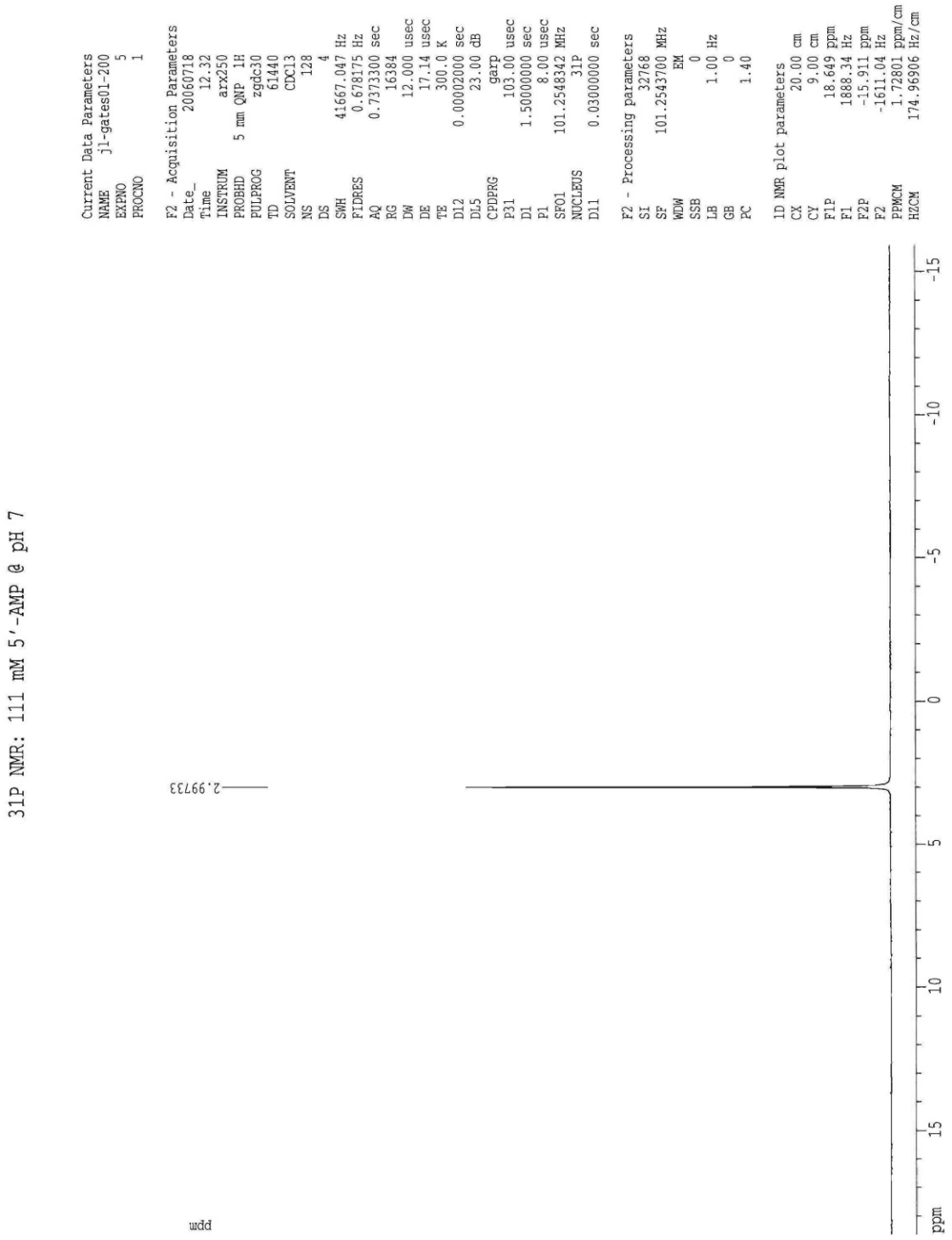

Figure 5.5 ^{31}P NMR of a negative control for peroxykinase activity that contained 100 mM 5'-AMP in pH 7.0 buffer (3 ppm).

AcpA, in the presence of 5'-AMP and hydrogen peroxide was found to generate a product with a chemical shift similar to that of peroxymonophosphate (7.8 ppm, Figure 5.3). Addition of iodate to the sample destroyed this peak (data not shown). Importantly, controls that lacked either hydrogen peroxide or AcpA failed to produce such a product (Figures 5.4 and 5.5).

To further support our hypothesis that phosphoryl transfer to hydrogen peroxide can be accomplished by a variety of phosphohydrolases, we included alkaline phosphatase in our NMR studies. Alkaline phosphatase is another phosphohydrolase that has been shown to exhibit phosphotransferase activity.[4]

Observed chemical shifts are highly dependent on the solvent environment under which they are measured[9] (pH, solvent dipole moment), therefore it was necessary to carefully prepare each sample with identical constituents. A positive control for peroxymonophosphate would entail fortifying a sample with an authentic standard of known quantity. Due to the fact that the preparation of peroxymonophosphate involves the use of perchloric acid, and that the authentic standard would therefore contain millimolar concentrations, it was necessary to fortify the test samples with an identical amount of the acid to maintain an equal solvent environment for NMR.

Figure 5.6 shows the results of ^{31}P NMR analysis of a sample containing alkaline phosphatase, 5' adenosine monophosphate and hydrogen peroxide, an identical sample fortified with authentic peroxymonophosphate standard and an associated negative control. The presence of a peroxymonophosphate peak at 5.2 ppm is clear in both the test and positive control samples. This data provides direct evidence that supports our

concept of peroxykinase activity by a member of the phosphoric monoester hydrolase class of enzymes.

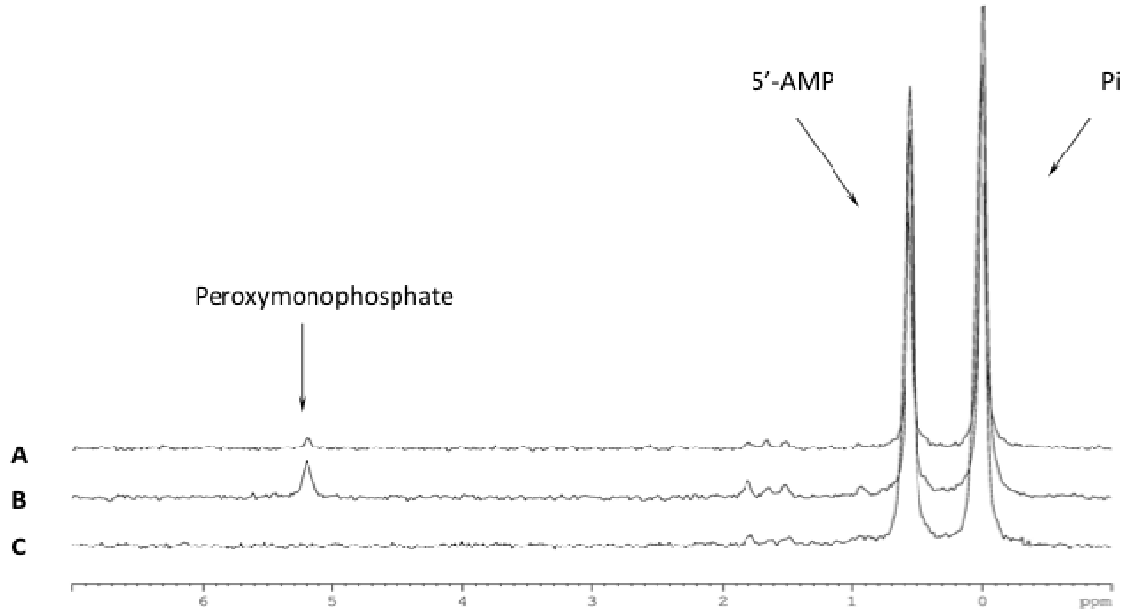

Figure 5.6 Detection of peroxymonophosphate generated by alkaline phosphatase in the presence of 5'-adenosine monophosphate and hydrogen peroxide. A: alkaline phosphatase + 100 mM 5'-adenosine monophosphate + 1M hydrogen peroxide. B alkaline phosphatase + 100 mM 5' adenosine monophosphate + 1M hydrogen peroxide fortified with peroxymonophosphate authentic standard to ~ 10 mM. C: alkaline phosphatase + 100 mM 5'-adenosine monophosphate.

5.5 Conclusions

Both the acid phosphatase AcpA and alkaline phosphatase have demonstrated peroxykinase activity. These results are a proof-of-concept for the notion that peroxymonophosphate could be a biologically relevant redox regulator. There are 79 discreet sub-classes of phosphoric monoester hydrolases (EC 3.1.3.X) that possess a wide variety of active sites and respective substrates. In addition to the phosphoric monoester

hydrolase class, there exist other similar classes of enzyme that could possess peroxykinase activity including phosphoric diester (EC 3.1.4), diphosphoric monoester (EC 3.1.7), and phosphoric triester hydrolases (EC 3.1.8). Furthermore, classes of enzyme seemingly disparate from the phosphohydrolases such as non-heme and vanadium variants of chloroperoxidase (EC 1.11.1; oxidoreductases that act on peroxide as an acceptor) have been identified that exhibit phosphatase activity.[10, 11] This is not entirely surprising, because several investigators have noted similarities in active site architecture between these peroxidases and phosphatase class enzymes.[12, 13] These chloroperoxidase enzymes are particularly intriguing due to the fact that they have intrinsic affinity for and utilize hydrogen peroxide during their catalytic cycle. In fact, these enzymes have been found to transfer hydrogen peroxide to an acylated enzyme intermediate to produce peroxyacetic acid (Scheme 5.4). It seems reasonable, then, to hypothesize that production of peroxymonophosphate could occur from a phosphorylenzyme intermediate that was formed during phosphatase activity. The lack of commercial availability of these enzymes, however, precluded their inclusion in the studies presented here due to time constraints. Perhaps in the near future the Gates Lab will be able to clone the genes that encode these enzymes and express them for testing.

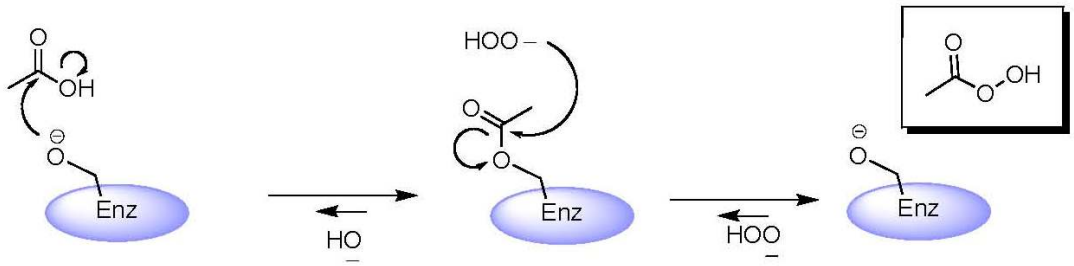

Scheme 5.4 Generation of peroxyacetic acid from the catalytic cycle of non-heme bacterial chloroperoxidase involves the use of hydrogen peroxide as an acyl acceptor.

We envision future studies that take advantage of both the selectivity of PC-1 towards peroxymonophosphate, and the resistance of peroxymonophosphate to decomposition by catalase to screen a wide array of enzymes for peroxykinase activity. For example, a native 2D proteomic gel could be screened for peroxykinase activity by bathing the gel in universal phosphatase substrate and hydrogen peroxide. Excess hydrogen peroxide would then be quenched with catalase, followed by bathing of the gel in a solution of PC-1. Analysis of the gel with fluorescence imaging could then identify discreet proteins that "light up" PC-1.

5.6 Experimental Procedures

Methods and Materials

Reagents were purchased from the following suppliers: Buffers, salts, *p*-nitrophenylphosphate (*p*NPP) (# N4645), 5' adenosine monophosphate (5'AMP, # A1752), hydrogen peroxide (# H325), bovine catalase (# C3155), human alkaline phosphatase (#P3895), bovine alkaline phosphatase (#P7923), purple acid phosphatase (#), were obtained from Sigma-Aldrich (St. Louis, MO). Zeba mini and micro centrifugal

buffer exchange columns (#89882) were purchased from Pierce Biotechnology (Rockford, IL). Amicon Centricon 30,000 MWCO centrifugal filter devices (# 4208) were purchased from Millipore (Milford, MA). PTP1B was prepared as described in Chapter 3. PC-1 was prepared as described in Chapter 4.

Utilizing PTP1B to Detect Peroxykinase Activity. To support our hypothesis that peroxyphosphate could be generated through enzymatic phosphoryl transfer, we utilized PTP1B as a probe. In the generation phase of this assay, AcpA (30 ng/ml), substrate (5'-adenosine monophosphate, 10 mM) and hydrogen peroxide (1, 10 and 100 mM) were combined in 1.0 mL of assay buffer (100 mM Bis-tris, pH 7.0) and allowed to incubate for 10 minutes at 37^{o}C. Excess hydrogen peroxide was then removed by adding ~1000 units of catalase and the resulting mixture was allowed to stand for five minutes at room temperature. AcpA was removed from the reaction volume with centrifugal filtration (Centricon, 30,000 MWCO, 30 minutes @ 5000 x g), and the resulting filtrate was tested for the presence of peroxymonophosphate with a PTP1B-based continuous enzymatic assay. In this assay, to 0.5 mL of filtrate was added 0.5 mL of a 20 mM solution of p-nitrophenyl phosphate dissolved in assay buffer, and 5 μL of thiol-free PTP1B that was prepared as described in Chapter 3 (~2 μg/mL, or 75 nM, final concentration). The apparent rate of time-dependent PTP1B inactivation was then determined by fitting the data to the equations described in chapter 3. Control incubations were performed with AcpA that lacked one of the following: hydrogen peroxide, substrate, or phosphotransferase with and without added catalase. In addition, substrate was combined with hydrogen peroxide and assayed for inactivation of PTP1B.

Detection of Peroxykinase activity with PC-1. The protocol to test for generation of peroxymonophosphate by phosphohydrolase-class enzymes was divided into three phases: generation, work-up, and observation. In the generation phase, enzyme (0.1 mg/ml), hydrogen peroxide (100 mM) and substrate (*p*-nitrophenylphosphate, or 5' adenosine monophosphate, 10 mM) were combined in 1.0 mL of assay buffer (100 mM Bis-tris, 120 mM NaCl, 1 mM $MgCl_2$) and incubated at room temperature for 30 minutes. Following the incubation, a work-up was performed in which 100 units of catalase was added to remove excess hydrogen peroxide in a five minute incubation at room temperature. We probed for the presence of peroxymonophosphate by adding 10 μL of a 100 μM solution of PC-1 in acetonitrile to the reaction volume in a fluorescence cuvette and measuring the increase in PC-1 fluorescence intensity every 5 seconds for one minute (Ex: 550 (4) nm; Em: 585 (4) nm). The apparent rate of PC-1 fluorescence increase was derived from plotting relative fluorescence intensity versus time and finding the slope of the resulting line by fitting the data to a linear equation.

Direct observation of enzyme-generated peroxymonophosphate with ^{31}P NMR. Confirmation of enzyme-generated peroxymonophosphate was accomplished via direct observation with ^{31}P NMR. Three reaction aliquots (1.0 mL final volume) of assay buffer (100 mM Bis-tris, pH 7.0) containing either AcpA or alkaline phosphatase and substrate, 5' adenosine monophosphate was prepared both with (1 aliquot) and without (2 aliquots) hydrogen peroxide and incubated as previously described. A sample lacking hydrogen peroxide was then fortified with peroxymonophosphate from quantified authentic standard to a final concentration of 10 mM. To maintain an equivalent NMR environment in the test sample that had contained hydrogen peroxide, it was fortified

with perchloric acid to a final concentration of 83 mM. Finally, another sample lacking hydrogen peroxide was unaltered for analysis as a negative control. The three samples were quickly analyzed with quantitative ^{31}P NMR (within 10 minutes of quenching hydrogen peroxide) as described in chapter 2 to minimize loss of peroxymonophosphate through degradation.

References

1. Thompson, P. R.; Cole, P. A., Probing the mechanism of enzymatic phosphoryl transfer with a chemical trick. *Proceedings of the National Academy of Sciences of the United States of America* **2001,** *98* (15), 8170-8171.

2. Herschlag, D.; Jencks, W. P., Nucleophiles of high reactivity in phosphoryl transfer reactions: α-effect compounds and fluoride ion. *J. Am. Chem. Soc.* **1990,** *112* (5), 1951-1956.

3. Coleman, J. E., Structure and Mechanism of Alkaline Phosphatase. *Annual Review of Biophysics and Biomolecular Structure* **1992,** *21* (1), 441-483.

4. Jackson, M. D.; Denu, J. M., Molecular Reactions of Protein Phosphatases-Insights from Structure and Chemistry. *Chem. Rev.* **2001,** *101* (8), 2313-2340.

5. IUPAC-IUBMB Joint Commission on Biochemical Nomenclature (JCBN) and Nomenclature Committee of IUBMB (NC-IUBMB). *European Journal of Biochemistry* **1999,** *264* (2), 607.

6. Reilly, T. J.; Baron, G. S.; Nano, F. E.; Kuhlenschmidt, M. S., Characterization and Sequencing of a Respiratory Burst-inhibiting Acid Phosphatase from Francisella tularensis. *J. Biol. Chem.* **1996,** *271* (18), 10973-10983.

7. B.C Jeong, H.-W. K., L.E Macaskie,, Phosphotransferase activity of acid phosphatases of a Citrobacter sp. *FEMS Microbiology Letters* **1997,** *147* (1), 103-108.

8. Dissing, K.; Uerkvitz, W., Class B nonspecific acid phosphatase from Salmonella typhimurium LT2: Phosphotransferase activity, stability and thiol group reactivity. *Enzyme and Microbial Technology* **2006,** *38* (5), 683-688.

9. Hunter, J. K. M. S. a. B. K., *Modern NMR Spectroscopy, A Guide for Chemists*. Oxford University Press: New York, 1991.

10. Preobrazhenskaya, Y. V.; Voskoboev, A. I.; Burd, V. N., Phosphatase activity of non-heme chloroperoxidase from the bacterium Serratia marcescens. *FEBS Letters* **2003,** *536* (1-3), 41-44.

11. Renirie, R.; Hemrika, W.; Wever, R., Peroxidase and Phosphatase Activity of Active-site Mutants of Vanadium Chloroperoxidase from the Fungus Curvularia inaequalis. IMPLICATIONS FOR THE CATALYTIC MECHANISMS. *J. Biol. Chem.* **2000,** *275* (16), 11650-11657.

12. Hemrika, W.; Renirie, R.; Dekker, H. L.; Barnett, P.; Ron, W., From Phosphatases to Vanadium Peroxidases: A Similar Architecture of the Active Site. *Proceedings of the National Academy of Sciences of the United States of America* **1997,** *94* (6), 2145-2149.

13. Jennifer Littlechild, E. G.-R. A. D. M. I., Structural and functional comparisons between vanadium haloperoxidase and acid phosphatase enzymes. *Journal of Molecular Recognition* **2002,** *15* (5), 291-296.

Chapter 6

A Tryptophan-based Fluorescence Assay for Measuring PTP1B Inactivation Kinetics

6.1 Introduction and Objectives

Measurement of the kinetics of enzymatic time-dependent inactivation is typically accomplished with either a continuous or discontinuous assay. A continuous assay is performed by combining an enzyme of interest with an appropriate substrate (typically chromogenic or fluorescent) and various concentrations of inactivator.[1, 2] Time-dependent loss of enzymatic activity is observed with the proper instrumentation; such as A UV/vis for chromogenic substrates, or a spectrofluorimeter for fluorescent substrates (Figure 6.1). The apparent rates of enzyme inactivation are then determined by fitting the resulting data for each concentration of inactivator to an exponential decay equation. An apparent second order rate of enzyme inactivation is then derived from these apparent pseudo-first order rates (see chapter three for a more detailed description of this type of data analysis).

A discontinuous assay, in contrast, is performed by combining an enzyme with various concentrations of inactivator, then removing aliquots at specific times and testing them for enzyme activity with an appropriate substrate.[3] This data is then plotted on a semi-log plot and the apparent rates of inactivation for each concentration of inactivator are determined by fitting the data to an equation that depicts a straight line (Figure 6.2). The apparent second order rate of inactivation is then derived from these rates.

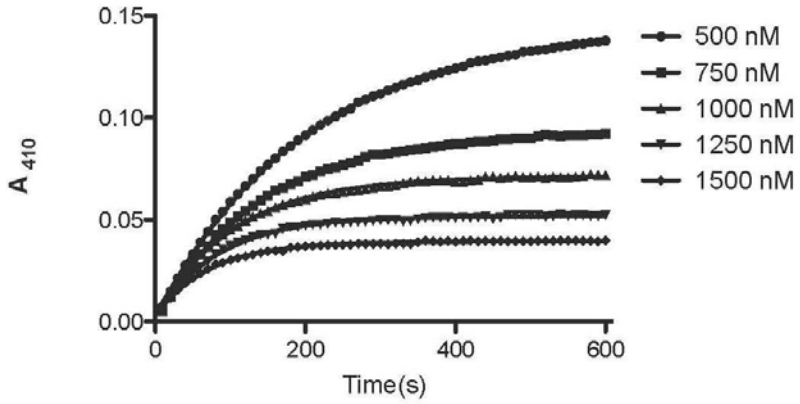

Figure 6.1 An example of time-dependent enzyme inactivation data generated with a continuous assay. This particular set of data was generated with PTP1B and the oxidative inactivator peroxymonophosphate.

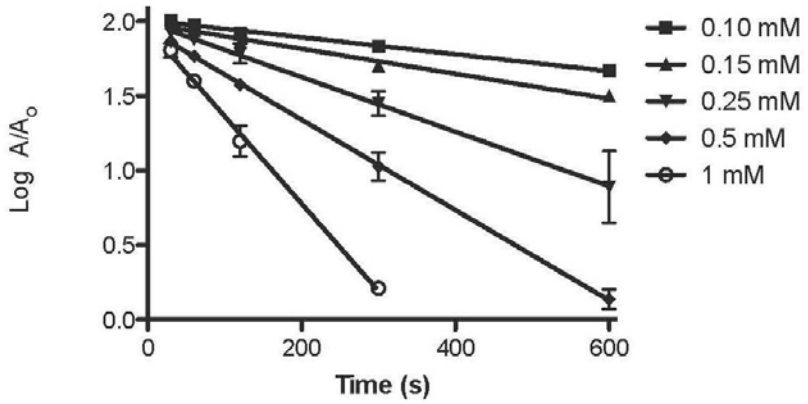

Figure 6.2 An example of time-dependent enzyme inactivation data generated with a discontinuous assay. This particular set of data was generated with PTP1B and the oxidative inactivator hydrogen peroxide.

There are advantages and disadvantages associated with each type of assay. An advantage of the continuous assay, for example, is the technical ease and speed at which it can be done. Specifically, a continuous assay for inactivation of PTP1B by peroxymonophosphate could be performed with five concentrations of H_2O_2 in triplicate in a few hours. Conversely, a discontinuous assay is cumbersome in comparison, taking approximately one full day of work (or more) to generate a similar set of data. Furthermore, this assay requires deft hand/eye coordination, situational awareness and very good organization on the part of the scientist due to the fact that one must keep track of several variables at once. Small errors in time, volume or concentration are amplified in the resulting data.

A general advantage of the discontinuous assay is that, in contrast to the continuous assay, there is no kinetic interference of substrate with the chemistry occurring at the enzyme active site. This provides for "clean" and direct analysis of the resulting data. Analysis of data from a discontinuous active site-directed assay requires

correcting for the presence of substrate during enzyme inactivation. The kinetics of oxidative inactivation of PTP1B by hydrogen peroxide and peroxymonophosphate have been determined using both of these techniques and are described in Chapter 3 of this dissertation.

The PTP1B catalytic subunit that we express and purify contains six tryptophan residues (Scheme 1), which is an unusually high number for a 322 amino acid protein. Of these six residues, Trp179 exists in the general space of the active site pocket as part of the so-called "WPD loop".[4] Oxidation of the catalytic cysteine thiolate (Cys215) to the sulfenic oxidation state leads to significant changes in the active site pockets secondary structure.[5, 6] In addition to these structural changes, there is an apparent increase in flexibility of the active site area due to neutralization of the cysteine thiolate negative charge and subsequent loss of its ionic interactions with positive charges.[7]

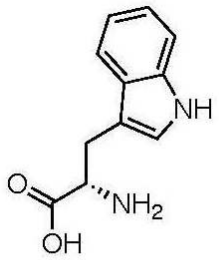

tryptophan (**1**)

Scheme 6.1 The amino acid tryptophan

It is known that the fluorescence quantum yield of tryptophans is very sensitive to the environment in which the indole side chain resides.[8, 9] We entered this line of experimentation with the following hypothesis: Due to the proximity of Trp179 to the

PTP1B active site (Figure 6.3), we hypothesized that the known changes in active site secondary structure that are associated with oxidative inactivation would cause a change in its solvation state. This change in solvation state would alter its quantum yield and change the overall fluorescence signature of the enzyme. Observed changes in fluorescence could therefore be utilized to measure rates of PTP1B oxidative inactivation.

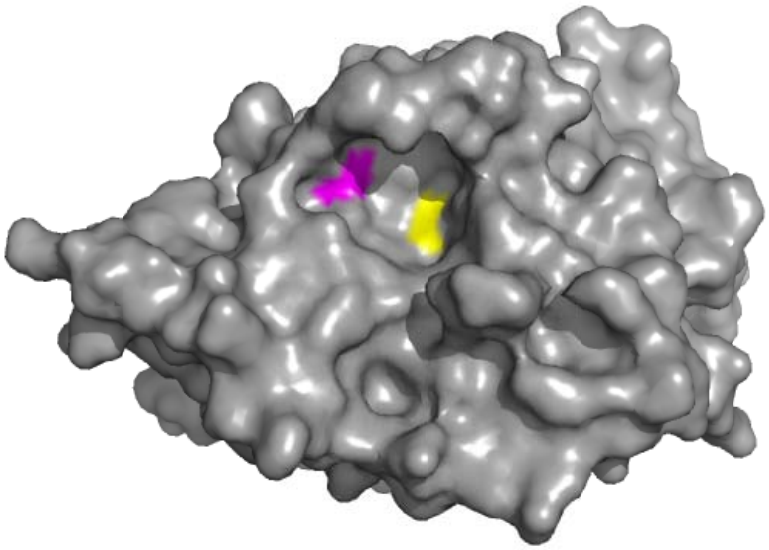

Figure 6.3 A surface model of native PTP1B derived from an X-ray crystal structure. This model shows the close proximity of Trp179 (magenta) to the active site catalytic cysteine thiolate (Cys215, yellow) and its position within the active site pocket.

6.2 Determining Optimum Excitation and Emission Parameters for Observing Tryptophan Fluorescence in Native and Oxidized PTP1B

While there were hints that tyrosine fluorescence could act as a reporter for PTP1B active site oxidation, there were no specific reports of such that we could find in the literature. Proof-of-concept studies were, therefore, necessary to start this project.

Our objective in these initial studies was to determine the optimum spectrofluorimeter excitation and emission settings to observe the kinetics of PTP1B active site oxidation.

To begin, thiol-free PTP1B was prepared, and then oxidized with hydrogen peroxide. We chose a concentration of 0.5 mM H_2O_2 because we had previously determined it would completely inactivate PTP1B within five minutes (see chapter 3). The SLM-Aminco spectrofluorimeter excitation monochrometer was set to 285 nm, which is at or around the known UV absorption maximum for tyrosine residues and provides good tryptophan fluorescence emission intensity.[10] Utilizing this excitation wavelength native PTP1B showed an emission spectrum with a broad maximum that ranged from approximately 315 to 340 nm (Figure 6.4). When this sample was treated with 0.5 mM H_2O_2 for five minutes, the fluorescence quantum yield was reduced approximately 25%, and the emission maximum became more defined at 335 nm. Tryptophan quantum yield (or relative fluorescence intensity) could therefore be used to measure the oxidation state of the PTP1B catalytic cysteine thiolate. Interestingly, when the enzyme was allowed to stand for 15 minutes with 0.5 mM H_2O_2, which most certainly caused "overoxidation" of the active site cysteine, there was little additional change in the emission spectrum. A difference spectrum between native and oxidized PTP1B showed that the optimal excitation wavelength to observe the kinetics of PTP1B oxidative inactivation was 320 nm.

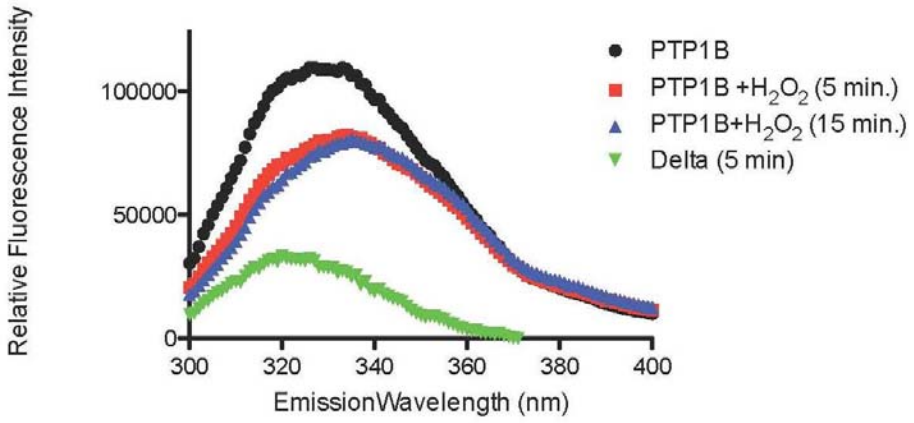

Figure 6.4 Fluorescence emission spectrum of PTP1B prior to (native) and after (oxidized) treatment with 0.5 mM hydrogen peroxide. Excitation monochrometer was set at 285 nm, with a 2 nm slit-width. Emission monochrometer was scanned from 300 to 400 nm with a 4 nm slit-width.

6.3 Optimal Spectrofluorimeter Settings for Observation of PTP1B Inactivation Kinetics

Initial experiments to measure the time-dependent inactivation of PTP1B by hydrogen peroxide were not successful due to irregularities in the data. Observation of PTP1B fluorescence when treated with 0.5 mM hydrogen peroxide showed what we thought was smooth single-phase exponential loss of fluorescence (Figure 6.5). When PTP1B was treated with hydrogen peroxide at or above concentrations of 1 mM, however, a biphasic decay of fluorescence was revealed (Figure 6.6). Upon further experimentation with buffer controls that contained only PTP1B, it was determined that several variables were dramatically affecting its fluorescence intensity. These uncontrolled variables, which will be discussed in the next few paragraphs, were the cause of the two decay phases observed at higher H_2O_2 concentrations. The apparent single phase exponential decay observed at lower concentrations was actually a combination of two rates.

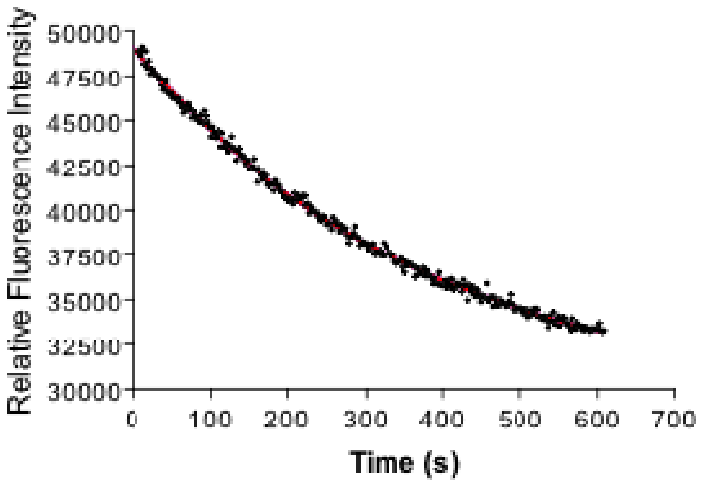

Figure 6.5 An example of apparent single-phase exponential decay of PTP1B fluorescence observed upon treatment of the enzyme with 0.5 mM hydrogen peroxide.

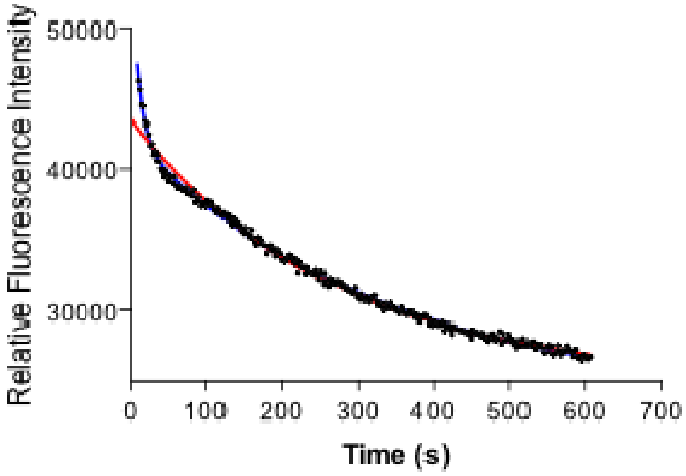

Figure 6.6 An example of biphasic PTP1B fluorescence decay observed upon treatment of the enzyme with 4 mM hydrogen peroxide. The blue and red lines represent curve fits for the first and second exponential rates of decay, respectively.

To obtain stable fluorescence emission at 320 nm, both the temperature and overall UV exposure of the sample had to be tightly controlled. Figure 6.7 shows that

changing the temperature of the sample a mere 3 degrees (from 25°C to 22°C) caused a decrease in quantum yield of approximately 10%. Furthermore, when a solution of PTP1B was continuously irradiated with 285 nm UV light, there was a clear exponential decay of tryptophan fluorescence at 320 nm. This is presumably the result of either tryptophan photobleaching or destruction through photooxidation.[9] When the temperature is held constant, and exposure to UV light minimized through employment of an excitation shutter (measurement of fluorescence intensity every 10 seconds), PTP1B fluorescence quantum yield is stable for at least ten minutes.

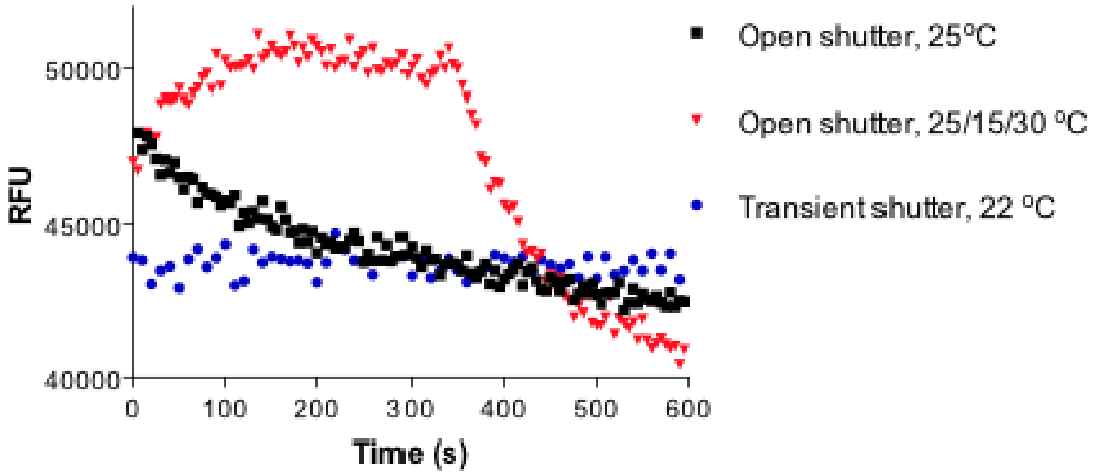

Figure 6.7 The effects of temperature and exposure to UV radiation on the fluorescence quantum yield of PTP1B. Temperature was either held constant, or varied from 25°C (@ 0 s) to 15°C (@10 s) to 30°C (@ 360 s). The observed changes in fluorescence intensity were representative of the time necessary for the cuvette to reach the programmed temperature.

6.4 Utilizing Fluorescence to Measure the Rate of PTP1B Oxidative Inactivation by H_2O_2

When combined with various concentrations of hydrogen peroxide under pseudo-first order conditions ([H_2O_2] > 10x [PTP1B]), the fluorescent yield of PTP1B decays in a time-dependent manner (Figure 6.8). The fluorescence decay appears to follow a single exponential rate, for when the data is plotted on a semi-log scale a straight line is obtained (Figure 6.9). This data was then fitted to the equation:

$$y = mx + b \qquad (1)$$

The resulting slope of each line represented the apparent pseudo-first-order rate of fluorescence decay, k_Ψ in units of s^{-1} (k_Ψ = m* 2.303). When these rates are then plotted as a function of hydrogen peroxide concentration, and the data again fitted to equation 1, the slope of the resulting line gave the apparent second order rate of PTP1B inactivation as 14.96 +/- 0.92 $M^{-1}s^{-1}$. This is in close agreement with data generated from both the discontinuous and continuous assays that yielded apparent second order inactivation rates with hydrogen peroxide of ~ 18 and 27 $M^{-1}s^{-1}$, respectively (see Chapter 3).

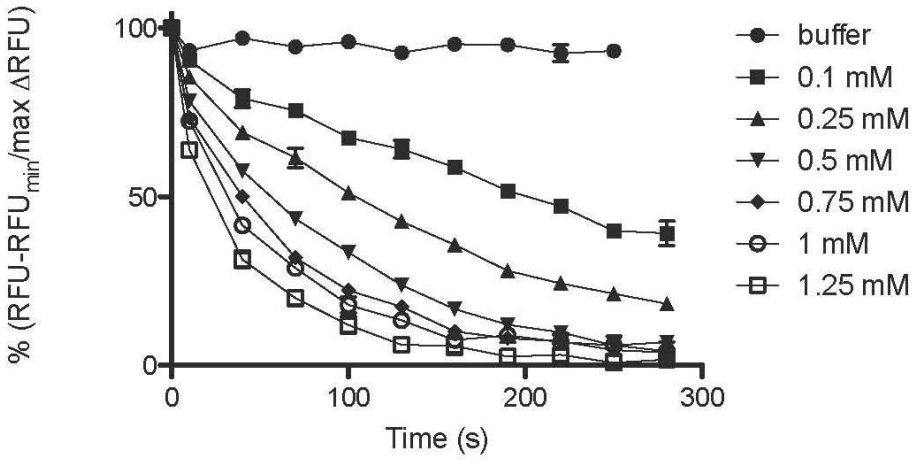

Figure 6.8 PTP1B, when treated with various concentrations of hydrogen peroxide, shows time dependent decay of fluorescence intensity.

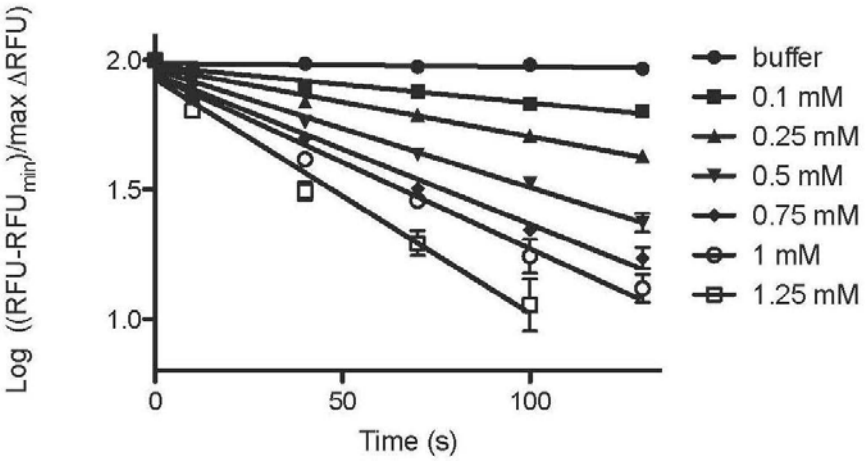

Figure 6.9 Data showing hydrogen peroxide mediated time-dependent loss of PTP1B fluorescence on a semi-log plot.

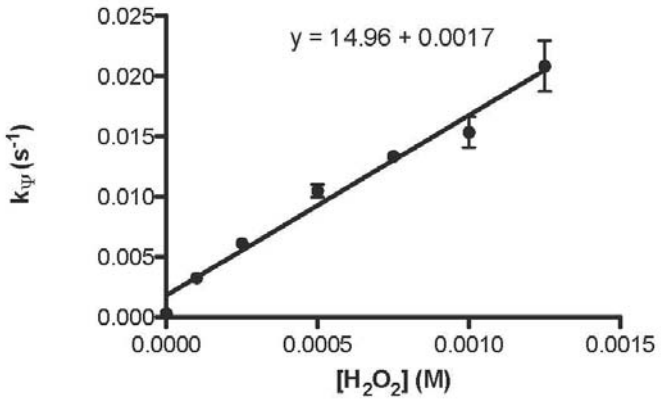

Figure 6.10 Replot of the apparent rate of PTP1B fluorescence decay as a function of H_2O_2 concentration.

6.5 Conclusions

We have developed a method for measuring the time-dependent oxidative inactivation of PTP1B by observing changes in the fluorescence intensity of its tryptophan residues. This method is, essentially, a hybrid of the well-known "gold standard" substrate-based discontinuous and continuous assays that are typically used to determine rates of time-dependent enzyme inactivation. Specifically, the fluorescent method allows for facile *continuous* monitoring of the enzyme active site oxidation state in the *absence* of substrate. The measurement of the second order rate of PTP1B inactivation (oxidation) by hydrogen peroxide that were obtained with this method are in agreement with those derived from the discontinuous and continuous methods (15 versus 18 and 27 $M^{-1}s^{-1}$, respectively).

The success of the method is most likely derived from the known changes in secondary structure that accompany PTP1B active site thiolate oxidation.[5, 6] The loss of ionic interactions that occurs when the cysteine thiolate (Cys215) is oxidized to a sulfenic acid triggers a collapse of the PTP1B active site and rearrangement of its tertiary structure.[11-14] In fact, analysis of PTP1B native and oxidized x-ray crystal structures, reveal dramatic changes in the orientation of the Trp 179 indole ring (Figure 6.11 and Figure 6.12). These changes in orientation could cause corresponding changes in its solvent environment and cause a reduction in its fluorescence quantum yield.[8]

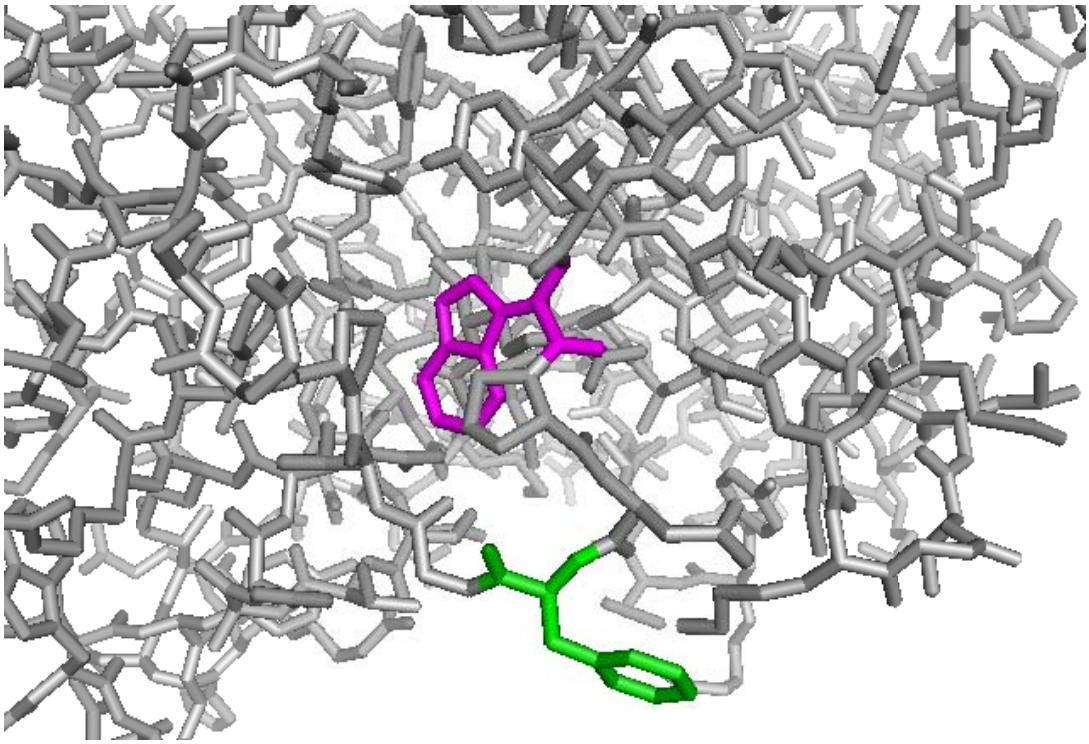

Figure 6.11 X-ray crystal structure of native PTP1B (PDB # 2HNP) showing orientation of the Trp179 indole ring (magenta) with Tyr 181 (green) as a spatial reference.

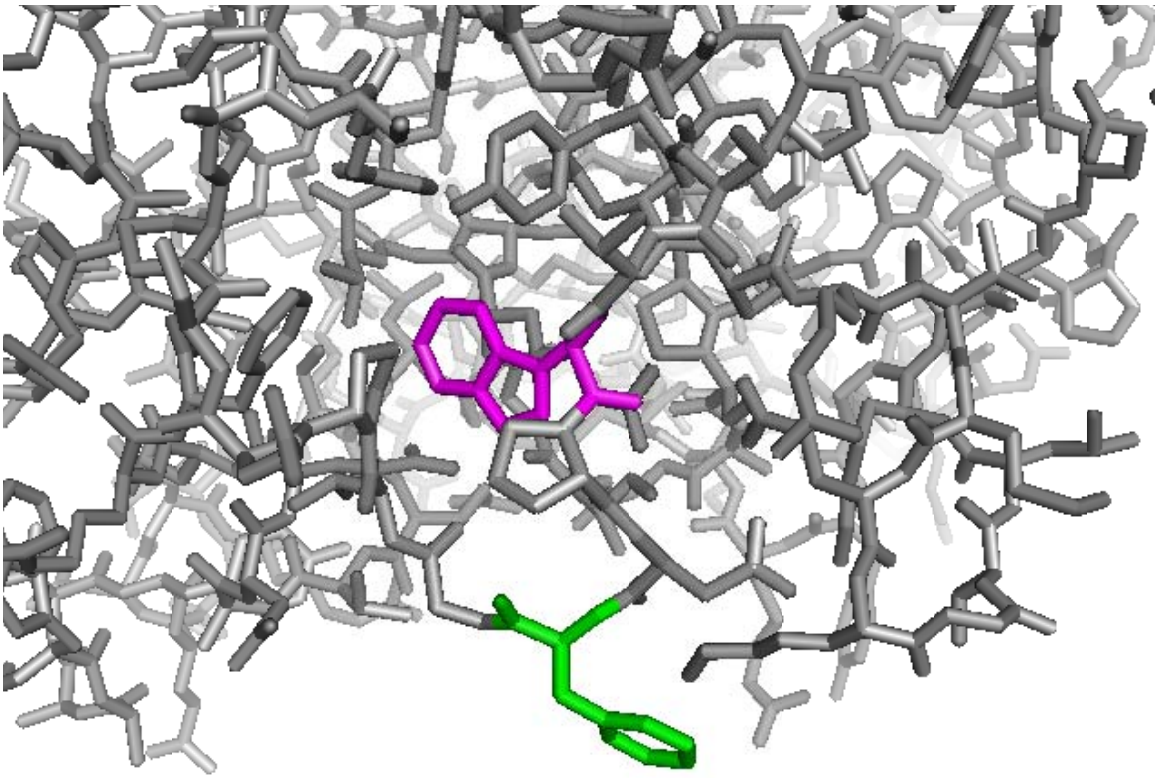

Figure 6.12 X-ray crystal structure of oxidized PTP1B (PDB# 1OEM) showing the change in the orientation of the Trp179 indole ring (magenta) with Tyr 181 shown in green as a spatial reference**.**

Due to the fact that there are a minimal number of physical manipulations necessary to conduct this assay, this assay may prove useful for robotic-based high throughput screening of PTP1B oxidative inactivators. Additionally, an intriguing potential application lies in the field of intracellular PTP redox regulation. With the proper fluorescence instrumentation, it may be possible to monitor the oxidation state of phosphatases in more complex experimental systems. An interesting twist to this would be to incorporate a non-natural Trp analogue, such as 7-azatryptophan (Scheme 6.2) or 5-hydroxytroptophan (Scheme 6.3) at the 179 position. These analogues exhibit strong absorbance at UV wavelengths greater than 300 nm and could therefore enable an

investigator to selectively observe their fluorescence intensity in the presence of proteins and peptides that contain natural Trp.[15]

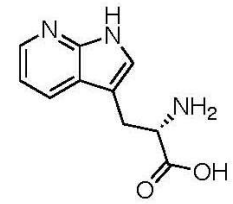

7-azatryptophan

Scheme 6.2 Structure of the non-natural amino acid 7-azatryptophan.

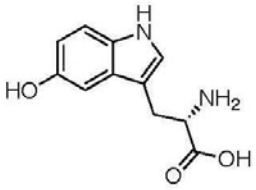

5-hydroxytryptophan

Scheme 6.3 Structure of the non-natural amino acid 5-hydroxytryptophan.

Finally, this assay may also be useful to monitor the oxidation state of the active site cysteine thiolates in other so-called "classical" protein tyrosine phosphatases. Due to the highly conserved nature of their active sites, most PTPs, such as PTP1B, the *yersinia* phosphatase YOP, T-cell protein tyrosine phosphatase (TCPTP) and SHP-2 possess the WPD motif.[4, 16-18] This motif contains the tryptophan residue (W) that we believe is responsible for the change in fluorescence observed with PTP1B after treatment with oxidizing agent. SHP-2, in fact, demonstrates a response similar to that of PTP1B when it is treated with hydrogen peroxide (Figure 6.13).

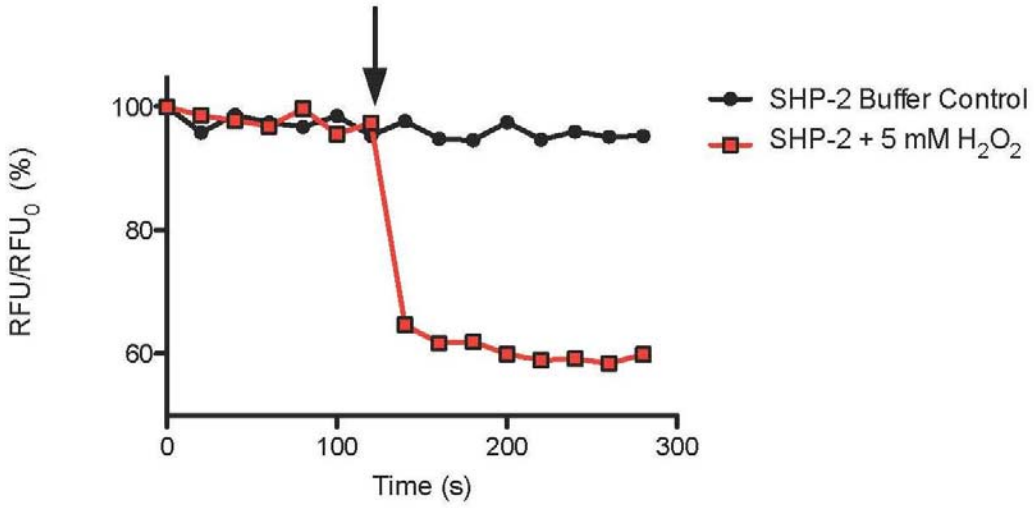

Figure 6.13 Fluorescence emission intensity of SHP-2 (Ex: 285 (4) nm, Em: 330 (4) nm) when treated with either buffer or 5 mM hydrogen peroxide (arrow indicates point of buffer or H_2O_2 addition @120s).

Of particular interest to the scientific community are the effects of intracellular signaling agents on the oxidative state of proteins such as PTP1B. To date, a majority of the data gathered on this topic has lacked a temporal aspect. An assay, such as this, that allows for direct observation of the active site oxidation state of PTPs could bring a new dimension of knowledge to the field of redox regulation.

6.6 Experimental Procedures

Materials and Methods

All fluorescence spectra were measured with an SLM-Aminco model 8100 spectrofluorimeter (Milton Roy/Spectronic Instruments, no longer in production) using 1.0 mL quartz fluorimeter cuvettes. Sodium acetate (# 241245), Bis-tris (# B9754), Tris (#T1378), diethylenetriaminepentaacetic acid (DTPA, Fluka # 32318) were obtained from Sigma-Aldrich Inc. (St. Louis, MO). 30% Hydrogen peroxide (# H325-500) was obtained from Fisher Scientific (Fairlawn, NJ). Crystal structures of PTP1B were visualized with the academic version of PyMol. PTP1B was expressed and purified as described in Chapter 3 of this dissertation. SHP-2 was expressed and purified in the Gates Lab by Derrick R. Seiner.

Determining Optimum Excitation and Emission Parameters for Observing Fluorescence in Native and Oxidized PTP1B. To determine the optimum parameters for observing changes in PTP1B tyrosine fluorescence, we first prepared thiol-free enzyme as described in chapter 3 with one major change to the exchange buffer constituents. Due to the large UV absorbance of NP-40 detergent, this was omitted from the exchange buffer used for removing thiols from the enzyme stock solution. While this

did reduce the overall recovery of enzyme from the buffer exchange step, maximum enzyme recovery was not important to achieve the goals of the experiment.

Native PTP1B samples were prepared by combining 50 μL of thiol-free enzyme (~ 0.5 mg/ml stock) with 0.45 mL of three-component assay buffer (100 mM sodium acetate, 50 mM Bis-tris, 50 mM Tris, 10 mM DTPA, pH 7.0). To observe oxidized PTP1B tyrosine fluorescence, 50 μL of thiol-free enzyme was combined with 0.45 mL of three-component assay buffer fortified with 0.5 mM H_2O_2 and allowed to stand at room temperature for five minutes. An identical sample was allowed to stand at room temperature for fifteen minutes. To observe PTP1B tyrosine fluorescence in all three samples, we utilized an excitation wavelength of 285 nm (2 nm slit width) and scanned the emission wavelength (4 nm slit width) every nm from 300 to 400 nm. The optimum emission wavelength for observing oxidation kinetics of PTP1B was determined by subtracting the spectrum of oxidized enzyme from the spectrum of native enzyme.

Optimizing Spectrofluorimeter Settings for Observation of PTP1B Inactivation Kinetics. Thiol-free enzyme was prepared and diluted with assay buffer to XX mg/ml. To a 1.0 mL of this solution (final volume) in a 1.0 mL quartz fluorescence cuvette was added hydrogen peroxide from 1.0 or 0.1 M stock solutions prepared in H2O. Immediately after addition of hydrogen peroxide, the cuvette was stoppered, inverted three times to mix and the fluorescence intensity was measured every 10 s for 10 min. The cuvette temperature was maintained at 25°C, 22°C, or ramped from 25 to 15 to 30°C. When the temperature was held at 22°C, the excitation monochrometer shutter was closed in between fluorescence intensity readings to minimize exposure of PTP1B to UV light. The shutter remained open for the duration of the other experiments.

Measurement of the rate of PTP1B Oxidative Inactivation by H_2O_2 with Fluorescence. To measure rates of oxidative inactivation, thiol free enzyme was prepared as previously described. To a quartz fluorescence cuvette was added 0.95 mL of thiol-free PTP1B solution (XX mg/ml/XX nM). Hydrogen peroxide from a 1 M stock solution in H2O was then added to final concentrations of 1, 2, 3, 4 and 5 mM (1, 2, 3, 4, 5 μL in 1.0 mL total volume). These concentrations were sufficient for pseudo-first order kinetic analysis. Immediately following addition of H_2O_2, the cuvette was stoppered, rapidly inverted three times to mix and the fluorescence intensity measured as described previously (Ex: 285 (2) nm; Em: 320 (4) nm). Fluorescence measurements were recorded every 30 s for 4.5 min, with each measurement being an average of twenty scans. In between measurements, the instrument was instructed to close the excitation shutter to minimize exposure of PTP1B to UV light. The log values of the resulting data were plotted for analysis as a function of time and fit to an equation describing a straight line. The second order rate of reaction between PTP1B and hydrogen peroxide was then derived by plotting the resulting apparent pseudo-first order rates of inactivation (k_Ψ, slopes of lines) as a function of inactivator concentration (in units of Molarity) and fitting the resulting data to a straight line. The slope of the line gave the rate in $M^{-1}s^{-1}$.

Observation of the Effects of Hydrogen Peroxide on SHP-2 Fluorescence

To a 0.95 mL aliquot of assay/exchange buffer (100 mM Na-Acetate, 50 mM Bis-Tris, 50 mM Tris-HCl, 10 mM DTPA, pH 7.0) in a quartz fluorescence cuvette was added 50 μL of thiol-free SHP-2 (~ 3 in μM exchange buffer, ~150 nM final concentration). Fluorescence emission intensity was monitored every 20 s. for 300 s. (Ex: 285 (4) nm,

Em: 330 (4) nm) with minimal exposure of the sample to UV light. Each data point was an average of 20 individual fluorescence emission scans. At 120 s., the acquisition was paused, and a one microliter aliquot of either exchange buffer or 1M H_2O_2 was added. The cuvette was stoppered, inverted three times to mix, and the acquisition immediately resumed.

References

1. Tian, W. X.; Tsou, C. L., Determination of the rate constant of enzyme modification by measuring the substrate reaction in the presence of the modifier. *Biochemistry* **1982,** *21* (5), 1028-1032.

2. Hart, G. J.; O'Brien, R. D., Recording spectrophotometric method for determination of dissociation and phosphorylation constants for the inhibition of acetylcholinesterase by organophosphates in the presence of substrate. *Biochemistry* **1973,** *12* (15), 2940-2945.

3. Silverman, R. B., *Mechanism-Based Enzyme Inactivation: Chemistry and Enzymology*. CRC Press: Boca Raton, 1988; Vol. I.

4. Hoppe, E.; Berne, P.-F.; Stock, D.; Rasmussen, J. S.; Miller, N. P. H.; Ullrich, A.; Huber, R., Expression, purification and crystallization of human phosphotyrosine phosphatase 1B. *European Journal of Biochemistry* **1994,** *223* (3), 1069-1077.

5. Salmeen, A.; Andersen, J. N.; Myers, M. P.; Meng, T.-C.; Hinks, J. A.; Tonks, N. K.; Barford, D., Redox regulation of protein tyrosine phosphatase 1B involves a sulphenyl-amide intermediate. *Nature* **2003,** *423* (6941), 769-773.

6. van Montfort, R. L. M.; Congreve, M.; Tisi, D.; Carr, R.; Jhoti, H., Oxidation state of the active-site cysteine in protein tyrosine phosphatase 1B. *Nature* **2003,** *423* (6941), 773-777.

7. Zongchao Jia, D. B., Andrew J. Flint, Nicholas K. Tonks, Structural Basis for Phosphotyrosine Peptide Recognition by Protein Tyrosine Phosphatase 1B. *Science* **1995,** *268*, 1754-1758.

8. Edward P. Kirby, R. F. S., Influence of Solvent and Temperature upon the Fluorescence of Indole Derivatives. *The Journal of Physical Chemistry* **1970,** *74* (26).

9. Mudry, C. A.; Frasca, A. R., Photo-oxidation of indole derivatives. *Tetrahedron* **1973,** *29* (4), 603-613.

10. Creighton, T. E., *Proteins Structures and Molecular Properties*. Second Edition ed.; W.H. Freeman and Company: New York, 1993.

11. Puius, Y. A.; Zhao, Y.; Sullivan, M.; Lawrence, D. S.; Almo, S. C.; Zhang, Z.-Y., Identification of a second aryl phosphate-binding site in protein-tyrosine phosphatase 1B: A paradigm for inhibitor design. *PNAS* **1997,** *94* (25), 13420-13425.

12. Johnson, T. O.; Ermolieff, J.; Jirousek, M. R., Protein tyrosine phosphatase 1B inhibitors for diabetes. *Nature Reviews Drug Discovery* **2002,** *1* (9), 696.

13. Tonks, N. K., Protein tyrosine phosphatases: from genes, to function, to disease. *Nat Rev Mol Cell Biol* **2006,** *7* (11), 833-846.

14. Zhang, Z.-Y., Protein tyrosine phosphatases: structure and function, substrate specificity, and inhibitor development. *Ann. Rev. Pharmacol. Toxicol.* **2002,** *42* (42), 209-234.

15. Ross, J. B. S., A.G.; Hogue, C.W.V., Enhancement of protein spectra with tryptophan analogs: fluorescence spectroscopy of protein-protein and protein-nucleic acid interactions. *Methods in Enzymology* **1997,** *278*, 151-190.

16. Stuckey, J. A.; Schubert, H. L.; Fauman, E. B.; Zhang, Z.-Y.; Dixon, J. E.; Saper, M. A., Crystal structure of Yersinia protein tyrosine phosphatase at 2.5 A and the complex with tungstate. *Nature* **1994,** *370* (6490), 571-575.

17. Iversen, L. F.; Moller, K. B.; Pedersen, A. K.; Peters, G. H.; Petersen, A. S.; Andersen, H. S.; Branner, S.; Mortensen, S. B.; Moller, N. P. H., Structure Determination of T Cell Protein-tyrosine Phosphatase. *J. Biol. Chem.* **2002,** *277* (22), 19982-19990.

18. Barr, A. J.; Ugochukwu, E.; Lee, W. H.; King, O. N. F.; Filippakopoulos, P.; Alfano, I.; Savitsky, P.; Burgess-Brown, N. A.; M¸ller, S.; Knapp, S., Large-Scale Structural Analysis of the Classical Human Protein Tyrosine Phosphatome. **2009,** *136* (2), 352-363.

VITA

Jason LaButti was born in 1972 in Providence, Rhode Island to proud parents Norman and Elaine LaButti. During his childhood, he spent the school months inland, and the summer months on the Atlantic coast in Narragansett, Rhode Island where he fished and swam the days away. During his senior year in high school he participated in the Honors Research Program at the National Synchrotron Light Source in Brookhaven, New York. Following graduation from Cranston High School West in 1990, he attended Rensselaer Polytechnic Institute where he was awarded a Bachelors Degree in biochemistry and biophysics in 1994. After testing out the graduate scene at Rensselaer, he decided to enter the industrial sector and began work in 1997 at Alkermes, Inc., a company in Cambridge, Massachusetts that specialized in developing controlled release formulations of pharmaceuticals. Jason was employed at Alkermes, Inc. for a little over a year before he left for an opportunity at Bion, Inc., a Cambridge-based biotech company that was developing digitaloid pregnane derivatives for the treatment of congestive heart failure. When Bion, Inc. folded, he found employment in the drug metabolism and pharmacokinetics group at Millennium Pharmaceuticals, also in Cambridge. During his five-year tenure at Millennium, Jason played a role in the development of a first-in-class boronic acid proteasome inhibitor, marketed as Velcade® (bortezomib), for the treatment of several types of cancer. Jason was married to Gretchen Overbaugh in the summer of

2001 in Glastonbury, Connecticut. They welcomed their first child, Anna Regina in January of 2005, after which Jason suddenly got the itch to return to academia to pursue a terminal degree at the University of Missouri in the laboratory of Professor Kent S. Gates. Interestingly, Jason's supervisor at Millennium was Dr. Gates' first graduate student: John Scott Daniels.